Continuous Deflection Testing of Highways at Traffic Speeds

Research Report 0-4380-1
Project Number 0-4380

Conducted for

Texas Department of Transportation
P.O. Box 5080
Austin, Texas 78763

October 2006

Center for Transportation Infrastructure Systems
The University of Texas at El Paso
El Paso, Texas 79968
(915) 747-6925

TECHNICAL REPORT STANDARD TITLE PAGE

1. Report No. FHWA/TX-06/0-4380-1	**2. Government Accession No.**	**3. Recipient's Catalog No.**
4. Title and Subtitle Continuous Deflection Testing of Highways at Traffic Speeds		**5. Report Date** October 2006 **6. Performing Organization Code**
7. Author(s) Jitin, Arora, B.Tech. Vivek Tandon, PhD, PE Soheil Nazarian, PhD, PE		**8. Performing Organization Report No.** 0-4380-1
9. Performing Organization Name and Address Center for Transportation Infrastructure Systems The University of Texas at El Paso El Paso, Texas 79968-0516		**10. Work Unit No.** **11. Contract or Grant No.** 0-4380
12. Sponsoring Agency Name and Address Texas Department of Transportation Research and Technology Implementation Office P.O. Box 5080 Austin, Texas 78763		**13. Type of Report and Period Covered** Technical Report: September 2003-December 2005 **14. Sponsoring Agency Code**

15. Supplementary Notes
Research performed in cooperation with the Texas Department of Transportation and the Federal Highway Administration.
Project title: Feasibility of Near Highway Speed Deflection Testing of Texas Pavements

16. Abstract

Nondestructive testing devices have been utilized for the last 50 years to assess the structural condition and bearing capacity of existing or newly-constructed pavement systems. A variety of devices have been developed to measure the deformation (deflection) of a pavement due to an applied load. Currently, the most commonly-used nondestructive testing device is the Falling Weight Deflectometer. The Falling Weight Deflectometer is a stop and go (discrete testing) operation rather than a continuous testing operation. The discrete test points are assumed to be representative of a specified length of the pavement under investigation. The stop and go process increases testing time, operational cost and creates unsafe working environment due to traffic interruptions.

To measure deflection profiles at or near highway speeds, various national and international research efforts have taken place in the last decade. However, the status, reliability, operational speed and cost, and limitations of the developed systems are unknown. The main objective of this research project was to summarize the state-of-the-art of continuous deflection measurement systems. Another objective of this study was to propose a specification for an ideal device, if the existing devices do not meet the needs of TxDOT. The results of the findings and ways to incorporate that device in the TxDOT's pavement management systems are reported here.

17. Key Words Rolling Wheel Deflectometer, High Speed Deflectometer, Continuous Deflection Testing, Deflection, Structural Condition Index.	**18. Distribution Statement** No restrictions. This document is available to the public through the National Technical Information Service, Spring field, Virginia 22161, www.ntis.gov

19. Security Classif. (of this report) Unclassified	**20. Security Classif. (of this page)** Unclassified	**21. No. of Pages** 152	**22. Price**

Continuous Deflection Testing of Highways at Traffic Speeds

By

Jitin Arora, B.Tech.
Vivek Tandon, Ph.D., PE
Soheil Nazarian, Ph.D., PE

Research Report No. 0-4380-1
Project Number 0-4380

Project Title: Feasibility of Near Highway Speed Deflection Testing of Texas Pavements Mix Design and Performance Testing of Crumb Rubber Modified Hot Mix Asphaltic Concrete (CRM-HMAC)

Performed in cooperation with the

Texas Department of Transportation
And the Federal Highway Administration

The Center for Transportation Infrastructure Systems
The University of Texas at El Paso
El Paso, Texas 79968-0516
October 2006

Disclaimer:

The contents of this report reflect the view of the authors, who are responsible for the facts and the accuracy of the data presented herein. The contents do not necessarily reflect the official views or policies of the Texas Department of Transportation or the Federal Highway Administration. This report does not constitute a standard, specification, or regulation.

The Unites States Government and the State of Texas do not endorse products or manufacturers. Trade or manufacturers' names appear herein solely because they are considered essential to the object of this report.

NOT INTENDED FOR CONSTRUCTION, BIDDING, OR PERMIT PURPOSES

Jitin Arora, B.Tech.
Vivek Tandon, Ph.D., PE (88219)
Soheil Nazarian, Ph.D., PE (69263)

ACKNOWLEDGEMENTS

The successful progress of this project could not have happened without the help and input of many personnel of TxDOT. The authors acknowledge Mr. Carl Bertrand, Dr. Mike Murphy, Dr. Dar Hao Chen, and Mr. Bryan Stampley for their valuable guidance and input towards successful completion of the project.

ABSTRACT

Nondestructive testing devices have been utilized for the last 50 years to assess the structural condition and bearing capacity of existing or newly-constructed pavement systems. A variety of devices have been developed to measure the deformation (deflection) of a pavement due to an applied load. Currently, the most commonly-used nondestructive testing device is the Falling Weight Deflectometer. The Falling Weight Deflectometer is a stop and go (discrete testing) operation rather than a continuous testing operation. The discrete test points are assumed to be representative of a specified length of the pavement under investigation. The stop and go process increases testing time, operational cost and creates unsafe working environment due to traffic interruptions.

To measure deflection profiles at or near highway speeds, various national and international research efforts have taken place in the last decade. However, the status, reliability, operational speed and cost, and limitations of the developed systems are unknown. The main objective of this research project was to summarize the state-of-the-art of continuous deflection measurement systems. Another objective of this study was to propose a specification for an ideal device, if the existing devices do not meet the needs of TxDOT. The results of the findings and ways to incorporate that device in the TxDOT's pavement management systems are reported here.

TABLE OF CONTENTS

LIST OF FIGURES

LIST OF TABLES

CHAPTER 1 INTRODUCTION

1.1 Problem Statement

Backed by extensive research and experience, the Falling Weight Deflectometer (FWD) is a common device used for evaluating the structural condition of pavements. The Texas Department of Transportation (TxDOT) owns and operates fifteen FWDs to evaluate the condition of the existing pavement network. The FWD needs to stop at every location where a reading is required. Not only does this require lane closure and causes traffic disruption, it also poses a hazard to the personnel who operates the device. Moreover, it may take several minutes to test a point. This stop and go nature of the device limits the frequency of testing along the length of a roadway. The fact that readings are taken at significant distances is another disadvantage.

Several international research efforts are now underway to develop a device that will overcome these deficiencies by measuring the deflections continuously at or at near highway speeds. Several organizations in the USA and Europe have developed devices for this purpose. These devices are currently in various phases of development, and some of them have been successfully implemented. This project aimed at identifying the devices that continuously measure pavement structural conditions, obtaining information about their current stage of development, and evaluating the effectiveness of such devices.

1.2 Objective

The main objective of this study was to evaluate the feasibility of using a continuous deflection testing device for pavement management. To achieve this objective, the project was subdivided into three tasks: 1) determining the status, limitations, and advantages of the available devices, 2) evaluating the applicability of the devices for using in conjunction with the TxDOT Pavement Management Information System (PMIS), and 3) proposing specifications for a device that can be adopted by TxDOT.

1.3 Organization of the Report

Problem statement, research objectives and report organization are presented in this chapter. Chapter 2 provides an overview of the emerging new devices and a summary of a survey that was conducted to obtain more information from their manufacturers. Chapter 3 describes the Structural Strength Index (SSI), the index currently being used by TxDOT in its Pavement Management Information System. The SSI is evaluated to determine its suitability for use with continuous deflection measuring devices.

Chapter 4 describes alternative indices of pavement structural condition that have been proposed by Zhang, et al (2003). Chapter 5 investigates the suitability of these indices for use with

continuous deflection measuring devices and reliability of selected device(s). Recently, one of the devices has been upgraded. These updates are discussed in Chapter 6. Chapter 7 provides a summary and presents recommendations for a suitable deflection measuring device for TxDOT.

CHAPTER 2 SURVEY OF EXISTING DEVICES

Various continuous deflection measuring devices are in the developmental stages. The methods for data acquisition and data analysis are different for each device depending on its characteristics such as the speed, applied load, and accuracy. This chapter contains an overview of the capabilities of the devices that are currently under development or have been developed. At the time of preparing this report, five different devices were under different stages of development. These devices are the Quest Airfield Rolling Weight Deflectometer (ARWD), the Swedish Road Deflection Tester (RDT), the Texas Rolling Dynamic Deflectometer (RDD), the Danish High Speed Deflectograph, and the Applied Research Associate's Rolling Wheel Deflectometer (RWD). Several other devices such as the British Deflectograph, French Lacroix Deflectograph, Flash Deflectograph, and French Curviameter are one-of-a-kind with no future development or commercialization planned for them. Therefore, a discussion on these devices is not included in this report.

2.1 Quest ARWD

Quest Integrated has developed a prototype Airfield Rolling Weight Deflectometer (ARWD) that measures runway deflections under a wheel load of 9 kips (40 kN) moving at a speed of 20 mph (35 km/h). The device uses four sensors to estimate the deflection due to an applied wheel load. The equipment (Figure 1) has been developed in collaboration with Dynatest, Inc. The theory of operation and results obtained with this device has been reported by Briggs et. al. (1999) and are included in Appendix A as reference.

FIGURE 1 ARWD Prototype by Quest Integrated

The ARWD has the advantage of being based on a sound principle that has been demonstrated to be effective at slow speeds. The factors that are likely to introduce error have been taken into account and suitable workarounds have been incorporated. In this device, it is assumed that the sensors pass sequentially over identical areas of pavement, and that sensors do not move with respect to each other. The reported limitations of the device are the loss of accuracy on curves and the length of the trailer. Moreover, this device has originally been designed to work at low speeds and may not be successful at or near highway speeds. Recently, Quest has received a Small Business Implementation Research grant to update the system to make it suitable for highway applications and increase the speed to 60 mph (100 km/h).

2.2 Swedish Road Deflection Tester

The Swedish National Road Administration and Swedish National Road and Transport Research Institute have developed a Road Deflection Tester (RDT). The RDT (Figure 2) consists of a truck that has been retrofitted with two arrays of laser range finders, each consisting of 20 sensors arranged in a line transverse to the direction of travel. The device can impart forces from 8 to 14 kips (40 to 70 kN) and travel up to a speed of 60 mph (100 kph). The theory of operation and results obtained from this device are reported by Andr´en et. al. (2000a, 2000b and 2004), which are included in Appendix B for reference.

FIGURE 2 Swedish Road Deflection Tester (Andr´en and Lenngren, 2000a)

The RDT has the advantage of providing an entire transverse deflection profile instead of a single deflection value provided by some of the other devices. In principle at least, it should be possible to backcalculate the properties of the pavement layers.

The RDT implicitly makes certain assumptions regarding the nature of the deflections and the measurement process. It assumes that the RDT is moving faster than the speed at which the deflection wave travels along the pavement, so that the maximum deflection occurs a little distance behind the load wheels. Thus, the RDT measures the deflection as the difference

between the deflections beneath the loaded wheels and the maximum deflection which is assumed to occur at a distance of 0.5 m behind the wheels. The validity of this assumption needs to be investigated. It is likely that the location of the maximum deflection behind the wheel would depend on the speed at which the RDT moves and the pavement stiffness, rather than being a fixed value. The RDT also does not account directly for the possible errors introduced due the vertical motion of the device. Instead it relies on averaging of several data points to reduce this error.

2.3 Texas Rolling Dynamic Deflectometer

The Rolling Dynamic Deflectometer (RDD) consists of a vibroseis truck on which a servo-hydraulic vibrator is mounted to generate dynamic loads (Figure 3). The dynamic forces of (35 kips) are transferred to the pavement with a set of loading wheels. Vertical pavement deflections generated by the dynamic force are measured with up to four rolling deflection sensors which can be positioned in any number of configurations. The theory of operation and results obtained from this device are reported by Bay et al. (2000) and are included in Appendix C for reference.

This device seems to provide good estimate of the pavement stiffness. In addition, the measured deflections provide a good indication of the load transfer efficiency of joints in rigid pavement. This device has been successfully used by TxDOT on various forensic investigations.

The RDD travels at speeds of of 1 mph (1.5 km/hr) and is therefore not suitable for testing at highway speeds.

FIGURE 3 Rolling Dynamic Deflectometer

2.4 Danish High Speed Deflectograph (HSD)

The Danish Road Institute and Greenwood Engineering A/S have developed a device for measuring pavement bearing capacity and the funding was provided by the Danish Agency for Trade and Industry. The device uses lasers for velocity (that can be converted to deflection) measurements as shown in Figure 4. The device uses two laser sensors based on the Doppler technique to measure the undeflected and the deflected profiles of the pavement. The difference of these two values is the deflection of the pavement. Wheel loads of up to 11 kips (50 kN) are applied and monitored using a servo-control system. The motion of the sensors is monitored using inertial systems. The theory of operations and test results obtained from this device as reported by Hildebrand, et. al. (2002) are included in Appendix D for reference.

FIGURE 4 Danish High Speed Deflectograph (Hildebrand, et. al. 2002)

The HSD has the advantage of using a simple and well known principle. The HSD trailer is neither long nor bulky. The device has shown good repeatability and good correlation with the results of the FWD.

2.5 Applied Research Associate's Rolling Wheel Deflectometer

Applied Research Associates, Inc. (ARA) is developing a Rolling Wheel Deflectometer (RWD) with the grant from the Federal Highway Administration. A prototype of the RWD has been assembled and tested in 2002 and 2003. A picture of the RWD is shown in Figure 5. Since one of the objectives of this study was to evaluate the data provided by the manufacturer, a detailed discussion of the device along with some analysis of the data is included in here. The information about theory of operation and initial data analyses is reproduced from Hall and Steele (2004).

FIGURE 5 Picture of the ARA RWD (Hall, et al., 2004)

2.5.1 Theory of Operation

The RWD is based on the spatially coincident methodology for measuring pavement deflections. Three lasers are used to measure the unloaded pavement surface (i.e., forward of and outside the deflection basin), and a fourth laser, located between the dual tires and just behind the rear axle, measures the deflected pavement surface. Deflection is calculated by comparing spatially coincident scans as the RWD moves forward (Hall, et. al., 2004). The RWD applies a 9 kip (40 kN) load through 2 wheels spaced 13 in. (330 mm) apart.

The deflection profile is obtained by subtracting the profile of the deflected shape from that of the undeflected shape measured at the same location. The method is identical to that used in the Quest ARWDas explained in Harr, et al. (1977). The ARA RWD employs a 2 kHz sampling rate

and averages the deflection values collected over a 100 ft length to produce a single deflection measurement.

The RWD employs an aluminum beam of 25.5 ft (7.78 m) length and a custom built trailer of 53 ft (16.2 m) length. The beam uses a curved extension to pass under and between the dual tires, placing the rear most laser approximately 6 inches rear of the axle centerline and 7 inches above the roadway surface. Figure 6 shows the rear laser and part of the beam between the RWD tires. The three forward lasers on the RWD are mounted 12 in (305 mm) above the road surface while the fourth is mounted 6 in (153 mm) above the road surface.

FIGURE 6 Rear Laser Between the Wheels of RWD (Hall, et. al., 2004)

2.5.2 Test Results

The RWD was field tested in 2004 in Texas. The deflections measured with the device were compared to other devices including the FWD, the Texas RDD, and on a more limited basis, the MDD. The sections chosen for the test are indicated in Table 1. Most of the test runs were carried out at a nominal speed of 55 mph (90 km/h). Each road section was tested 5 times. Figure 7 shows typical results of the five test runs on one road. The repeatability of the RWD deflection measurements are good as the peaks and valleys in all except one deflection profile coincide. It is also noticed that the deflection measurements on the same section of the road tended to decrease over the course of the day where a reverse trend is expected.

A comparison of the deflections obtained from the RWD with those obtained from the FWD and RDD are shown in Figures 8 and 9, respectively. Figure 8 shows that some relationship exists between the RWD and FWD deflections. The data exhibits some scatter, especially at smaller deflection values.

TABLE 1. RWD Test Locations

Road	Reference Marker and Direction	Characteristics of Interest	Pavement Structure
SH 47	RM 412.2 to 418.7 Northbound RM 411.8 to 418.3 Southbound	Medium and low deflections. Horizontal and vertical curves, and tangents. Fine and medium textured pavement surfaces	3 in. of AC 6 in. of granular base (majority) 2 in. of AC 6 in. of CTB (selected areas)
SH 21	RM 628.0 to 630.9 Westbound	Undulating longitudinal profile due to swelling soils (aka, bumpy)	2 in. of AC unspecified base
FM 50	RM 412.0 to 413.7 Northbound	High deflections	N/A
SH 21	RM 634.0 to 635.6 Westbound	Coarse surface texture	2 in. of AC unspecified base
FM 2154	RM 626.0 to 632.0 Southbound	High deflections and rutted surface	Chip seal 6-in. flexible base 5-8 in. of subbase
IH 45	RM 168.0 to 184.0 North and South	Continuously Reinforced Concrete Pavement (CRCP) and AC/CRCP	8-in. CRCP 4-in. AC stabilized base

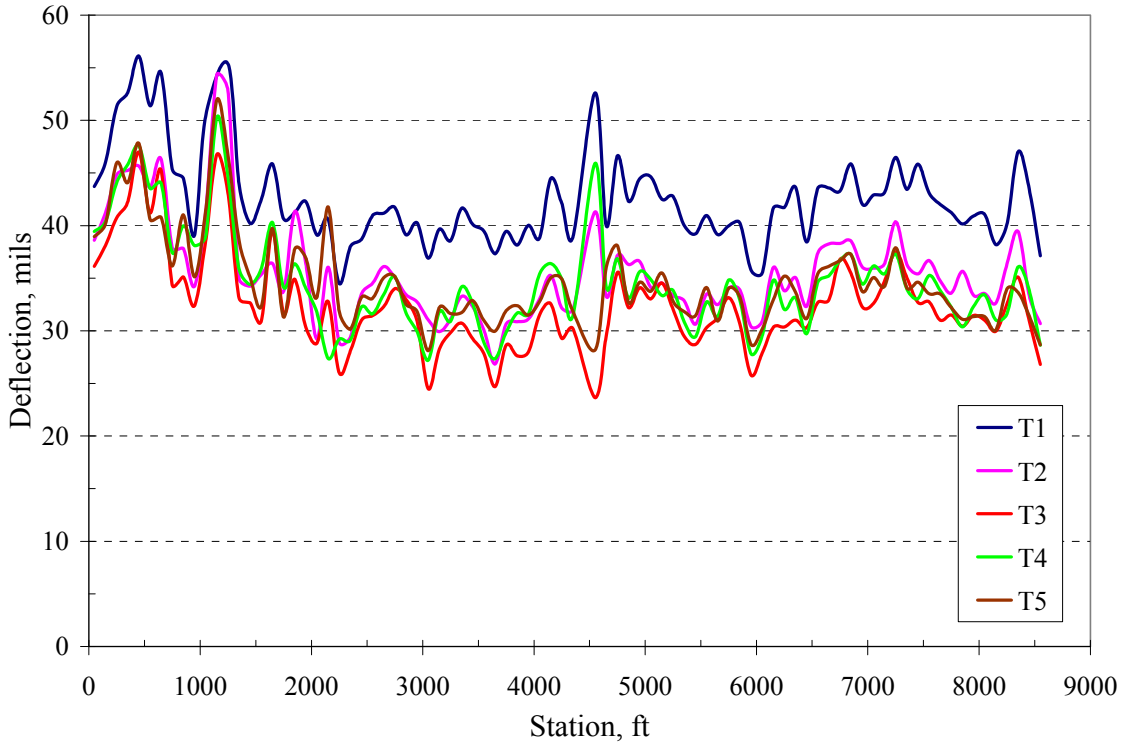

FIGURE 7 Plot of 5 Test Runs of the RWD for FM50 (Hall, et. al., 2004)

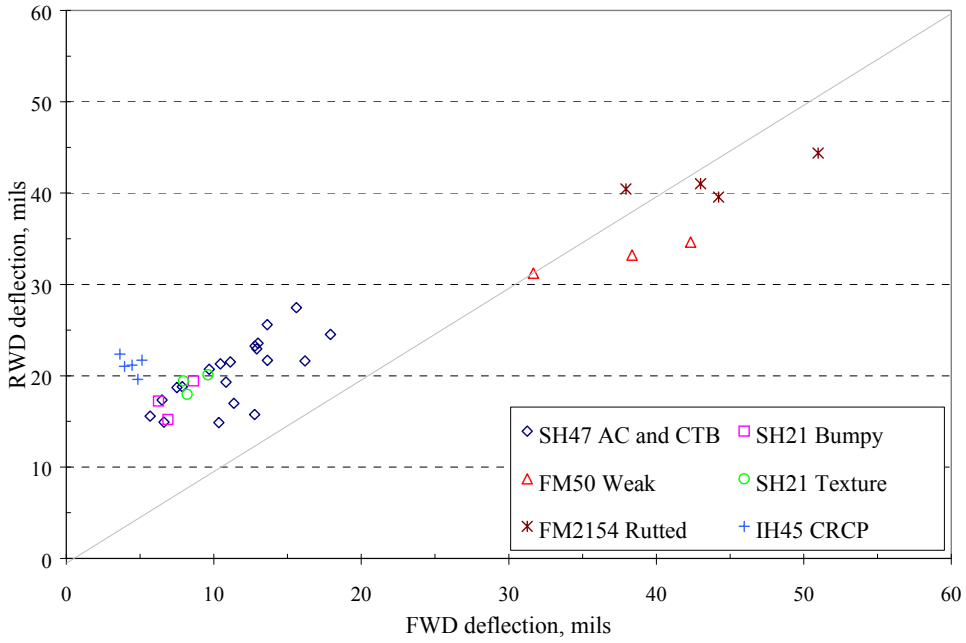

FIGURE 8 RWD Deflections vs. FWD Deflections (Hall, et. al., 2004)

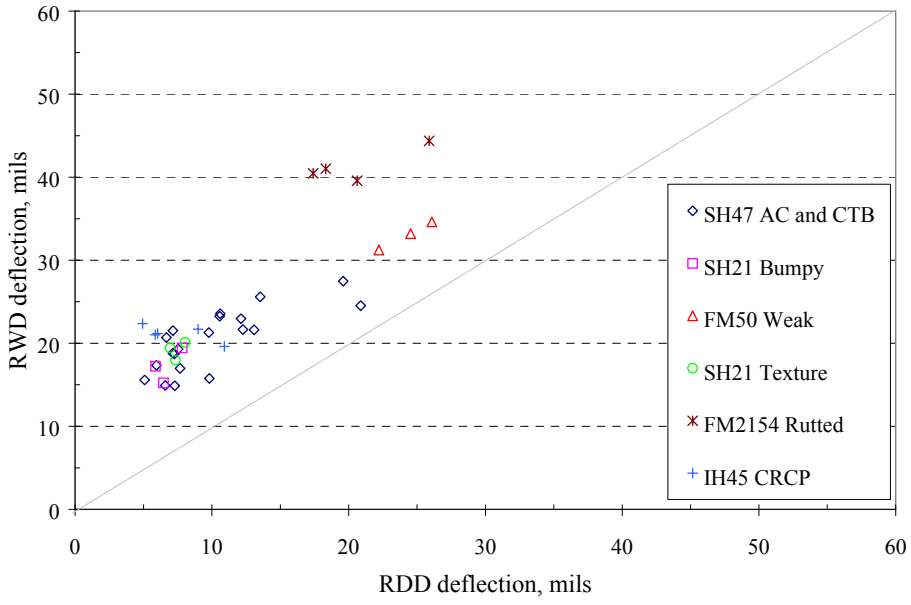

FIGURE 9 RWD Deflections vs. Texas RDD Deflections (Hall, et. al., 2004)

A comparison of the results obtained from the RWD with those obtained from the Texas RDD also shows similar trends (Figure 9). A comparison of the RWD results with the MDD results is presented in Table 2. The RWD values are consistently higher than those obtained from the MDD. Further, unlike the MDD values, the values obtained from the RWD show a decreasing trend with increase in temperature. A summary of mean values obtained from RWD, RDD, and FWD are presented in Table 3. Different devices provide different deflections. The FWD and RDD deflections are closer to one another.

TABLE 2. Deflection Values From RWD and MDD (Hall et. al., 2004)

Date	Speed, mph	Time, hh:mm	Temp, F	RWD, mils		MDD, mils	
				Section R5	Section R6	Section R5	Section R6
7/16/03	50	11:10	118	15.51	21.63	4.88	N/a
		11:16	119	14.04	20.79	5.13	11.72
		11:21	122	14.61	19.85	5.31	10.99
		11:27	123	13.63	19.12	5.55	11.23
		11:32	123	13.28	19.00	5.25	11.60
		11:37	123	12.18	18.20	5.55	10.93
		11:47	124	10.15	16.04	5.37	12.08
		11:52	126	9.37	15.73	5.74	12.57
		11:57	127	8.86	15.02	5.49	11.29
		12:02	128	8.66	14.59	5.43	11.41
		12:07	129	8.22	14.68	5.49	10.68
		12:13	130	7.90	14.58	5.55	11.47
		12:18	131	7.26	13.16	6.29	14.22
		12:22	132	8.27	14.54	N/a	11.23
	15	12:52	126	7.82	N/a	6.59	11.84
		12:59	126	8.05	N/a	6.23	14.16
		13:01	127	8.04	N/a	6.35	14.89
	10	13:11	130	7.07	13.56	7.57	13.61
		13:18	128	6.87	12.33	5.86	14.10
	5	13:28	131	5.57	12.57	5.49	15.01
	50	17:20	106	19.71	27.51	5.25	15.38
		17:25	108	20.50	27.96	5.86	11.66
	60	17:30	108	20.53	27.75	5.19	11.60
		17:35	108	19.97	27.08	5.19	11.54
	65	17:40	108	19.38	25.60	5.13	N/a
		17:45	108	18.70	25.98	5.86	11.72
		17:54	108	14.58	20.60	5.13	11.54

TABLE 3. Summary of mean RWD, FWD, and RDD Deflections by section (Hall et. al., 2004)

Road and Direction	Section No.	RWD, Mils	FWD, mils	RDD, mils
SH 47 Southbound	R1	15.76	12.77	9.82
	R2	14.87	10.34	7.28
	R3	16.98	11.36	7.67
	R4	21.62	16.18	13.09
	R5	15.58	5.68	5.09
	R6	23.55	13.00	10.61
	R7	21.29	10.45	9.78
	R8	20.70	9.69	6.68
	R9	17.34	6.49	5.94
	R10	25.59	13.62	13.53
	R11	27.46	15.60	19.60
SH 47 Northbound	R12	24.53	17.91	20.88
	R13	14.92	6.62	6.60
	R14	21.67	13.63	12.26
	R15	23.25	12.80	10.58
	R16	22.95	12.91	12.13
	R17	18.80	7.87	7.14
	R18	18.72	7.50	7.26
	R19	21.52	11.13	7.15
	R20	19.30	10.83	7.54
SH 21 Westbound	R22	15.21	6.90	6.46
	R23	17.24	6.25	5.88
	R24	19.43	8.62	7.84
FM 50 Northbound	R25	33.21	38.36	24.53
	R26	31.23	31.66	22.22
	R27	34.62	42.32	26.09
SH 21 Westbound	R28	19.43	7.95	6.96
	R29	20.10	9.60	8.05
	R30	17.97	8.20	7.34
FM 2154 Southbound	R31	40.46	37.94	17.40
	R32	41.02	43.00	18.33
	R33	44.38	50.97	25.88
	R34	39.57	44.22	20.62
IH 45 Northbound	R35	21.70	5.13	9.00
	R36	21.16	4.45	6.03
IH 45 Southbound	R37	22.36	3.63	4.93
	R38	21.04	3.94	5.86
	R39	19.61	4.85	10.91

2.5.3 Analysis of the Data Provided by ARA

It would have been advantageous to obtain raw data of the device because fast Fourier transform and other signal analysis techniques could have been applied. However, only the average deflections at 100-ft interval were available.

The RDD and RWD deflections from all sites are compared with the FWD deflections in Figure 10a. The relationship between the high-speed devices and FWD deflections are best represented by a power equation. The R^2 values obtained for these relationships are 0.67 for the RWD and 0.80 for the RDD. Ignoring the data from IH-45, the R^2 values improved to about 0.87 for both relationships (as shown in Figure 10b). This suggests that the IH-45 data needs further evaluation.

The variations in deflections with distance from Northbound and Southbound IH-45 tested at a speed of 55 mph (the analysis assumes that the speed is constant throughout the test section) are shown in Figures 11 and 12, respectively. In addition,. The deflections with no restrictions on Y-axis are shown in Figure 11a while Y-axis with deflections only up to one standard deviation (from mean) and with no negative deflections are shown in Figure 11b. The data shown in Figure 11a suggests that the RWD vehicles movements might be inducing artificial peaks (or noise) because peaks were observed at different locations at different trial runs. Therefore, the data needs to be filtered out which have been proposed by Hall and Steele (2004).

To minimize the influence of noise, the Y-axis was expanded (Figure 11b) to show the differences between trial runs and compare the data with FWD measurements. The data was averaged in two different fashions. In the first method, it was decided to average out the each trial run data and standard deviations (SD) were estimated for that trial run as well. The average ± one standard deviation (SD) was then used to identify the upper and lower limits. If the data falls above or below these limits, then the data should be discarded. The average values and the limits for the data set are shown as lines in the Figure 11b. The small dashed lines represent upper limits, solid lines represent the mean values and larger dashed lines represent lower limits. The data presented this way shows that the average of three trial runs are pretty close to each other including upper and lower limits indicating that the device is reasonably repeatable. The average value varied from 20 to 22 mils for the entire test section. However, this analyses method assumes that the entire length of pavement section is the same which may not be the case. On the other hand, the data from MDD or FWD is collected at the discrete points and it is assumed that the test section is the same between measured data points.

The other method of averaging is to average the data obtained for each trial assuming that the deflections measured at each point is the same. The data averaged in this fashion is shown as diamond marker points in the figure. The data presented this way allowed a better representation of the test section. The averaged RWD deflection varied from 17 mils to 23 mils (excluding outliers identified using average ± SD). In addition, SD values were less than 10 mils with this method in comparison to 12 to 17 mils with the previous method.

When the average values (either method) of RWD are compared to FWD, the deflection values are quite different. The FWD data for the entire length is roughly 4.8 mils which is roughly four to five times lower than the averaged RWD deflections. In addition, the measured deflections

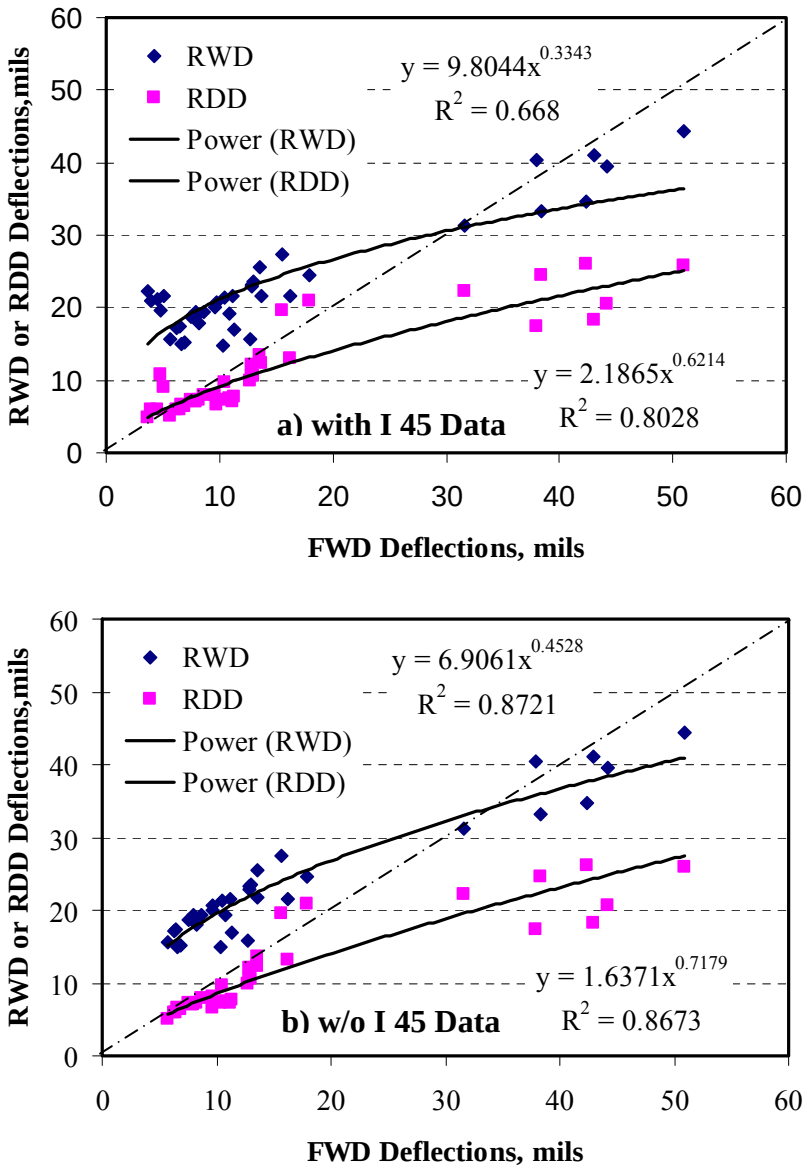

FIGURE 10 FWD Deflections vs. RDD and FWD Deflections (Hall, et. al., 2004)

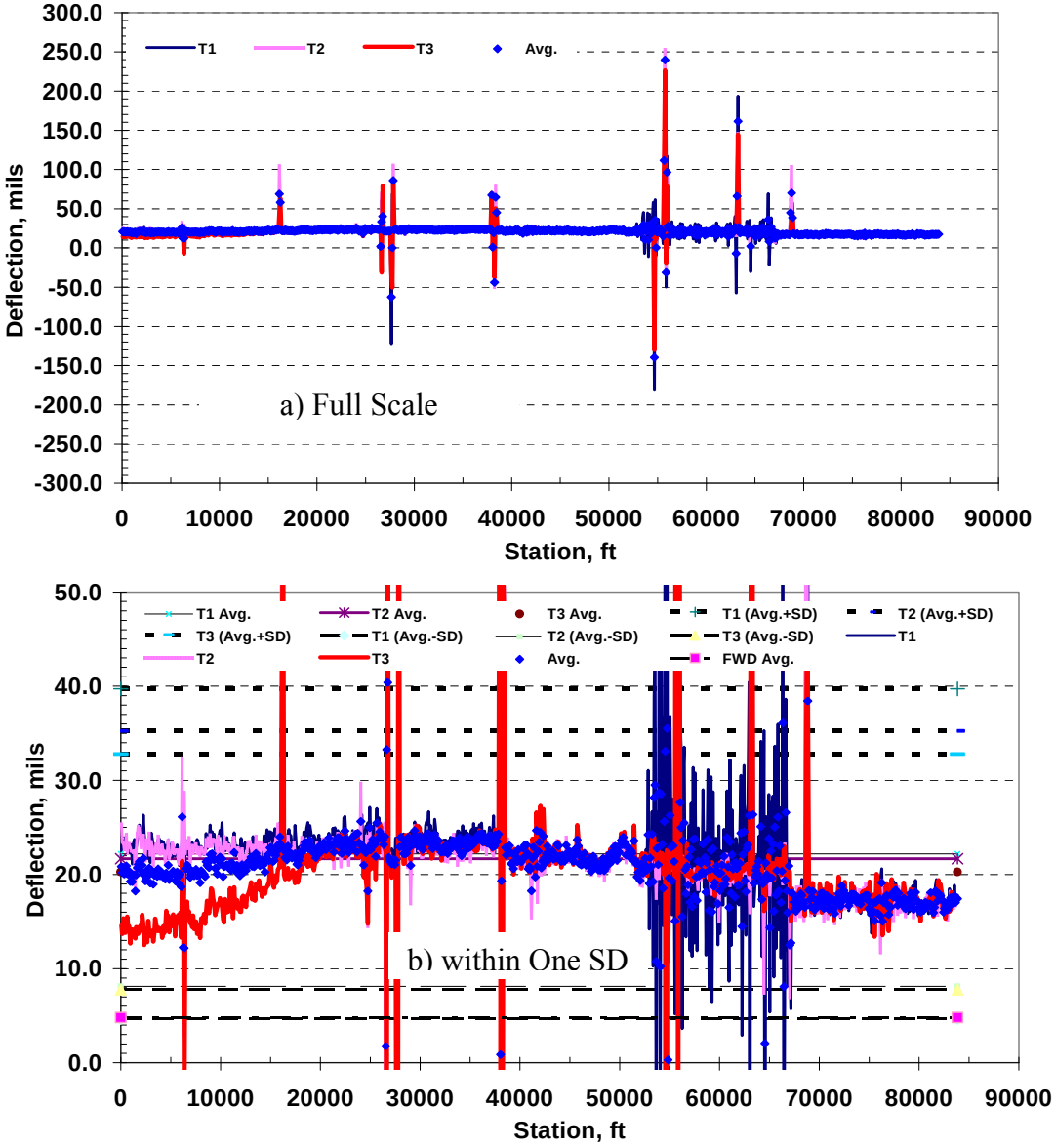

FIGURE 11 RWD Deflections from Northbound I 45

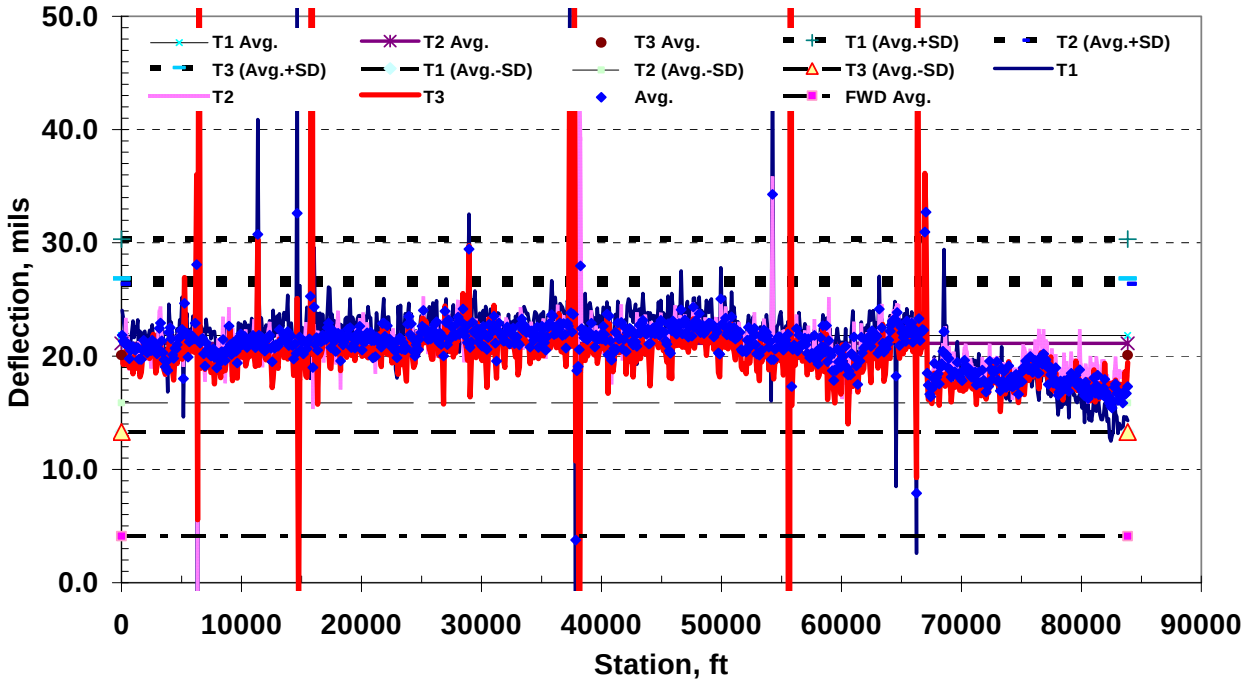

FIGURE 12 RWD Deflections from Southbound I 45

were always higher than 10 mils (excluding noise data) throughout the test section. To further evaluate this difference, the FWD data collected at various intervals were compared with RWD individual points and the results are shown in Figure 13. The data suggests that overall RWD is measuring higher deflections in comparison to FWD even though the tested pavement is structurally sound (based on data collected with RDD and PMIS database).

Another important observation is the data at the beginning and at the end of the test sections. The measured deflections dropped from 20 mils to 17 mils at the end of the test section (from 6,750 to 8,500 feet) indicating that the pavement is structurally better in comparison to the remainder section. On the other hand, the trail run 3 (T3) measured lower deflection (from 22 mils to almost 15 mils) at the starting of the test section (from 0 to 1,500 ft) in comparison to other two trials. The drop in deflection reduces the averaged deflection to a lower value which indicates that the section is better than the section beyond 2000 ft which may not be the case.

This discrepancy leads to question that whether lower deflection means structurally sound pavement or is a manifestation of some other measurement issues. The other question comes to mind is whether the device has the capability of measuring deflections lower than 10 mils. However, the data presented in Table 2 suggests that the RWD was able to measure the

deflections at the levels of 5 to 6 mils but at lower speeds. Therefore, it is quite possible that the levels of measured deflections change with speed.

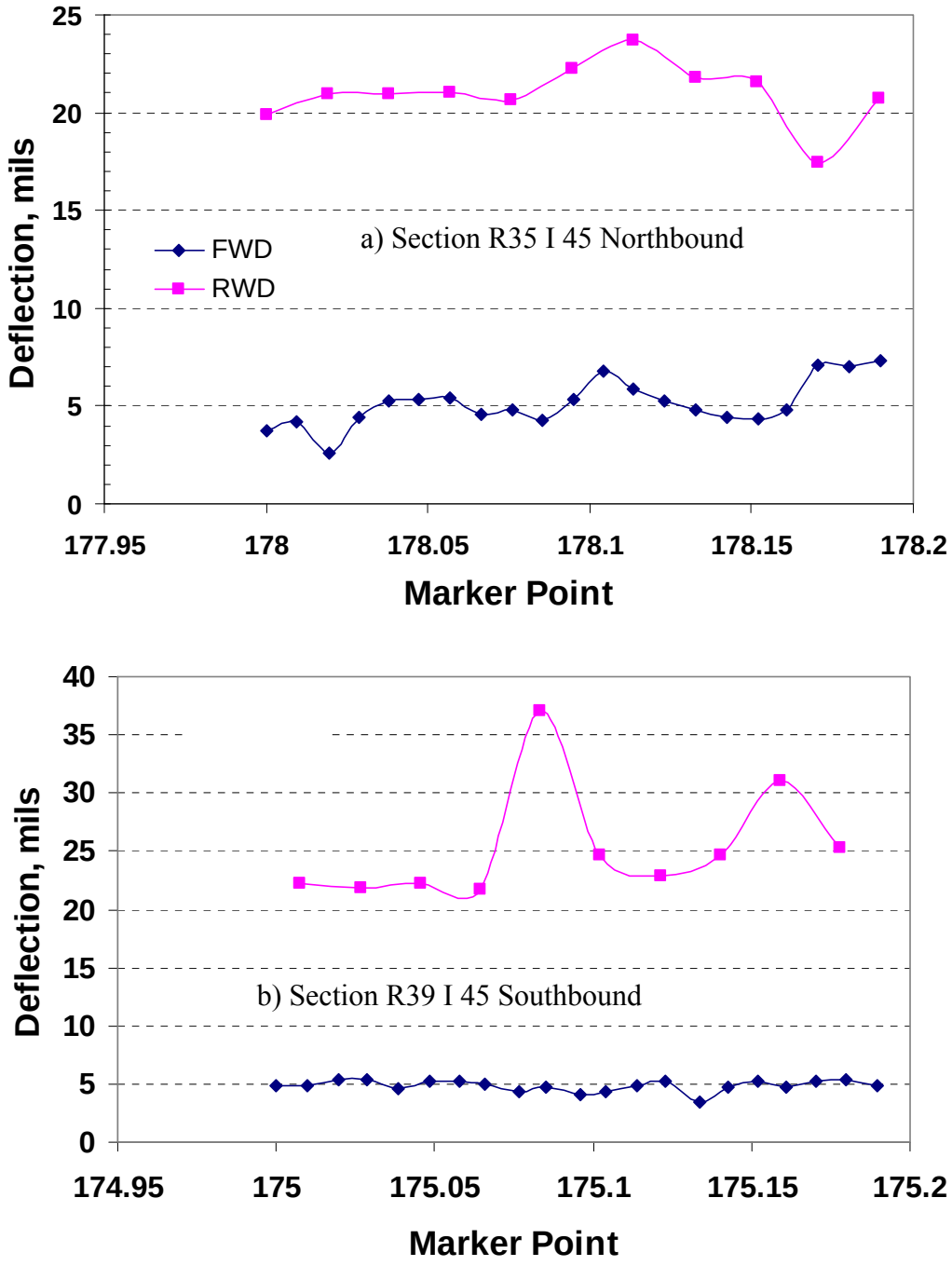

FIGURE 13 RWD vs. FWD Deflections from I 45

The data presented in Table 2 suggests that the measured deflections are dependent on the speed of the device. Tests were performed at different speeds along SH47 on July 16th for Section R5. The variations in deflection with distance at different speeds are summarized in Figure 14. Figure 14a contains the results from tests carried out in the afternoon. An increase in speed from 5 mph to 65 mph results in an increase in the measured deflections, even though the pavement temperature dropped from 125 to 108 °F. On the other hand, the MDD data presented in Table 2 shows a decrease in deflection with decrease in temperature as expected; thus, indicating that there is an influence of speed on measured deflection. The data presented in Figure 14b is for the testing performed in the morning of July 16th at a speed of 50 mph except one data point (tested at 65 mph around 17:25 PM). The overall trend for the morning data suggests that the deflections decrease even though temperature is increasing.

The data presented in Figure 14b suggests that the section is weaker at 150 ft in comparison to 50 ft or 250 ft because the deflection values increased by 10% for almost all of the runs at 150 ft. Similarly, the measurements at 750 ft indicate that this section is weaker than 650 ft or 850 ft because of higher deflections at 750 ft. This information can be easily missed with the FWD measurements; thus, showing the benefits of using RWD. However, one thing needs to be kept in mind is that the vehicle speed plays an important role. If the increase or drop in deflection is a manifestation of change in speed (due to traffic constraints) rather than pavements structural capacity, then the pavement section will be assigned a lower rating which is an issue for the TxDOT.

Overall, the data analyses indicate that there is an influence of speed on the measured deflections; therefore, the use of constant speed over the entire section may not be a valid assumption. In addition, the data suggests that the minimum deflection that can be measured at highway speeds (50 mph) is roughly 15 mils (Figures 11 and 12) that will eliminate evaluation of TxDOT Pavement Types 1 through 4 because CRCP pavements are expected to have less than 6 mils of deformation under traffic loads.

To overcome this problem, the data can be collected, under minimal traffic conditions and a relationship between speed and measured deflections can be developed for various pavements types. This relationship can be used in conjunction with the actual vehicle speed at the time of data collection to estimate actual deflections at lower speeds which can be closer to RDD speeds. To test this assumption, the data of Table 2 in the afternoon session is plotted (Figure 15) in terms of speed and measured deflections for section R5. The data shows very good relationship (R^2 of 0.94) between speed and measured deflections. Therefore, a deflection of 5 mils at the speed of 5 mph translates into a deflection of roughly 17 mils at 55 mph speed. Now if we compare the I 45 data obtained using FWD and RWD, the data shows similar levels of deformation. The FWD data was roughly 4.8 mils on I 45 while the averaged RWD data varied from 17 to 22 mils suggesting that the deflections are pretty close. This way of data analysis can reduce the discrepancy between the RWD and static devices.

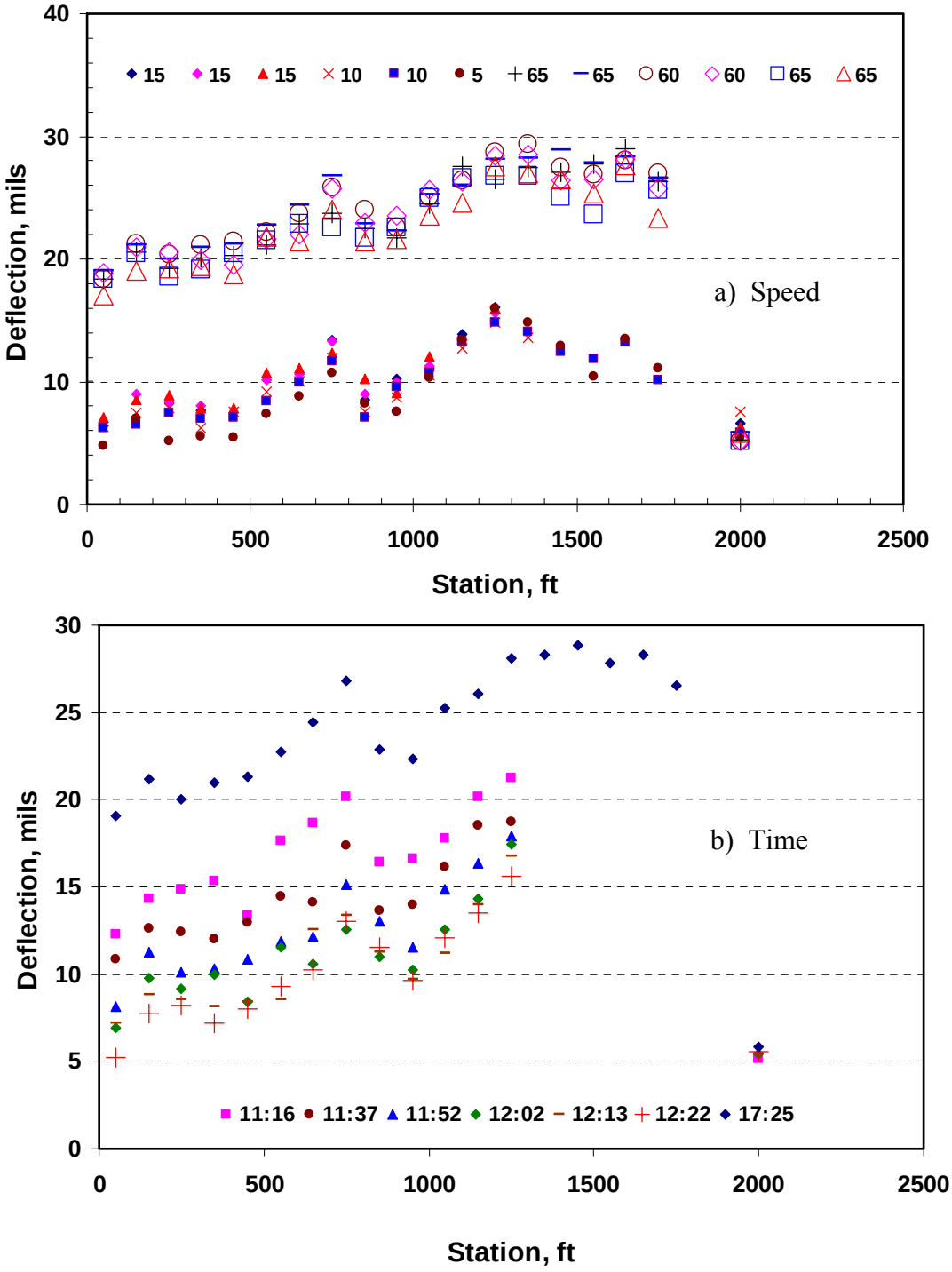

FIGURE 14 RWD and MDD Deflections from SH47 at Section R5

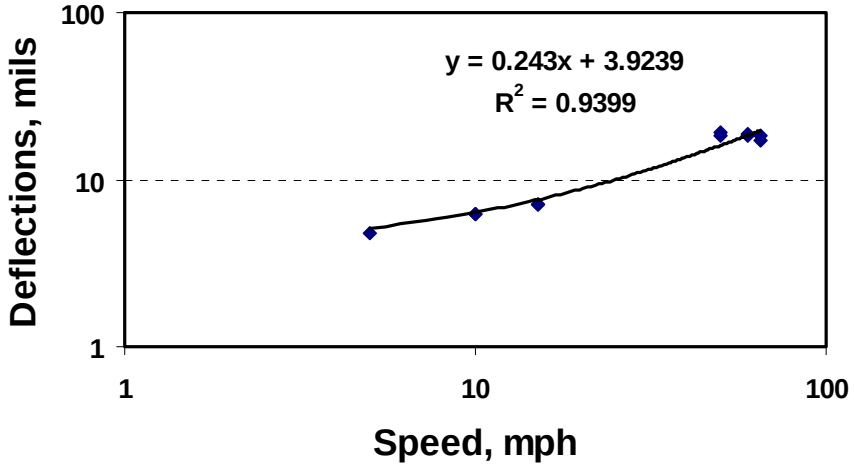

FIGURE 15 Influence of RWD Speed on Measured Deflections

2.6 Comparison of Devices

The questionnaire enclosed in Appendix E was sent to the manufacturers to obtain more information about each device. The results of this survey are summarized in Table 4. Since a response was not received from the manufacturer of the ARWD, information from the published papers and brochures were used to complete the information. None of the device ideally fulfills all the intended functions, although some are close.

The survey results suggest that typically two operators would be needed to perform tests with any of the devices. The applied load levels range from 5 kips to 18 kips. The operational speeds of the device range from 20 mph to 60 mph with the exception of RDD which operates at a speed of about 1 mph. The frequency of data collected varies from every 0.5 in. to every 9 ft depending on the speed of the vehicle. Typically, the data are collected at higher rates but are reported at a specified interval after averaging. The accuracy of the deflection or velocity measuring transducers varies from 0.05 mils to 4 mils/seconds. Some of the devices have GPS equipment for referencing purposes.

All of the devices are in various development stage and likely need to undergo significant changes before they can be commercialized. The HSD and RWD devices have recently performed some field demonstration and shown to have the potential to be available in the near future.

Currently, TxDOT PMIS system uses FWD which has seven sensors while the HSD or RWD devices have only one sensor. Therefore, it was decided to identify how the information form one sensor can be used for the pavement management as discussed in the following chapter.

TABLE 4. Summary of Dynamic Deflection Devices

Device	Texas Rolling Dynamic Deflectometer (RDD)	Highway Rolling Weight Deflectometer (ARWD)	Rolling Wheel Deflectometer (RWD)	Rolling Deflection Tester (RDT)	High Speed Deflectograph (HSD)
Manufacturer	UT Austin	Dynatest Consulting and Quest Integrated	Applied Research Associates	Swedish National Road Administration and VTI	Greenwood Engineering,Denmark
Estimated Cost	N/A	N/A	N/A	N/A	$ 2,400,000
Operational Speed	1 mph	20 mph	45 to 65 mph	60 mph	50 mph
Distance between readings	2 to 3 ft	9 ft	0.5 in	0.75 in.	0.80 in. (20 mm)
Applied Load	10 kips static + 5 kips dynamic	9 kips	18 kips fixed	8 to 14 kips (40 to 70 kN)	11 kips (49 kN)
Deflection Sensor Accuracy	0.05 mils	N/A	± 2.75 mils (± 0.070 mm)	±10 mils (± 0.256 mm)	±4 mils/s (± 0.1 mm/s)
System Accuracy	N/A	1 mil at 6 mph	N/A	N/A	0.2 mils (5 μm)
Other Features	GPS Equipped	N/A	GPS Equipped	N/A	GPS Equipped
Number of Operators	2	N/A	2	2	2
Calibration Process	Yes	N/A	Yes	Yes	Yes
Comments	Too slow for network level.	No Release Date Available.	No Release Date Available.	No Release Date Available.	Sold two devices so far.

CHAPTER 3 EVALUATION OF SSI

3.1 TxDOT PMIS and SSI

The Texas Department of Transportation (TxDOT) utilizes a Pavement Management Information System (PMIS) to monitor and record the condition of pavements. Pavements are classified into 10 categories depending on their sectional details. These categories along with their description are shown in Table 5.

TABLE 5. Pavement Types in the TxDOT PMIS

Pavement Code	Pavement Type	Pavement Category
01	Continuously Reinforced Concrete Pavement	C
02	Jointed Reinforced Concrete Pavement	J
03	Jointed Plain Concrete Pavement	J
04	Thick Asphaltic Concrete Pavement (greater then 5½")	A
05	Intermediate Thickness Asphaltic Concrete Pavement (2½" to 5½")	A
06	Thin Surfaced Flexible Base Pavement (less than 2½")	A
07	Composite Pavement (Asphalt Surfaced Concrete Pavement)	A
08	Overlaid and/or Widened Old Concrete Pavement	A
09	Overlaid and/or Widened Old Flexible Pavement	A
10	Thin Surfaced Flexible Base Pavement (Surface Treatment-Seal Coat Combination)	A

Information about the structural condition of the pavements is obtained from FWD testing. The seven measured deflections are normalized to 9 kips (40 kN) and are used along with pavement type, traffic load in ESAL, and average annual rainfall information to compute an index called the Structural Strength Index (SSI). The SSI is used to determine the structural condition of the pavement according to Table 6.

The Quest ARWD, Danish HSD and ARA RWD provide only a single deflection which may not be sufficient to estimate the strength of the pavement section. Moreover, since these are moving devices, the level of the deflections measured may not be the same as that of the FWD (as shown in Figure 16). The FWD measures the peak deflections under a single impulse load. The moving devices measure the deflection under a wheel load that may be moving at a significant speed (up to 50 mph). The single deflection provided by moving devices may be from different locations. For example the maximum deflection velocity measured by HSD happens at a certain distance ahead of the wheel (Figure 16). Another thing to keep in mind is that the deflection

bowl developed using FWD data depends on the peak deflections obtained from seven geophones. However, the reported peak occurs at different times as the stress wave generated by the imparted load travels through the pavement system. On the other hand, the addition of more than one sensor in the moving device will provide deflections at the same time which will be different from the typical FWD deflection bowl. It is therefore important to know the amount of information that can be obtained about the pavement structural condition from a single deflection.

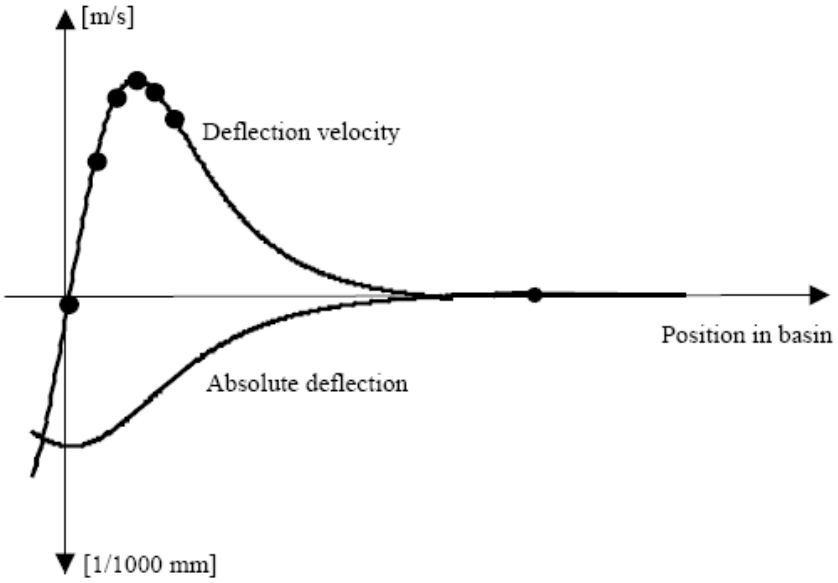

FIGURE 16 Velocity Curve vs. Deflection Bowl (Simonin et al, 2005)

The feasibility of relating the FWD center deflection (referred to as W1) to the SSI is reported here. The FWD center deflection is chosen because it has the closest correspondence to the deflection measured by the moving devices. If a relationship between W1 and SSI can be developed, or if a significant amount of information about the pavement structural condition can be obtained from W1, they can be extended to the single deflection provided by most moving devices.

TABLE 6. Pavement Structural Condition According to SSI

SSI Score	Class	Description
90-100	"A"	"Very Strong"
80-89	"B"	"Strong"
70-79	"C"	"Fair"
60-69	"D"	"Weak"
01-59	"F"	Very Weak
0	Null	Not Calculated

3.2 Computation of SSI

The SSI is based on three parameters: the utility value (U_{FWD}) computed from the measured FWD deflections and pavement types, the rainfall factor and the traffic factor. To calculate the utility factor (U_{FWD}), the FWD deflections (specifically W1, W2, and W7) are utilized. The FWD deflections are first normalized to 9 kips using Equation 3.1.

$$NW_i = W_i \times \left(\frac{9000}{Load} \right) \tag{3.1}$$

In this equation, W_i is the measured deflection value, Load is the measured load at which the deflection was measured and NW_i is the normalized deflection.

The Surface Curvature Index (SCI) is computed using

$$SCI = NW_1 - NW_2 \tag{3.2}$$

where NW_1 and NW_2 are the normalized deflections from the first and second sensors.

The utility factor (U_{FWD}) is estimated using SCI, NW_7 (normalized deflection from the seventh sensor of FWD) and the pavement type. The U_{FWD} values are documented in the TxDOT PMIS manual and are included in Appendix F (Tables F1 through F3). Typically, U_{FWD} varies between 1.00 and 0.10 with 1.00 describing a very strong pavement.

The Rainfall Factor is based on the average rainfall and is obtained from Table F4 in Appendix F. This factor typically varies from 1.00 (for less than 20 in. of rainfall) to 0.94 (for more than 40 in. of rainfall). Similarly, the Traffic Factor (TF) is based on the pavement type and the 18-kip ESAL count and is obtained from Table F5 in Appendix F. This factor typically varies from 0.70 (for heavy traffic count) to 1.30 (for low traffic count) depending on applied ESALs and pavement type. Finally, the SSI is calculated using

$$SSI = 100 \times U_{FWD}^{[1/RF \times TF]} \tag{3.3}$$

3.3 Dallas Area Data

To evaluate the relationship between W1 and SSI, the actual pavement deflections from the TxDOT PMIS for the Dallas area were used. The database contained the FWD deflections, the applied FWD load, and the pavement type. The database, with 3,165 entries, contained records for different pavement types shown in Table 5 and from more than one season for some pavements. This data was used to compute the utility value (U_{FWD}) and the SSI. To calculate the SSI, three different values of the TF were used while a RF value of 0.97 was used for all records. The RF and TF values are not needed for U_{FWD} calculations. The Utility Values were plotted against three parameters: the normalized center deflection (NW1), the SCI, and NW7 in Figures 17 through 19, respectively.

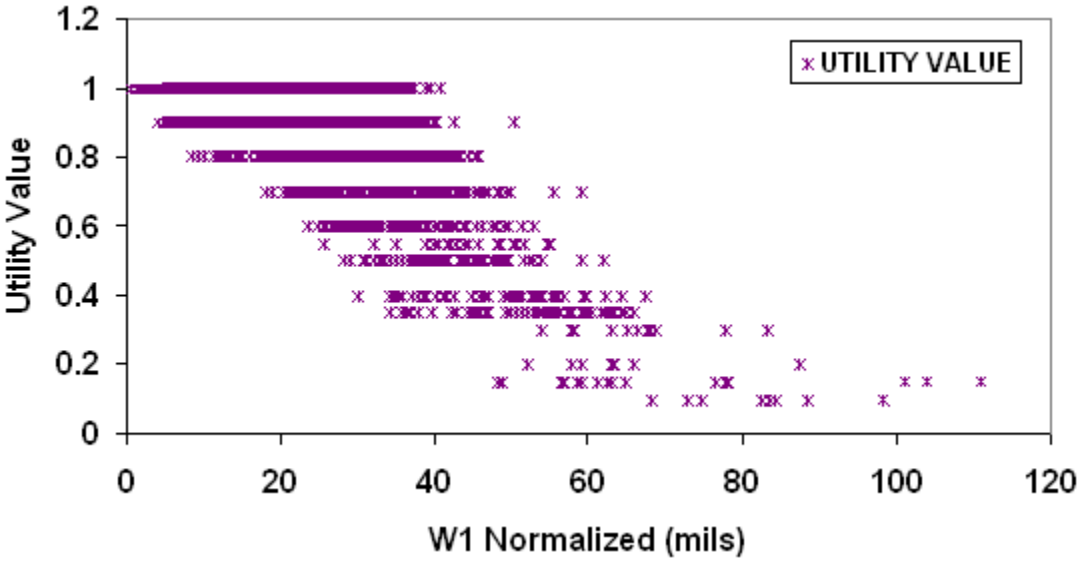

FIGURE 17 Utility Value Compared with the Center Deflection

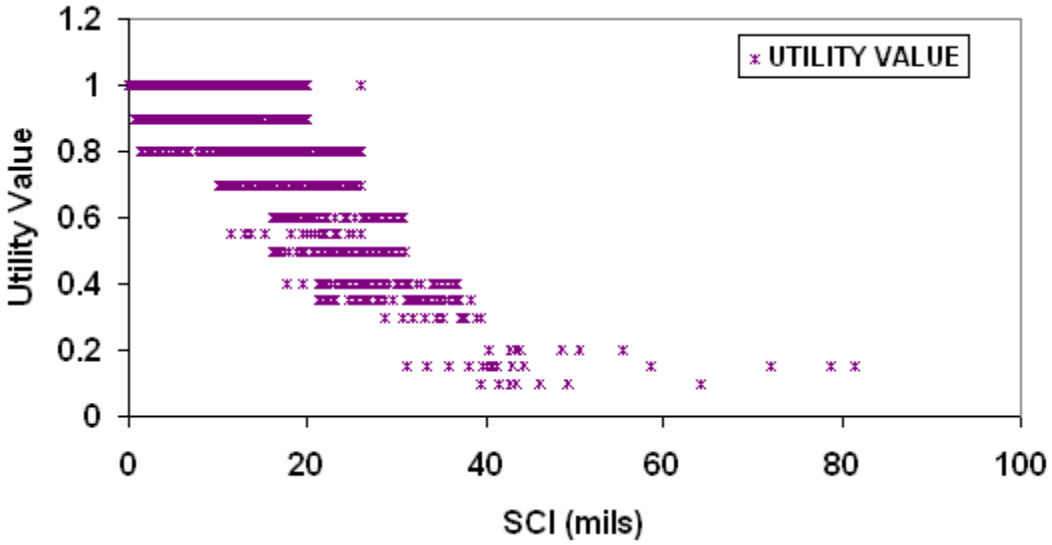

FIGURE 18 Utility Value Compared with the SCI

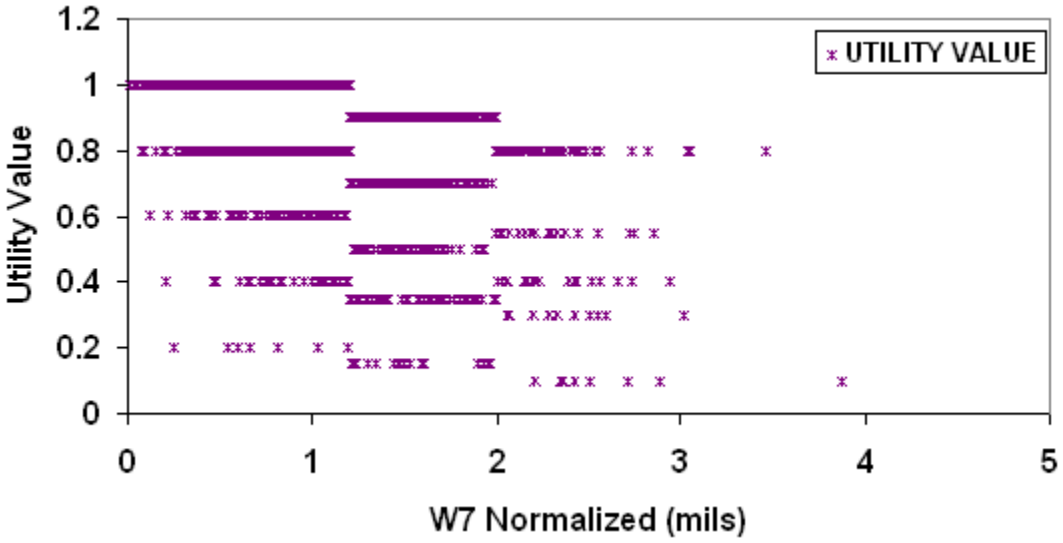

FIGURE 19 Utility Value Compared with W7

The graphs show that the Utility Value decreases with an increase in any of the three deflection parameters, but the relationships are not strong. There is a wide spread in the U_{FWD} values covering a range from a strong pavement to a weak pavement. For example, U_{FWD} of 1.0 was observed (Figure 17) for normalized W1 ranging from almost 0 to 40 mils, suggesting that W1 may not be able to discriminate between strong and weak pavements. Similar trends were observed when normalized W7 and SCI values were used. As a consequence, it does not seem feasible to predict the utility value on the basis of only a single deflection parameter.

To determine whether the SSI can be used as an indicator of the pavement strength, the SSI was plotted against normalized W1 and W7, and SCI for three different TF values as shown in Figures 20 to 22. A strong correlation between the SSI score and any of the three deflection parameters cannot be observed. A particular value of any of these deflection parameters may correspond to a wide range of possible SSI's. In other words, different pavements in very different structural conditions may register the same SSI value for any of these deflection parameters.

The data points were then sorted and examined individually according to the pavement type. The SSI scores were plotted against the same three deflection parameters. Typical plots for pavement Type 4 are shown in Figures 23 to 25. Once again, no clear relationships could be observed. The data from the remaining pavement types is included in Appendix G. The additional information provided by the pavement type does not seem to be adequate to distinguish between structurally-sound and weak pavements on the basis of a single deflection value.

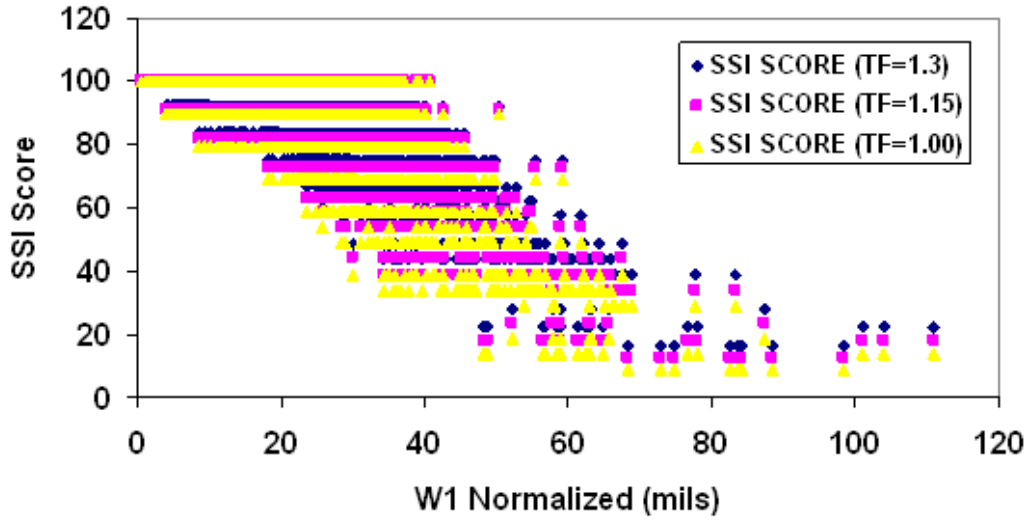

FIGURE 20 SSI Score Compared with W1

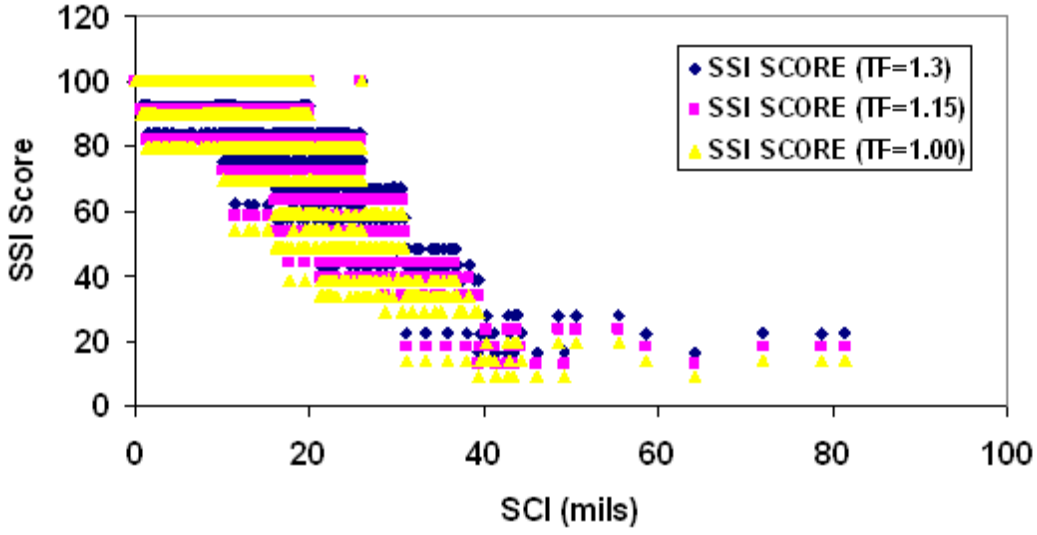

FIGURE 21 SSI Score Compared with the SCI

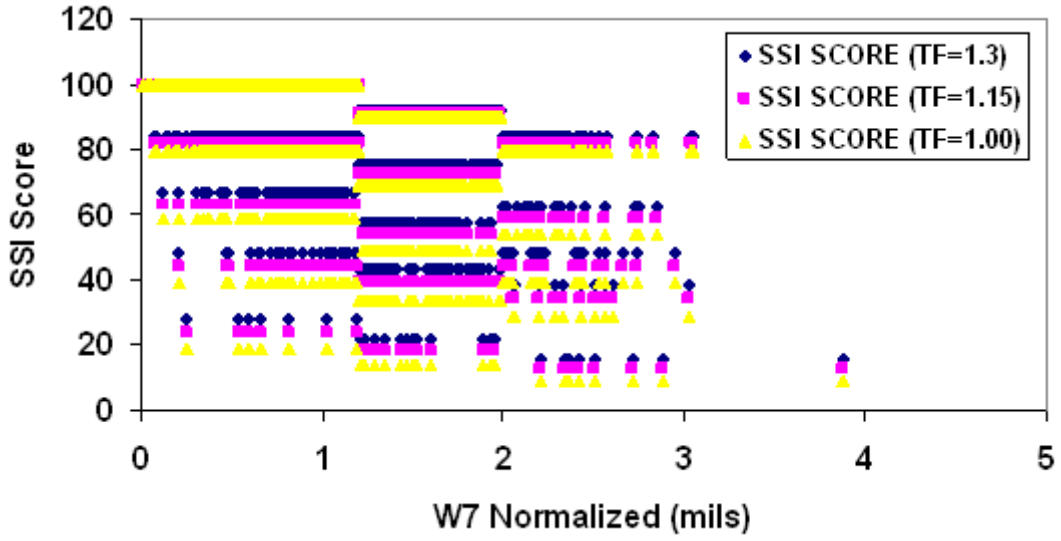

FIGURE 22 SSI Score Compared with W7

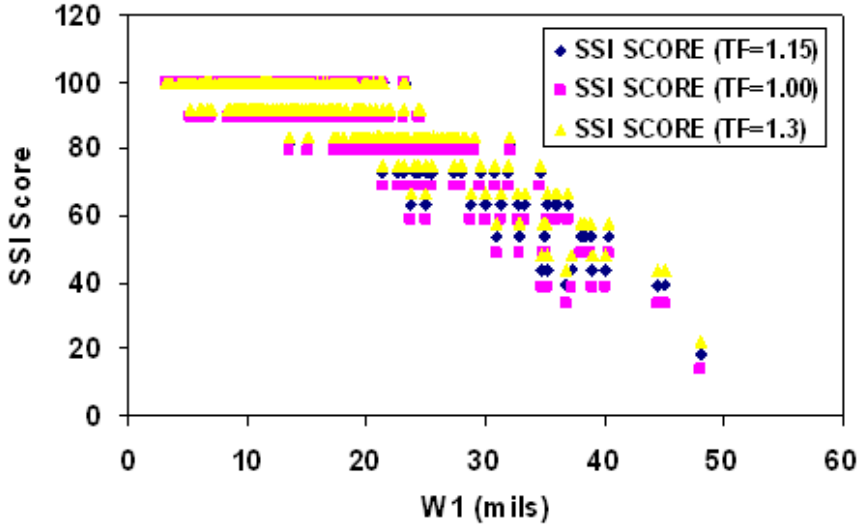

FIGURE 23 SSI Score Compared to W1 for Pavement Type 4

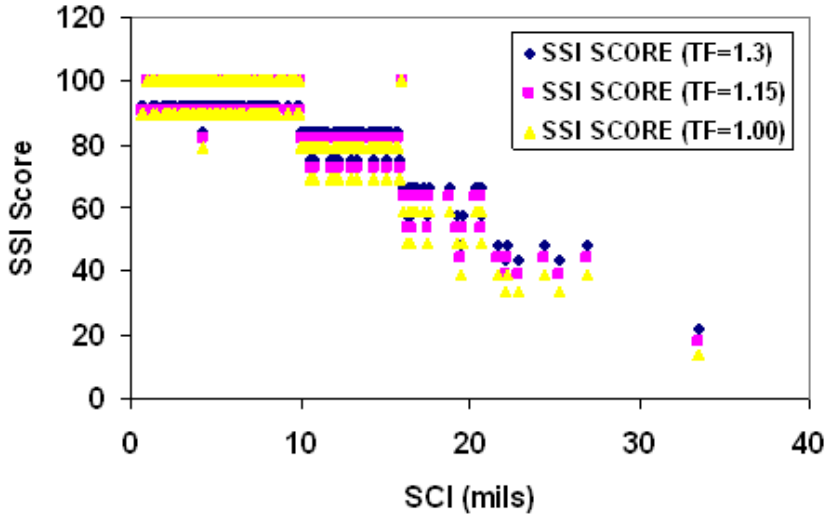

FIGURE 24 SSI Score Compared to SCI for Pavement Type 4

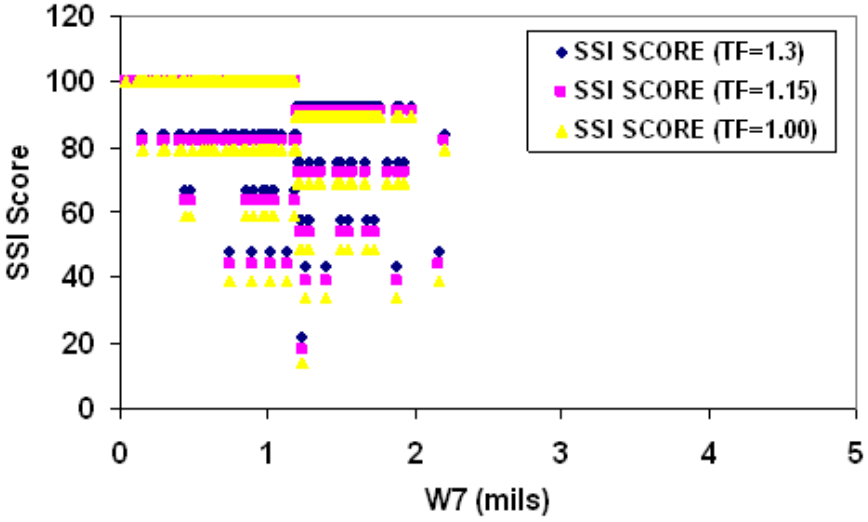

FIGURE 25 SSI Score Compared to W7 for Pavement Type 4

Since no correlation could be found based on SSI and SCI, it was decided to see if there is relationship between condition score and W1 or W7. Again, the relationship was evaluated using the Dallas area Database. The relationship between W1 and W7 with condition score is shown in Figure 26. At first the relationship was evaluated using W1 versus condition score for all pavement types (Figure 26a) and then with only Pavement Type 4 for W1 (Figure 26b) as well as W7 (Figure 25c). The data suggests that there is no relationship between condition score and W1 or W7. The evaluation of limited data set suggests that only one deflection point is not sufficient to describe condition of the pavement or structural strength of the pavement. Since the PMIS database for Dallas District did not contain sufficient data for all pavement types, the pool of data was expanded by numerically generating a large database as presented in the following sections. The main advantage of simulating data is that series of data sets can be generated without any field testing. An added advantage is that the pavement properties can be selected to simulate structurally sound or poor pavements.

3.4 Simulated Data

To supplement the investigation and increase the range of pavement properties, a layer elastic program (BISAR) was used to generate additional records. This program takes the thickness and modulus of the layers as input to compute deflections that are expected from the FWD tests. Representative values of these parameters are necessary for each of the pavement types in order to generate an accurate data set. TxDOT currently does not maintain this information in its PMIS system. A survey conducted by Murphy (1998) provides representative values for Texas. These values are summarized in Table 7.

TABLE 7. Representative Values of Pavement Parameters

	Pavement Types 1, 2 and 3	Pavement Type 4	Pavement Type 5	Pavement Type 6	Pavement Type 10
Surface Thickness (in)	10, 11, 12, 13, 14	6, 8, 10, 12	2.5, 4, 5.5	1, 1.5, 2	1, 2
Surface Modulus (ksi)	2000, 3000, 4000, 5000, 6000, 8000	50, 100, 200, 300, 400, 500, 600, 750, 1000, 1250	50, 100, 200, 300, 400, 500, 600, 750, 1000, 1250	50, 100, 200, 300, 400, 500, 600, 750, 1000, 1250	50, 100, 150, 200, 300, 400, 500, 600, 750, 1000, 1250
Base Thickness (in)	Not Applicable	6, 10, 14, 18	6, 10, 14, 18	6, 10, 14, 18	6, 10, 14, 18
Base Modulus (ksi)	Not Applicable	5, 10, 20, 30, 40, 80, 100, 200	5, 10, 20, 30, 40, 80, 100, 200	5, 10, 20, 30, 40, 80, 100, 200	5, 10, 20, 30, 40, 80, 100, 200
Subgrade Thickness (in)	250, 500, 700	250, 500, 700	250, 500, 700	250, 500, 700	250, 500, 700
Subgrade Modulus (ksi)	1, 5, 10, 15, 20, 25, 30, 40	1, 5, 10, 15, 20, 25, 30, 40	1, 5, 10, 15, 20, 25, 30, 40	1, 5, 10, 15, 20, 25, 30, 40	1, 5, 10, 15, 20, 25, 30, 40

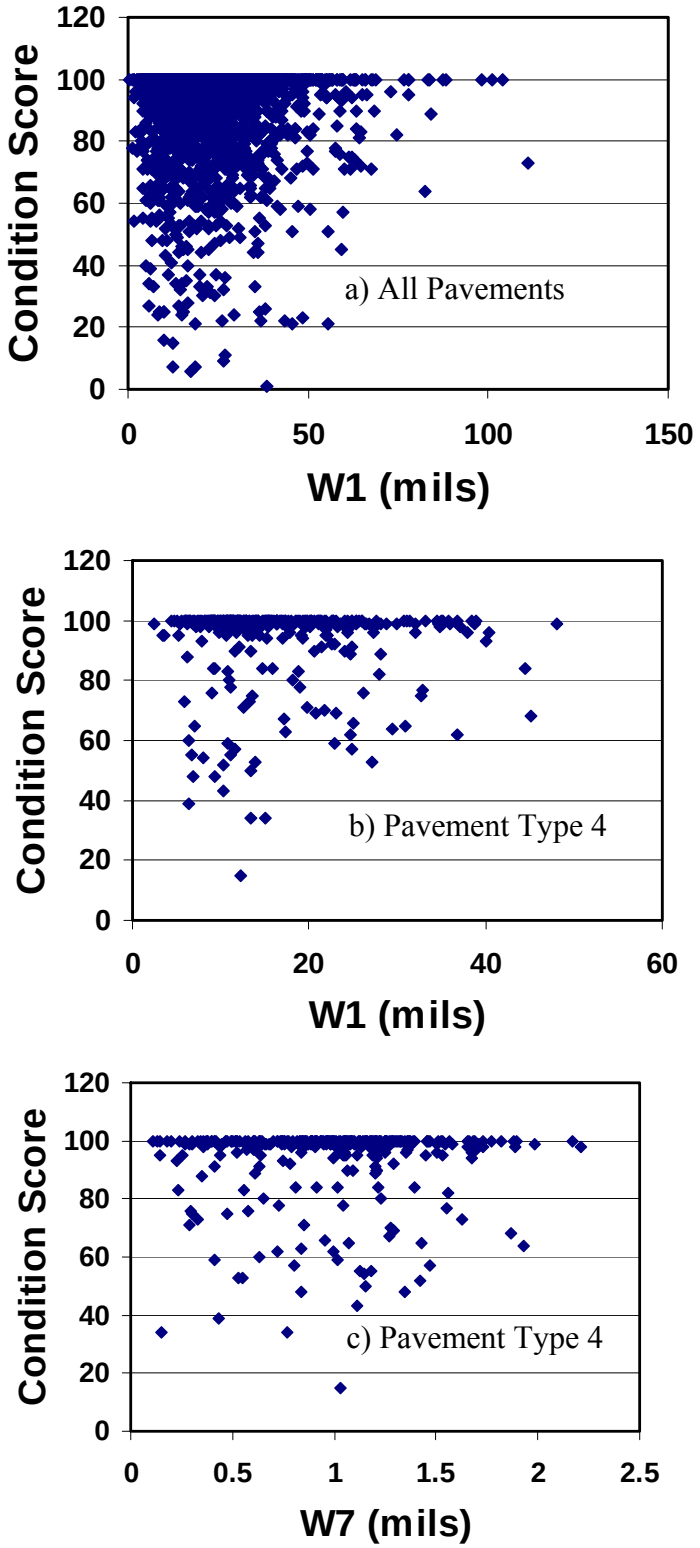

FIGURE 26 Condition Score vs. Deflection

These sets of values were used to compute the seven deflections and subsequently the SSI using traffic and rainfall factors of 1. Figures 27 through 31 shows the SSI plotted against W1 for each pavement type. The plots of SSI against SCI and W7 are included in Appendix H.

The results from these sets of data are quite similar to those from the Dallas area. Once again, while higher deflection values are associated with lower structural strength scores, there is no predictable relationship that can be used to assess the structural condition from only one of these deflection parameters. The SSI is most sensitive to the center deflection W1 and least sensitive to W7. This is consistent with known theories which state that W1 is more closely related to the top layer of the pavement structure while W7 is mostly dependent on the deeper layers such as the subgrade.

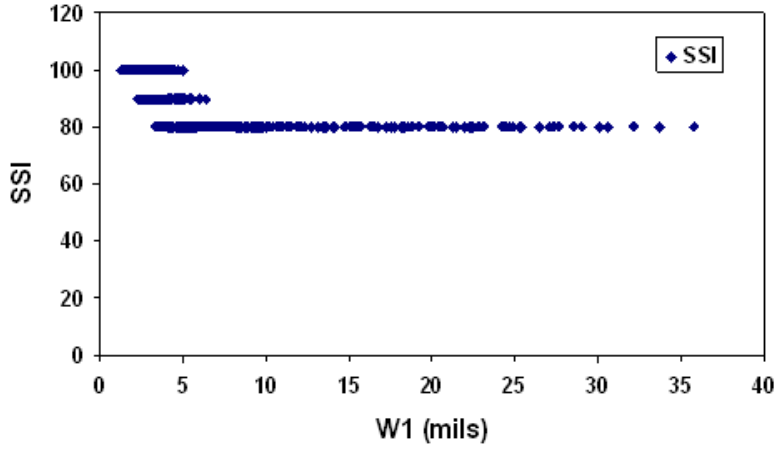

FIGURE 27 SSI Compared with W1 for Pavement Types 1, 2 and 3

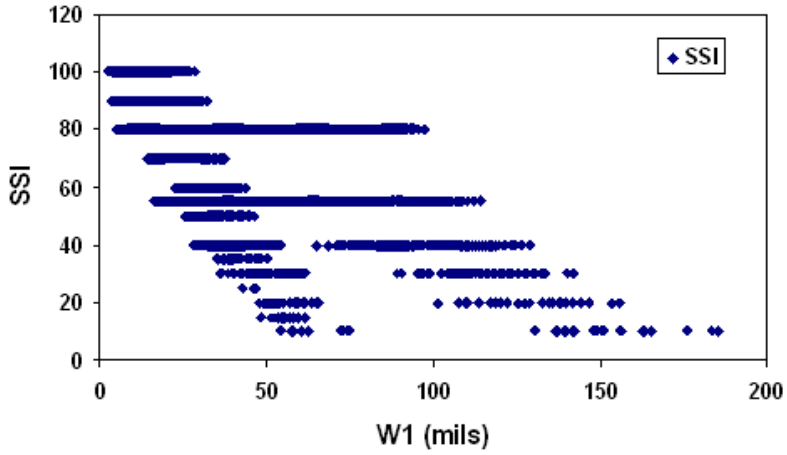

FIGURE 28 SSI Compared with W1 for Pavement Type 4

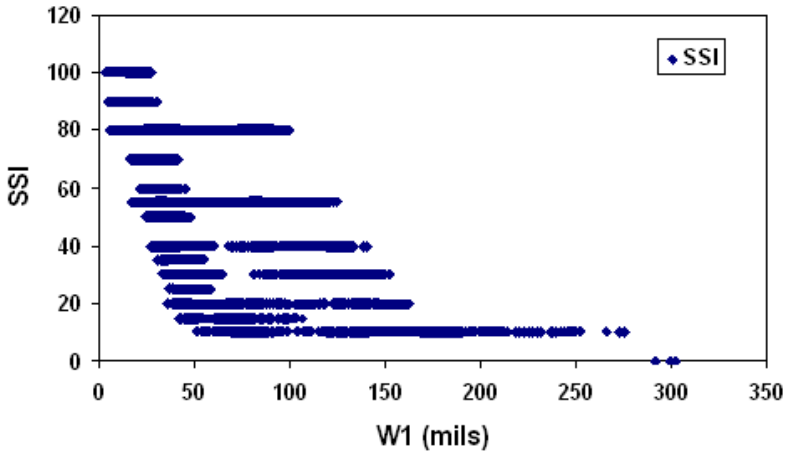

FIGURE 29 SSI Compared with W1 for Pavement Type 5

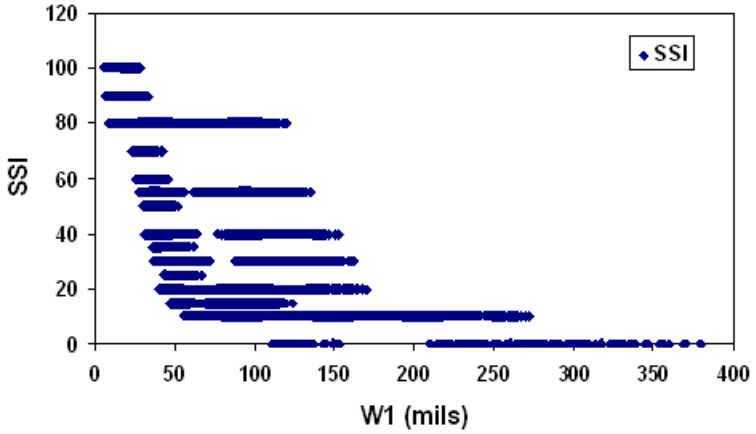

FIGURE 30 SSI Compared with W1 for Pavement Type 6

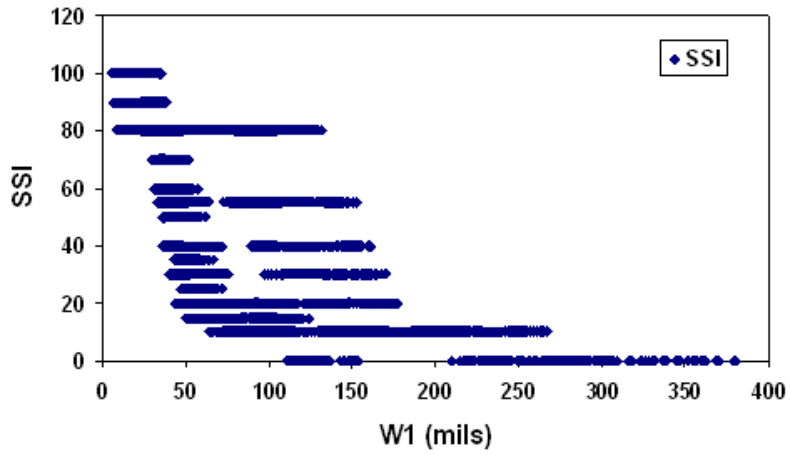

FIGURE 31 SSI Compared with W1 for Pavement Type 10

According to Zhang, et. al. (2003), the current SSI is not sensitive enough to discriminate one highway from another even if there is a significant difference in the structural capacity between the two highways. In other words, the SSI cannot be effectively used at the network level to identify pavement sections with structural deficiencies. Zhang identified five different methods to evaluate the structural conditions using FWD deflections. These alternative methods are discussed in the next chapter.

CHAPTER 4 NEW METHODS FOR STRUCTURAL EVALAUTIONS

Zhang, et. al. (2003) identified five alternative methods that require different types of input to provide different indices to assess the structural condition of pavements. They have also attempted to validate these methods by relating their indices to the pavement structural conditions. The information for each of the methods is briefly discussed here. Readers are encouraged to review Zhang et al. (2003) for an in-depth understanding of the methods.

4.1 Method I – The Modulus and Deflection Ratios

The first step in this method is to estimate the subgrade modulus using Equation 4.1. The ratio of the pavement modulus to the subgrade modulus is then calculated using Equation 4.2. The constants in the regression equation depend on the total thickness of the pavement, as summarized in Table 5. The existing pavement modulus is then obtained by multiplying the ratio obtained in the last step (Equation 4.2) by the subgrade modulus (Equation 4.1), as shown in Equation 4.3. The design pavement modulus is then estimated using Equation 4.4. Finally the design pavement modulus is compared with the existing pavement modulus to determine structural adequacy.

$$E_{subgrade} = 0.24 \times \frac{P}{W7 \times 72} \tag{4.1}$$

$$\frac{E_P}{E_{subgrade}} = A \times \left(\frac{W7}{W1}\right)^{\frac{5}{2}} + B \times \left(\frac{W7}{W1}\right)^{\frac{4}{2}} + C \times \left(\frac{W7}{W1}\right)^{\frac{3}{2}} + D \times \left(\frac{W7}{W1}\right)^{\frac{2}{2}} + E \times \left(\frac{W7}{W1}\right)^{\frac{1}{2}} \tag{4.2}$$

TABLE 8. Constants for Regression Equation 6.2

Pavement Thickness (in)	A	B	C	D	E
12	-1693.4	3035.9	756.71	100.68	-2.5058
15	847.37	-167.85	251.45	-24.01	3.081
18	672.02	-245.62	207.83	5.9825	1.7989
21	516.94	214.46	159.56	6.143	1.0826
24	421.55	-192.16	131.78	12.33	0.7697
27	356.26	172.52	112.71	16.095	0.6075
30	311.37	-158.63	100.05	18.393	0.5278

$$E_p = \left(\frac{E_p}{E_{subgrade}} \right) \times E_{subgrade} \quad (4.3)$$

$$E_{design} = \frac{(500 \times D_{ACP} + 60 \times D_{FB} + 45 \times D_{LT})}{D_{Total}} \quad (4.4)$$

$E_{subgrade}$ = the backcalculated subgrade modulus in psi.
P = the applied load in pounds.
W7 = the deflection at sensor 7 in inches.
E_{design} = the design modulus of the pavement in ksi.
D_{ACP} = the depth of the asphalt pavement layer in inches.
D_{FB} = the depth of the flexible base layer in inches.
D_{LT} = the depth of the lime treated subbase layer in inches.
D_{TOTAL} = the total depth of the pavement layers in inches.

According to the TxDOT internal analysis, this method is sensitive enough to differentiate pavements that need additional structural capacity from those that do not. Certain improvements were needed for the method to be implemented for network-level applications (Zhang, 2003).

4.2 Method II – The Modified Modulus and Deflection Ratios

This method is the modified version of the previous method. The first step in this method is to estimate the subgrade modulus using Equation 4.1. The ratio of the pavement modulus to the subgrade modulus is computed using a series of regression equation similar to the one presented above (for example Equation 4.5 for 21-in. pavement). The existing pavement modulus is computed using this ratio, as in the previous method (Equation 4.3). The required design pavement modulus ($E_{required}$) for the existing subgrade and the expected future ESALs is computed using Equation 4.6. The existing pavement modulus is compared with the design pavement modulus to determine the structural adequacy.

$$E_P / E_{subgrade} = -1.8497 + 29.952 * \left(W_7 / W_1 \right)^{0.5} - 124.62 * \left(W_7 / W_1 \right) + 331.3 * \left(W_7 / W_1 \right)^{1.5} \quad (4.5)$$

$$E_{required} = 6.06 \times 10^6 \times \frac{(ESAL)^{0.307}}{(E_{subgrade})^{1.6881}} \quad (4.6)$$

Zhang et al. suggest using a confidence interval to estimate the requirements for pavement strengthening. The main drawback of this modified method is that it does not relate to the structural number value used in the pavement design.

4.3 Method III – The Method Using Structural Number

In this method, the subgrade modulus, the ratio of the pavement modulus to the subgrade modulus, and the pavement modulus are computed as in the previous two methods. Thereafter the existing structural number (SN_{eff}) is estimated using Equation 4.7.

$$SN_{eff} = 0.0045 \times D \times E_p^{0.333} \quad (4.7)$$

D = the total thickness of the pavement layers.
E_p = the existing pavement modulus of all layers above the subgrade.

The estimated structural number serves as an indicator of structural condition. In order to evaluate the pavement's structural adequacy, the required SN is compared with the effective SN. The structural deficiency can be characterized as the difference between the required and the effective SN.

4.4 Method IV – An Alternative Method for Determining SN from FWD Data

This method is based on the idea that the surface deflections measured at an offset of 1.5 times the pavement thickness originate entirely in the subgrade. To use this method, the Structural Index of Pavement (SIP) is calculated using Equation 4.8. The structural number is then computed using this value of SIP and the total pavement thickness from Equation 4.9.

$$SIP = W_1 - W_{1.5Hp} \quad (4.8)$$

$$SN_{eff} = k1 \times SIP^{k2} \times Hp^{k3} \quad (4.9)$$

SIP = Structural Index of Pavement in microns.
W_1 = normalized FWD center deflection in microns.
H_P = total pavement thickness (excluding stabilized subgrade) in mm.
$W_{1.5Hp}$ = surface deflection measured at offset of 1.5 times of H_p under a standard 9 kips FWD load in microns.
SN_{eff} = existing pavement structural number in inches.
k1, k2, k3 = regression coefficients listed in Table 6.

TABLE 9. Regression Coefficients for Method IV

Surface Type	k1	k2	k3
Surface Seals	0.1165	-0.3248	0.8241
Asphalt Concrete	0.4728	-0.4810	0.7581

To calculate the deflection at an offset of 1.5 times the total pavement thickness ($W_{1.5\ Hp}$), the deflections from fixed sensor positions can be interpolated as per Equation 4.10:

$$D_X = \left[\frac{(R_X - R_B)\times(R_X - R_C)}{(R_A - R_B)\times(R_A - R_C)}\right]\times D_A + \left[\frac{(R_X . R_A)\times(R_X . R_C)}{(R_B . R_A)\times(R_B . R_C)}\right]\times D_B + \left[\frac{(R_X - R_A)\times(R_X - R_B)}{(R_C - . R_A)\times(R_C - R_B)}\right]\times D_C$$

… (4.10)

D_X = deflection at offset of R_X.
D_i = deflection at sensor i.
R_i = offset of Sensor i.
i = A, B, C, the three closest sensors to Point X.
X = point for which deflection is determined.

The method proposes to estimate the required Structural Number (SN) using Table 7 for known subgrade moduli. The required SN is estimated based on future traffic predictions. If the subgrade modulus (M_r) is unknown, Zhang et al. suggest multiplying the subgrade modulus obtained from Equation 4.1 by 0.33. The ratio of SN_{eff} to SN_{req} is then used to estimate the structural condition index (SCI). A value of one or more would indicate that the pavement is in excellent structural condition, while values significantly less than one would indicate a structurally weak pavement. This method has been currently proposed to be implemented for structural integrity evaluation of pavements by TxDOT.

TABLE 10. Required SN for Different Categories of Accumulated ESAL Traffic and M_r (Zang, et al. 2003)

			20-Year Accumulated Traffic in ESALs					
			Category	**Very Low**	**Low**	**Medium**	**High**	**Very High**
			Range	50,000 – 945,000	945,000 – 1,687,000	1,687,000 – 2,430,000	2,430,000 – 3,172,000	3,172,000 – 50,000,000
M_r (psi)	**Category**	Range	Average	498,000	1,316,000	2,059,000	2,801,000	26,586,000
	Low	1,000 – 5,400	3,200	4.3	5.1	5.3	5.6	7.1
	Medium	5,400 – 7,500	6,400	3.5	3.9	4.2	4.3	6.0
	High	7,500 – 40,000	24,000	2.3	2.6	2.8	2.8	3.9

4.5 Method V – Simple Approach to Estimate the SN of Pavements

This method uses regression equations to directly compute the structural number from the FWD deflections. Different equations for pavements having a stabilized base layer (Equation 4.11) and pavements having granular base and subbase layers (Equation 4.12) are proposed.

$$SN = 6.45 - 3.676 \times \log(D_0) + 3.727 \times \log(D_{1500}) \quad (4.11)$$

$$SN = 6.96 - 0.196 \times [(AREA) - 450 \times (D_{1200})]^{0.5} \quad (4.12)$$

$$D_{1500} = D_{600} - 3 \times D_{900} + 3 \times D_{1200} \quad (4.13)$$

$$AREA = 25.48 \times [4 \times D_0 + 6 \times D_{200} + 5 \times D_{300} + D_{450}] \quad (4.14)$$

SN = structural number.
D_0 = temperature corrected center deflection in microns.
D_{1500} = deflection at an offset of 1500 mm (60 in).
D_{600} = deflection at an offset of 600 mm (24 in).
D_{900} = deflection at an offset of 900 mm (36 in).
D_{1200} = deflection at an offset of 1200 mm (48 in).
D200 = deflection at an offset of 200 mm (8 in).
D300 = deflection at an offset of 300 mm (12 in).
D450 = deflection at an offset of 450 mm (18 in).

The structural number is then used to determine the structural condition of the pavement.

4.6 Review of the Methods

The five methods discussed above have different requirements and unique advantages and disadvantages. The requirements are summarized in Table 8. Each method requires certain pavement parameters beyond a single deflection. The total thickness of the pavement or the thickness of the individual pavement layers is also required. Each method was evaluated by Zang et al. (2003) and problems and benefit of each method was also discussed in the report. The information from the report is reproduced here. However, readers are encouraged to read the report for better understanding of each methods limitations and benefits.

According to the TxDOT internal analysis, the Method I is sensitive enough to differentiate pavements that need additional structural capacity from those that do not. However, certain improvements are needed for the method to be implemented for network-level applications. These improvements include: a) simplification is needed to reduce the fifth degree polynomial equations; b) the layer thicknesses required for determining the design pavement modulus are not currently available, c) a ratio of the existing pavement modulus to the required design pavement modulus is needed to develop threshold values that can be used to identify pavements requiring additional strengthening.

The Method II is modified version of the Method I and has several advantages over the original method. It is easier to calculate and it takes into consideration the required design modulus for the ESALs and environmental conditions in Method II. The new ratio can be directly used to identify pavement sections requiring strengthening. As in the original method, the modified method can calculate the minimum values of deflection ratios to be used in identifying the

TABLE 11. Summary of Method Requirements

Method	W7	W1	Total Thickness	Traffic Load (ESAL)	Other Deflections (W2, W6)	Individual Layer Thicknesses
I	✓	✓	✓			✓
II	✓	✓	✓	✓		
III	✓	✓	✓			
IV	✓	✓	✓	✓	✓	
V	✓	✓		✓	✓	

potential weakness of the base layer. The main drawback of this modified method (Method II) is that it does not relate to the SN value used in pavement design.

The Method III uses effective structural number (SN_{eff}) to characterize the adequacy of a pavement which is not sufficient. To evaluate the pavement's structural adequacy, one needs the required SN. With the required and the effective SN, the structural deficiency can be characterized as the difference between the required and the effective SN.

The Method IV overcomes the problems of Method III by using a procedure for calculating the Structural Number (SN) from the deflection data using methodology based on the "two-third" rule. This process is fairly simple and easily implementable in the PMIS.

During the preliminary analysis, the estimates of SN from Method V did not fall under the normal range of the SN values. The method yielded negative or unrealistically big values of the SN, such as 100 or more. Consequently, the conclusion from the preliminary analysis was that Method V was unsuitable for further evaluation.

Although TxDOT is in the process of implementing Method IV for PMIS (based on Zang et al., 2003 evaluation), all five methods are evaluated in this study because some of the methods

include only two deflection measurements, which could be typically available with current devices.

CHAPTER 5 EVALUATION OF ALTERNATIVE METHODS

In this chapter we investigated the indices proposed by Zhang, et. al. (2003) in an attempt to discover if any of them is better correlated with W1. Even though it is not the goal of this project to completely characterize the pavement structure, it seems likely that more than one deflection value may be needed to provide an indication of the structural capacity of the pavement. Therefore we also investigate if a better correlation may be obtained by using a combination of two deflections.

5.1 Preliminary Evaluation of Curve Fit Method

To evaluate the five new methods proposed by Zhang, et. al. (2003), a preliminary set of data was simulated. The values used for the structural parameters are listed in Table 12. The simulation generated 43,200 data points. Initially, the data points were not divided according to pavement types. The SCI (or SN in case of Method III) was computed with each of the 5 methods and was plotted against W1 as shown in Figure 32. The graph show a lot of scatter, some more so than the others. It is also evident that the relationships are not linear.

TABLE 12. Values of Structural Parameters Used in the Initial Investigation

Parameter	Minimum	Maximum	Step
AC Modulus (ksi)	50	750	50
AC Thickness (in)	6	12	2
Base Modulus (ksi)	25	200	25
Base Thickness (in)	4	18	4, except 2 for last step
Subgrade Modulus (ksi)	1	25	5, except for first step
Subgrade Thickness (in.)	200, 500, 720		

Different types of curves were fitted to the data in an attempt to quantify the relationship between W1 and the computed indices. Thirty one different relationships were attempted on the SCI produced by Method I ranging from linear and quadratic to exponential, rational, Gaussian, power and sum of sine series using MATLAB software. Out of thirty one relationships, the quadratic, cubic, exponential, and sum of two exponentials nonlinear relationships were identified to be the ones that provided maximum coefficient of determination (R^2) and minimum sum of squared errors (SSE). Therefore, only these four relationships are further discussed.

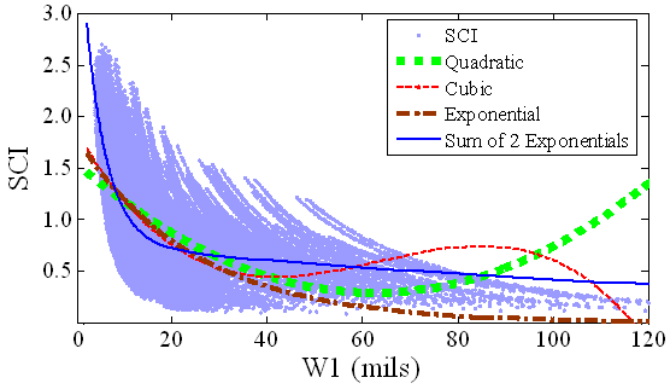

a) Method I

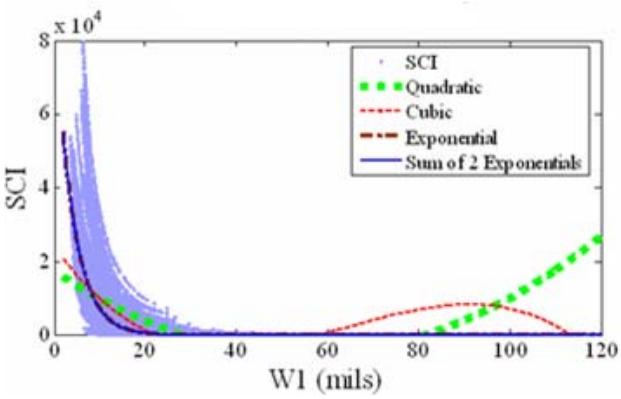

b) Method II

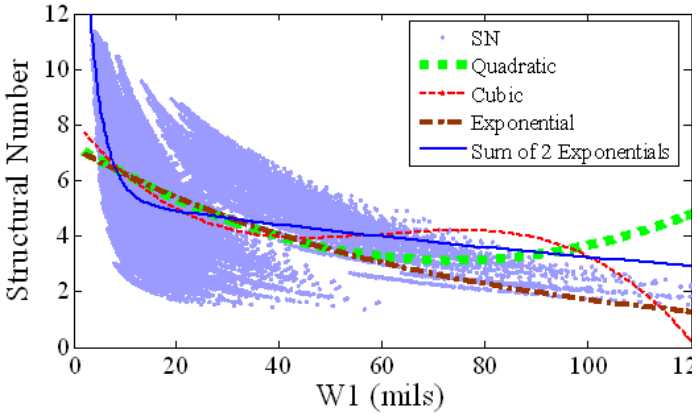

c) Method III

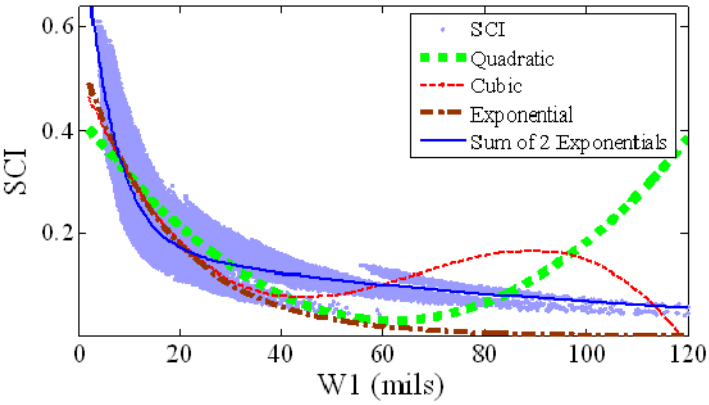

d) Method IV

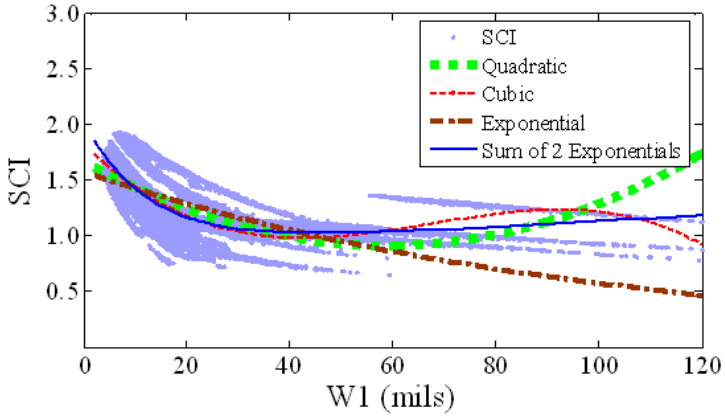

e) Method V

FIGURE 32 Nonlinear Curve Fits for Pavement Type 4 and for all Methods

The relevant equations for these relationships are shown in Equations 5.1 through 5.4 where A, B, C, and D are regression coefficients.

$$\text{Quadratic:} \quad Y = AX^2 + BX + C \tag{5.1}$$

$$\text{Cubic:} \quad Y = AX^3 + BX^2 + CX + D \tag{5.2}$$

$$\text{Exponential:} \quad Y = Ae^{BX} \tag{5.3}$$

$$\text{Sum of Two Exponentials:} \quad Y = Ae^{BX} + Ce^{DX} \tag{5.4}$$

The curve fits to the preliminary set of data are shown in Figure 31 and the R^2 values and the sum of squared errors (SSE) are tabulated in Table 13. The selected nonlinear relationships fitted the data reasonably well at smaller deflections, but diverged rapidly at higher deflections (Figure 32). The R^2 value ranged from 0.26 to 0.86 while SSE varied from $0.5*10^{03}$ to $2.6*10^{12}$. The data presented in Table 10 suggests that none of the relationships estimate SCI very well for the Method II (R^2 of less than 0.6 and SSE of more than $1.7*10^{12}$). However, the sum of two exponential relationship provided a R^2 value of 0.86 and SSE of $0.5*10^{03}$ for Method IV, indicating it to be a good fit. The relationships for the remaining methods either provided lower R^2 values of very high SSE values. This suggests that Method IV is the most promising method to be pursued for further investigation.

TABLE 13. Regression Coefficients for the 5 Methods

Method	Quadratic		Cubic		Exponential		Sum of Two Exponentials	
	R^2	SSE	R^2	SSE	R^2	SSE	R^2	SSE
I	0.36	$6.5*10^{03}$	0.43	$5.8*10^{03}$	0.39	$6.2*10^{03}$	0.52	$4.8*10^{03}$
II	0.33	$2.6*10^{12}$	0.42	$2.3*10^{12}$	0.56	$1.7*10^{12}$	0.56	$1.7*10^{12}$
III	0.26	$1.0*10^{05}$	0.31	$9.7*10^{04}$	0.26	$1.0*10^{05}$	0.42	$8.1*10^{04}$
IV	0.68	$1.1*10^{03}$	0.77	$0.8*10^{03}$	0.76	$0.8*10^{03}$	0.86	$0.5*10^{03}$
V	0.45	$1.6*10^{03}$	0.52	$1.4*10^{03}$	0.37	$1.9*10^{03}$	0.53	$1.4*10^{03}$

5.2 Further Investigation of Curve Fit for Data Analyzed Using Method IV

To further evaluate the feasibility of using Method IV, the data was simulated for different pavements types and was stored in five different databases. The selected pavement properties for generation of database are shown in Table 14. Again the data was selected based on the properties identified by Murphy (1998). The simulated data and corresponding best-fit curves are shown in Figure 33 while the results of the goodness of the fits are summarized in Table 15. A significant spread in the data is observed for each pavement type and none of the equations used provided a reasonably good fit for all the pavement types.

TABLE 14. Ranges of Values Used for Simulation of Different Pavement Types

	Pavement Types 1, 2 and 3	Pavement Type 4	Pavement Type 5	Pavement Type 6	Pavement Type 10
Surface Thickness (in)	10, 11, 12, 13, 14	6, 8, 10, 12	2.5, 4, 5.5	1, 1.5, 2	1, 2
Surface Modulus (ksi)	2000, 3000, 4000, 5000, 6000, 8000	50, 100, 200, 300, 400, 500, 600, 750, 1000, 1250	50, 100, 200, 300, 400, 500, 600, 750, 1000, 1250	50, 100, 200, 300, 400, 500, 600, 750, 1000, 1250	50, 100, 150, 200, 300, 400, 500, 600, 750, 1000, 1250
Base Thickness (in)	Not Applicable	6, 10, 14, 18	6, 10, 14, 18	6, 10, 14, 18	6, 10, 14, 18
Base Modulus (ksi)	Not Applicable	5, 10, 20, 30, 40, 80, 100, 200	5, 10, 20, 30, 40, 80, 100, 200	5, 10, 20, 30, 40, 80, 100, 200	5, 10, 20, 30, 40, 80, 100, 200
Subgrade Thickness (in)	250, 500, 700	250, 500, 700	250, 500, 700	250, 500, 700	250, 500, 700
Subgrade Modulus (ksi)	1, 5, 10, 15, 20, 25, 30, 40	1, 5, 10, 15, 20, 25, 30, 40	1, 5, 10, 15, 20, 25, 30, 40	1, 5, 10, 15, 20, 25, 30, 40	1, 5, 10, 15, 20, 25, 30, 40

TABLE 15. Adjusted R^2 and Sum of Squared Errors (SSE) Values

Fit Type	Statistical Parameter	Type 1, 2 & 3	Type 4	Type 5	Type 6	Type 10
Quadratic	**R^2**	0.22	0.43	0.43	0.46	0.37
	SSE	21.56	334.30	111.4	77.04	8.85
Cubic	**R^2**	0.32	0.52	0.51	0.54	0.43
	SSE	18.70	284.60	96.04	65.55	8.03
Exponential	**R^2**	0.20	0.45	0.46	0.51	0.37
	SSE	22.98	322.80	105.50	70.51	8.83
Sum of Two Exponentials	**R^2**	0.20	0.45	0.67	0.69	0.37
	SSE	21.98	322.80	65.38	45.11	8.83

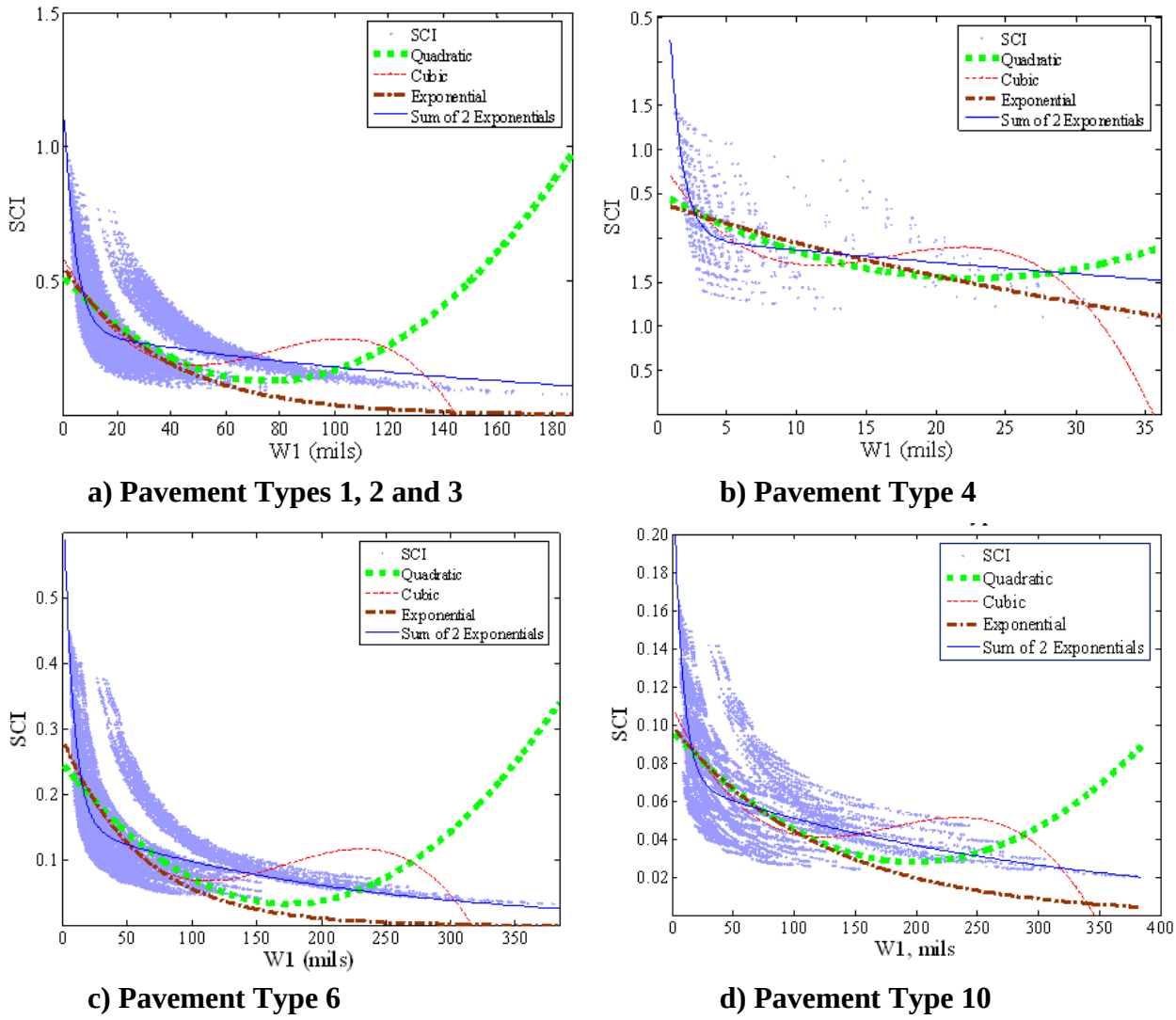

FIGURE 33 Nonlinear Curve Fits for Various Types of Pavements

The R^2 values ranged from 0.20 to 0.69 for various pavement types while SSE values varied from 8 to 350 depending on pavement types and nonlinear relationships. The data presented in Table 15 suggests that the sum of two exponentials provided best estimate for Pavement Types 5 and 6 (R^2 values of 0.67 and 0.69 with SSE values of less than 70). However, the R^2 values decreased or SSE values increased for other pavement types. The R^2 and SSE values did not change significantly for Pavement Type 10 for all of the nonlinear regression relationships. Therefore, the results suggest that the nonlinear relationships do not provide a good estimate of the structural condition of the evaluated pavement structure.

In addition, attempts were also made to develop a relationship between the SCI or SN_{eff} and two deflections (W1/W7 or W1-W2, etc.) but a suitable relationship could not be found. The plots generated for this activity are included in Appendix I.

5.3 Cut-Off Method

One of the ways to evaluate the condition of a pavement structure is to select an acceptable deflection for a specific pavement type. For example, a deflection of less than 4 mils may be considered structurally sound for pavement Types 1, 2 and 3. On the other hand, more than 10 mils deflection may be considered to be a weak pavement. To evaluate this type of criterion, the pavements were selected to be good (strong) or bad (weak) based on the moduli of the layers. The assumption was that if one or more layer(s) had lower than desirable modulus value then the pavement is categorized as bad (weak) pavement section and vice versa. For instance, a pavement is considered weak if PCC modulus is less than or equal to 3,000 ksi or subgrade modulus is less than 15 ksi or both for Pavement Types 1, 2 and 3. The selected pavement types and their properties are included in Table 16. Also, the moduli considered to represent a bad (weak) pavement, for each pavement type, are italicized and underlined. In addition, the simulated data was analyzed using Methods I through IV.

TABLE 16. Ranges of Values Used for Simulation of for Cut-Off Method

Pavement Layer Properties	Pavement Types 1, 2 and 3	Pavement Type 4	Pavement Type 5	Pavement Type 6	Pavement Type 10
Surface Thickness (in)	10, 11, 12, 13, 14	6, 8, 10, 12	2.5, 4, 5.5	1, 1.5, 2	1, 2
Surface Modulus (ksi)	*2000*, *3000*, 4000, 5000, 6000, 8000	50, 100, 200, 300, 400, 500, 600, 750, 1000, 1250	*50*, *100*, *200*, *300*, *400*, 500, 600, 750, 1000, 1250	*50*, *100*, *200*, *300*, *400*, 500, 600, 750, 1000, 1250	*50*, *100*, *150*, *200*, 300, 400, 500, 600, 750, 1000, 1250
Base Thickness (in)	Not Applicable	6, 10, 14, 18	6, 10, 14, 18	6, 10, 14, 18	6, 10, 14, 18
Base Modulus (ksi)	Not Applicable	*5*, *10*, *20*, *30*, 40, 80, 100, 200	*5*, *10*, *20*, *30*, 40, 80, 100, 200	*5*, *10*, *20*, *30*, 40, 80, 100, 200	*5*, *10*, *20*, *30*, 40, 80, 100, 200
Subgrade Thickness (in)	250, 500, 700	250, 500, 700	250, 500, 700	250, 500, 700	250, 500, 700
Subgrade Modulus (ksi)	*1*, *5*, *10*, *15*, 20, 25, 30, 40	*1*, *5*, *10*, *15*, 20, 25, 30, 40	*1*, *5*, *10*, *15*, 20, 25, 30, 40	*1*, *5*, *10*, *15*, 20, 25, 30, 40	*1*, *5*, *10*, *15*, 20, 25, 30, 40

A typical result for Pavement Type 4 analyzed using Method IV is shown in Figure 34. The simulated data is divided in good or bad pavement types depending on the modulus values. The data suggests that W1 deflection of greater than 12 mils is an indication of weak pavement. Similarly, an SCI value of less than 0.5 suggests that the pavement is weak. Therefore, it is possible to suggest that if the deflection value of more than 12 mils and SCI value of less than

0.5 is observed (for Pavement Type 4) or both than the pavement can be considered to be a weak pavement. The results for the remaining pavement types and methods are included in Appendix J and the selected cut-off values based on the SCI or SNeff and W1 are summarized in Table 17.

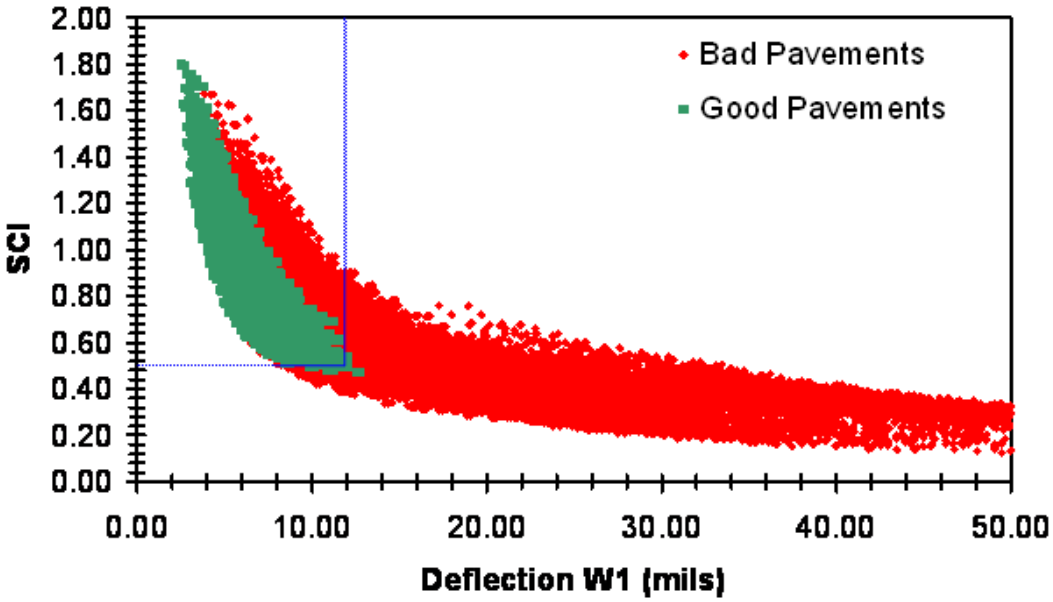

FIGURE 34 Typical Result for Method IV and Pavement Type 4

The cut-off values for W1 deflections as well as SCI or SNeff were selected in a manner that almost none of the strong pavements were considered to be weak pavements. Since W1 values remain the same regardless of analysis method, the selected W1 values are not method dependent. In other words, a W1 value of less than 4 mils is an indication of strong Pavement Types 1, 2, and 3 regardless of analysis method. Similarly, a W1 value of less than 25 mils is acceptable for thin AC pavements (Types 6, 7, 8, 9, and 10) while less than 12 mils are acceptable for Type 4 pavements for all type of methods. The values of SCI or SNeff are method dependent; therefore, these values did change depending on analysis method, as shown in Table 17. For example, a SCI value of less than 0.7 indicates a weak pavement (when data is analyzed using Method IV) while a SCI value of less than 4 indicates weak pavement for Pavement Type 4 (when data is analyzed using Method I or II).

The data presented in Figure 34 also suggests that a number of pavement sections with deflections less than 12 mils do contain weak layers. Since the selection of deflection levels (cut-off values) for each pavement type was such that the no good (strong) pavement can be identified as bad (weak) pavement, it was decided to identify the influence of changes in cut-off levels on reliability of the device. In other words, if the cut-off level for Pavement Type 4 is changed from 12 mils to 14 mils what influence it will have on the reliability of the device. To

evaluate the reliability, it was decided to identify false positive and false negatives as a criterion. A false positive indicates that the pavement is identified to be good when actually it is a bad pavement. A false negative indicates that the pavement is identified to be bad when actually it is a good pavement.

Another factor that can influence the reliability of the device is the accuracy of the sensor that measures deflection. For instance, if a deflection sensor is under predicting deflection by 10% (especially around the cut-off levels) then a pavement section can be identified as a good pavement when it is bad. Therefore, it was decided to identify the influence of sensor accuracy on the reliability using false positives and negatives as well.

To identify the influence of cut-off values on reliability, it was decided to change the cut-off values by ±5%, ±10%, ±15%, and ±20% for each pavement type. Similarly, the influence of accuracy was evaluated by changing the accuracy levels by ±5%, ±10%, and ±15%. A typical result for Pavement Type 4 analyzed using Method IV is shown in Table 18. The results are presented in terms of false positive or false negatives (both in numbers as well as in percentages). The influence of changes in cut-off values is shown in columns while the influence of deflection accuracy (W1) is shown in rows (W1 factors). A W1 factor of 1.00 indicates that the sensor is 100% accurate while a W1 factor of 0.85 suggests that the sensor is under predicting the deflections by 15%. Similarly, a cut-off value of 14.4 mils indicates the influence of changing the cut-off value by +20%.

TABLE 17. Cut-Off Values for Various Pavement Structures

Pavement Type		1, 2, and 3 (PCC)	4 (Thick AC)	5 (Inter. AC)	6, 7, 8, and 9 (Thin AC)	10 (Overlaid AC)
Method I	**Bad**	W1 > 4 Or SCI < 5.2	W1 > 12 Or SCI < 0.7	W1 > 20 Or SCI < 0.3	W1 > 25 Or SCI < 0.3	W1 > 25 Or SCI < 0.3
	Good	SCI > 5.2 and W1 < 4	SCI > 0.7 and W1 < 12	SCI > 0.3 and W1 < 20	SCI > 0.3 and W1 < 25	SCI > 0.3 and W1 < 25
Method II	**Bad**	W1 > 4 Or SCI < 80	W1 > 12 Or SCI < 4	W1 > 20 Or SCI < 4	W1 > 25 Or SCI < 2	W1 > 25 Or SCI < 2
	Good	SCI > 80 and W1 < 4	SCI > 4 and W1 < 12	SCI > 4 and W1 < 20	SCI > 2 and W1 < 25	SCI > 2 and W1 < 25
Method III	**Bad**	W1 > 4 Or SN Eff < 6	W1 > 12 Or SN Eff < 3	W1 > 20 Or SN Eff < 1.6	W1 > 25 Or SN Eff < 1.1	W1 > 25 Or SN Eff < 1
	Good	SN Eff > 6 and W1 < 4	SN Eff > 3 and W1 < 12	SN Eff > 1.6 and W1 < 20	SN Eff > 1.1 and W1 < 25	SN Eff > 1 and W1 < 25
Method IV	**Bad**	W1 > 4 or SCI < 1.3	W1 > 12 or SCI < 1.5	W1 > 20 or SCI < 0.4	W1 > 25 or SCI < 0.2	W1 > 25 or SCI < 0.2
	Good	SCI > 1.3 and W1 < 4	W1 < 12 and SCI > 0.5	W1 < 20 and SCI > 0.4	W1 < 25 and SCI > 0.2	W1 < 25 and SCI > 0.2

TABLE 18. False Positive and Negative for Pavement Type 4

W1 Factors		Cut-off Levels for W1									
			9.6	**10.2**	**10.8**	**11.4**	**12**	**12.6**	**13.2**	**13.8**	**14.4**
	0.85	False Positives	8254	9199	10132	10957	11705	12429	13142	13761	14384
		Percentage	26.9%	29.9%	33.0%	35.7%	38.1%	40.5%	42.8%	44.8%	46.8%
		False Negatives	146	83	48	24	12	5	2	0	0
		Percentage	0.5%	0.3%	0.2%	0.1%	0.0%	0.0%	0.0%	0.0%	0.0%
	0.9	False Positives	7331	8321	9199	10079	10868	11574	12288	12930	13550
		Percentage	23.9%	27.1%	29.9%	32.8%	35.4%	37.7%	40.0%	42.1%	44.1%
		False Negatives	229	142	83	50	29	13	6	3	0
		Percentage	0.7%	0.5%	0.3%	0.2%	0.1%	0.0%	0.0%	0.0%	0.0%
	0.95	False Positives	6497	7436	8380	9199	10025	10776	11470	12143	12769
		Percentage	21.1%	24.2%	27.3%	29.9%	32.6%	35.1%	37.3%	39.5%	41.6%
		False Negatives	340	221	138	83	50	31	15	7	3
		Percentage	1.1%	0.7%	0.4%	0.3%	0.2%	0.1%	0.0%	0.0%	0.0%
	1.00	False Positives	5733	6649	7526	8431	9199	9982	10692	11371	12008
		Percentage	18.7%	21.6%	24.5%	27.4%	29.9%	32.5%	34.8%	37.0%	39.1%
		False Negatives	472	319	213	134	83	52	32	16	8
		Percentage	1.5%	1.0%	0.7%	0.4%	0.3%	0.2%	0.1%	0.1%	0.0%
	1.05	False Positives	5022	5901	6776	7613	8462	9199	9957	10628	11274
		Percentage	16.3%	19.2%	22.1%	24.8%	27.5%	29.9%	32.4%	34.6%	36.7%
		False Negatives	621	434	298	201	131	83	54	33	17
		Percentage	2.0%	1.4%	1.0%	0.7%	0.4%	0.3%	0.2%	0.1%	0.1%
	1.1	False Positives	4413	5229	6066	6893	7679	8489	9199	9915	10560
		Percentage	14.4%	17.0%	19.7%	22.4%	25.0%	27.6%	29.9%	32.3%	34.4%
		False Negatives	795	566	403	282	193	128	83	55	34
		Percentage	2.6%	1.8%	1.3%	0.9%	0.6%	0.4%	0.3%	0.2%	0.1%
	1.15	False Positives	3813	4620	5414	6206	7006	7750	8525	9199	9889
		Percentage	12.4%	15.0%	17.6%	20.2%	22.8%	25.2%	27.8%	29.9%	32.2%
		False Negatives	984	723	525	377	269	184	128	83	55
		Percentage	3.2%	2.4%	1.7%	1.2%	0.9%	0.6%	0.4%	0.3%	0.2%

The cut-off value of 12 mils and W1 factor 1.00 indicates that only 0.3% of the time a pavement will be identified as bad (false negative) when the pavement is actually good. However, the same cut-off value will identify 30% of the time a pavement to be a good (false positive) when actually it is not. If cut-off value is increased to 14.4 mils (+20% of 12 mils) then the false positives will increase to 40% while false negatives will decrease to almost 0%. Similarly, a decrease in cut-off value to 9.6 mils (-20% of 12 mils) will decrease false positives to 19% but will increase false negatives to 1.5%. Although 1.5% seems small, the selected data set for this evaluation is 20,480 and even 1.5% translates to 472 pavement types being identified as bad pavements while they are good pavements.

On the other hand if the deflection sensor losses its accuracy by -10% (under prediction) then false positives increase to 35% from 30% for 12 mils as a cut-off level. If the deflection sensor losses its accuracy by +10% (over prediction) then false positives decrease to 23% while false negatives increase to 0.9% from 0.3%.

The best cut-off value identified with this analysis is for cut-off value of 9.6 (20% less of 12 mils) and the sensor is over predicting by 15% (W1 factor =1.15). At this level, the percentage of false positive is close to 12% and false negatives are 3.2%. However, the selected data set for this evaluation is 20,480 and even 3.2% translates to 984 pavement types being identified as bad pavements while they are good pavements. Similar, trends were observed for various analysis methods and pavement types and are included in Appendix L for reference purposes. The reliability analysis suggests that the W1 deflection alone is not sufficient to discriminate between strong and weak pavements.

Although various other methods to identify reliability of the devices were performed, the data indicated that one or two deflection levels are not sufficient to identify the structural integrity of the pavements within the state of Texas. Since none of the devices had more than one deflection values, it is not feasible to use these devices to reliably use these devices to identify pavements structural integrity.

Recently, one of the devices (HSD) has been modified to increase number of sensors to provide more than one velocity values which has the feasibility of implementation within the state of Texas and an update on the device has been included in the next chapter. In addition, RWD device has been evaluated by various other agencies and a brief update has been also included in the next chapter.

CHAPTER 6 UPDATE ON THE DEVICES

After the initial evaluation and survey of the devices, there are some new developments in the area of continuous deflection testing. The latest information gathered about the devices is included in this chapter. Since the further developments have been reported only for two devices (Rolling Wheel Deflectometer and High Speed Deflectograph), an update on these two devices is included in here.

6.1.1 Rolling Wheel Deflectometer (RWD)

An article on the update of RWD has been issued by Thomas Van of FHWA in the March issue of Focus Magazine. The article is reproduced here for reference purposes and can be accessed at the website: http://www.tfhrc.gov/focus/mar06/05.htm.

Now providing a high-speed alternative for evaluating highway pavements is the Federal Highway Administration's (FHWA) new Rolling Wheel Deflectometer (RWD). The RWD is a specially designed tractor-trailer with laser measuring devices mounted on a beam under the trailer and a computerized data collection system contained in the cab. The device can measure pavement deflections while traveling at highway speeds of up to 100 km/hr (70 mi/hr). Data can be collected on 320 to 480 km (200 to 300 mi) of roadway per day, usually without the need for traffic control vehicles. "The primary use for the RWD is to scan roadways for areas with high and variable deflections. These areas would then be targeted for more detailed inspection and testing using a falling weight deflectometer, coring, or other types of testing," says Thomas Van of FHWA. "With an RWD, agencies can concentrate resources on those areas most needing attention."

During the past year, FHWA has tested the RWD in Indiana, Kentucky, Minnesota, New Jersey, Ohio, Virginia, and West Virginia. These tests were designed to familiarize State departments of transportation and others with the RWD. FHWA's review of the test data to date has confirmed the original design criteria for the device. "Comparison of the RWD data with that from falling weight deflectometers has also been remarkably good," says Van. In addition to the State demonstrations, testing has been conducted on the entire length of the Natchez Trace Parkway, which runs through Alabama, Mississippi, and Tennessee, and at the National Center for Asphalt Technology test facility in Alabama, the Minnesota Road Research Project facility in Minnesota, and the Smart Road in Virginia. "Each testing program had unique objectives, and each agency has different plans for using the RWD data," says Van. New Jersey, for example, is considering using the data in conjunction with its pavement management system (PMS), while Minnesota is looking at using it to identify seasonal load restrictions on its roadways.

"We are now working to identify ways that RWD information can be effectively used in a PMS and to develop an analytical process to link the deflections to remaining service life and other pavement performance measures," notes Van. The goal of these efforts is to demonstrate that the RWD is a cost-effective tool that State transportation departments and others can use to help manage highway pavements. FHWA will continue testing and demonstrating the RWD this year, including tests planned for California, Iowa, and Kansas.

In addition, Indiana DOT has proposed that at the equivalent temperature of 68 °F and load levels of 9 kips, the deflection (in mils) levels should as per the Table 15. As the data in Table 15 suggests that any increase in deflection levels of more than 10 mils makes it a poor pavement indicating that the interstate needs closer scrutiny. The only problem with this approach is that the one deflection level is not enough (Chapter Five) to identify strong or weak pavements.

TABLE 19. Approach Proposed by Indiana Dot for RWD

Condition	Interstate Traffic > 30 Million EASLs	Heavy Traffic 10- 30 Million EASLs	Medium Traffic 3-10 Million EASLs	Light Traffic <3 Million EASLs
Excellent	<4	<5	<6	<8
Very Good	4-6	5-7	6-8	8-10
Good	6-8	7-9	8-10	10-12
Fair	8-10	9-11	10-12	12-14
Poor	>10	>11	>12	>14

6.2 High Speed Deflectograph (HSD)

There are some significant developments in the device to better predict bearing capacity of the pavements. The device uses laser sensors based on the Doppler technique to measure the deflection velocity of the road surface (a discussion on the sensor is included in Appendix D). The Laboratoire Central des Ponts et Chaussées (LCPC), Danish Road Institute (DRI) and Greenwood Engineering performed the assessment of the HSD prototype in the north of France in October 2003. The results of the assessment have been presented by Simonin et al. (2005) during Bearing Capacity of Road, Railways and Airfields (BCRA) conference at Trondheim in June 2005. Based on the experience from this assessment, the following developments were recommended:

- Four Doppler sensors instead of two
- Climate controlled environment for the equipment

- Improved design of the stiff beam with low susceptibility to changes in temperature and narrowing of the range of velocities measured
- Suspension system for protecting the electronics against shock
- New gyros with increased accuracy
- Electro-hydraulic system for shorter calibration procedure
- Special hub between the twin wheels to allow measurements to take place close to the center of the load (100 mm)
- The integration of a set of measurements obtained with several Doppler sensors to calculate a deflection basin, as the designers of the HSD propose it, to process the measurements with existing methods like the Surface Curvature Index (SCI);
- The direct interpretation of the slope of the tangent, as the technical network of the LCPC does for the measurement of the radius of curvature with the inclinometer.

In addition, the HSD was also evaluated by Transportation Research Laboratory (TRL) of United Kingdom (UK) along with Swedish RDT. Although report has been published yet, the personal conversation with Dr. Brian Ferne (representative of TRL) indicated that the initial assessment of HSD was successful but needed some modifications to improve the viability of the device.

Based on these two evaluation, Greenwood Engineering has modified the device and the new consists of four sensors. The sensors are placed at 4 in. (100 mm), 8 in. (200 mm) and 12 in. (300 mm) in front of the moving load. The remaining sensor is placed outside the deflection bowl as a reference. Because the deflection velocity is zero at the center of the load, a sensor has not been placed there. The slope of the deflection bowl can be calculated where the sensors are positioned since the driving speed is known. Therefore, the situation is somewhat different from that of a FWD. With information about the slope of the deflection bowl at 3 different positions, a 2 parameter model can be used to calculate the maximum deflection, as shown in Figure 35. It is possible to increase number of sensors if required.

The first modified system was delivered to DRI last year and DRI measured the entire Danish highway network successfully in three weeks. The second system was delivered to the UK in the autumn of 2005 and TRL is evaluating the device for implementation as a pavement management tool (as per email discussion with Mr. Ramesh Singhal of Highway Agencies, UK). Apart from processing and studying data from the devices Greenwood Engineering is now developing dedicated post processing software to improve the interpretation methods (as per email discussion with Dr. Soren Ramussen). A photo and a schematic of the modified version included in Figure 36 Since the device is measuring deflection velocity, it would be in appropriate to develop a pavement management system using deflection models as suggested by Zhang et al. (2003). Thus, raw data from the device is needed to identify the feasibility of implementing this device within the State of Texas.

Since the deflection velocity transducer is relatively new, the influence of the following properties: asphalt layer thickness, pavement temperature, speed of the vehicle, and thermo-susceptibility of the binder needs to be addressed. Since no published report is available yet, Dr. Rasmussen of Greenwood Engineering was contacted and the relevant information from the emails are included in the following paragraphs.

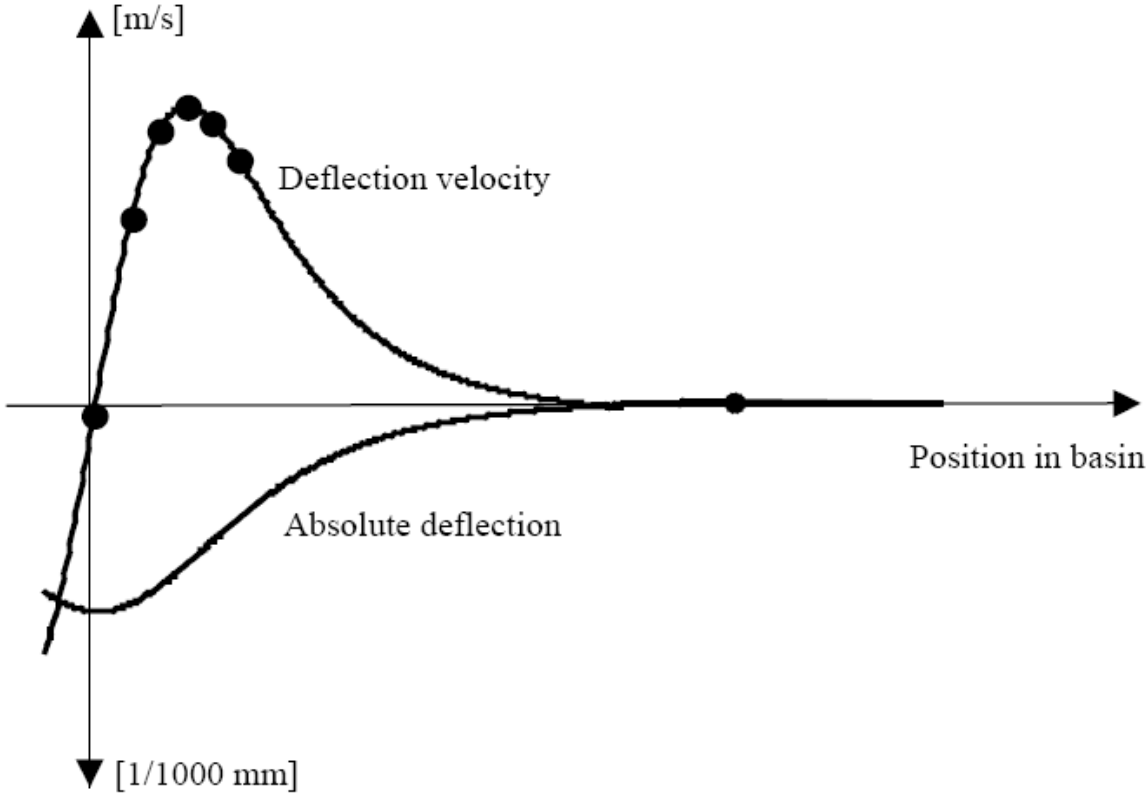

FIGURE 35 Deflection Velocity versus Absolute Deflection Bowl (Simonin et al., 2005)

FIGURE 36 Danish High Speed Deflectograph (Greenwood Engineering, www.greenwood.dk)

In general, the softer the structure is the deflection velocity will be higher. So the same structure with a high thermo-susceptibility will produce higher deflection velocities when the ambient temperature is high and vice versa. The device is equipped with an air temperature sensor for measuring the surface temperature of the road. But we do not have enough data to describe this relationship at this time. Also, because the deflection basin changes length with temperature it would be more practical to establish the relationship using a device with more than three sensors.

The device offers no information with respect to layer thicknesses. Only the response of the surface is measured. This has to be taken account when choosing an interpretation method. For roads with asphalt layer thicker than 6 in. (150 mm) a simple relationship between the structural surface index 300 and the asphalt strain at the bottom of the asphalt layer exists as shown in Equation 6.1(Krarup, et al., 2006)

$$\varepsilon = a * SCI_{300}^{b} \qquad (6.1)$$

where:
e =asphalt strain
SCI = structural surface index
a and b = regression coefficients.

The deflection velocity is directly proportional to the driving speed of the vehicle except for visco-elastic effects. However, visco-elastic effects are negligible at higher driving speeds (above ~40 km/h). So it is easier to use the slope of the deflection bowl. The slope is calculated by dividing the deflection velocity with the driving speed. That way the driving speed is "eliminated" when comparing data.

The discussion suggests that RWD and HSD are the only two devices that are operational at this point. However, HSD has been successfully evaluated by LCPC, DRI and TRL and is commercially available. Therefore, the specifications required to acquire the HSD device are included in Appendix L.

CHAPTER 7 CLOSURE

The Falling Weight Deflectometer (FWD) is the standard device used for evaluating the structural condition of pavements. It is backed by extensive research and experience. The Texas Department of Transportation (TxDOT) owns and operates fifteen of these devices to evaluate the condition of the existing pavement network. However, the FWD needs to stop at every location where a reading is required. Not only does this require lane closure and causes traffic disruption, it also poses a hazard to the personnel who operates the device. This stop and go nature of the device severely limits the length of roadway that can be covered with the device. To overcome this problem, several organizations in the USA and Europe have developed devices that can continuously measure the deflection profile of the pavement. These devices are currently in various phases of development, and some of them have been successfully implemented. The purpose of this research project was to identifying the devices that continuously measure pavement structural conditions, obtaining information about their current stage of development, and evaluating the effectiveness of such devices in incorporating within the TxDOT's pavement management system.

The review of the literature identified five different devices that have been developed. These devices are the Quest Airfield Rolling Weight Deflectometer (ARWD), the Swedish Road Deflection Tester (RDT), the Texas Rolling Dynamic Deflectometer (RDD), the Danish High Speed Deflectograph, and the Applied Research Associate's Rolling Wheel Deflectometer (RWD). The advantage and limitation of each device is discussed in the following sections.

7.1.1 Advantages and Limitations ARWD

The ARWD has the advantage of being based on a sound principle that has been demonstrated to be effective at slow speeds. The factors that are likely to introduce error have been taken into account and suitable workarounds have been incorporated. It is therefore to be expected that this device should perform well.

The limitations of the device are the loss of accuracy on curves and the length of the trailer. Moreover, this device has originally been designed to work at low speeds. Modification of this device is in progress to improve its applicability to highways by increasing its speed and reducing its dimensions. The FWD provides 7 deflection values which make it possible to backcalculate the pavement properties whereas the ARWD provides one deflection. The TxDOT PMIS is based on the FWD and its 7 deflections whereas the ARWD provides only 1 deflection value. A suitable means of adapting the ARWD to the TxDOT PMIS will have to be devised. The device is not commercially available.

7.1.2 Advantages and Limitations RDT

The RDT has the advantage of providing an entire transverse deflection profile instead of a single deflection value provided by some of the other devices. In principle at least, it should be possible to backcalculate the properties of the pavement layers and their thicknesses.

The RDT implicitly makes certain assumptions regarding the nature of the deflections and the measurement process. It assumes that the RDT is moving faster than the speed at which the deflection wave travels along the pavement, so that the maximum deflection occurs a little distance behind the load wheels. Thus the RDT measures the deflection as the difference between the deflections beneath the load wheels and the maximum deflection which is assumed to occur at a distance of 0.5 m behind the load wheels. The device thus depends on the dynamic nature of pavement response and would yield a value of zero or nearly zero when it is stationary.

The validity of this assumption needs to be investigated. Also, it is likely that the distance of the maximum deflection location behind the load wheel will depend on the speed at which the RDT moves and the pavement stiffness, rather than being a fixed value of 0.5 m. The errors introduced by this assumption need to be quantified. The RDT also does not have any system to account for the errors introduced by the vertical motion of the device. Instead it relies on averaging of several data points to reduce this error. The TxDOT PMIS is based on the FWD and its 7 deflections whereas the RDT provides deflection profile just below the loads. A suitable means of adapting the RDT to the TxDOT PMIS will have to be devised. The device is not commercially available.

7.1.3 Advantages and Limitations of RDD

The RDD provides three deflections values while the TxDOT PMIS is based on the 7 values provided by the FWD. It will therefore be necessary to devise a method to take this into account. The RDD travels at speeds of the order of 3 mph (5 km/h) and is therefore not suitable for testing on highways. The TxDOT PMIS is based on the FWD and its 7 deflections whereas the RDD provides less than 7 deflection values. Therefore, a suitable means of using adapting the RDD to the TxDOT PMIS will have to be devised. The device is commercially available and TxDOT has recently decided to acquire RDD device.

7.1.4 Advantages and Limitations of RWD

The RWD evaluated within Texas exhibited some relationship with the FWD and the Texas RDD. The device also exhibited reasonable repeatability. In addition, ARA has developed software to acquire and post process the data collected for quicker analysis of the data.

The RWD is 53 ft long which significantly limits the roads that can be tested with this device. The RWD deflection profiles decrease with an increase in temperature which opposite to what is expected and also display a warm up effect where in the first deflection profile is significantly different from the others. ARA has not specified how it accounts for errors generated by the vibration of the beam on which the sensors are mounted. The data evaluated suggested that there is an influence of speed on the measured deflection and it is not accounted for in the currently available system. Finally, the RWD provides only a single deflection value while the TxDOT PMIS is based on 7 deflection values provided by the FWD. Therefore a suitable method for using the RWD deflection data in the PMIS will need to be devised. The device is not commercially available.

7.1.5 Advantages and Limitations of HSD

The HSD has the advantage of using a simple, well known principle. The HSD trailer is neither long nor bulky unlike some of the other devices. There exists suitable data acquisition and analysis software to automate the task. The device shows good repeatability and good correlation with the results of the FWD. In addition, newer HSD device has the capability of measuring deflection velocity at more than one location; thus, allowing estimation of deflection velocity bowl that can be used to better estimate structural condition of the evaluated pavement. Since TxDOT PMIS database requires deflection measurements from 7 different locations, a new procedure will have to be devised to adapt the results of the HSD deflection velocity bowl in the TxDOT PMIS. This device is commercially available.

At present RWD and HSD devices are the only devices being evaluated by various agencies to identify feasibility of implementing them within their pavement management systems. Out of these two devices, only HSD is commercially produced and has been already procured by Highway Agencies of UK and Danish Road Institute. The device has been recently renamed to be Traffic Speed Deflectometer (TSD). Therefore, HSD or TSD device is the only device which has the possibility of implementation. It is difficult to develop a pavement management system without the availability of sufficient data and unsuitability of conventional computer programs like BISAR in estimating deflection velocity of the pavement system due to imparted dynamic loads. Since the device can be produced with more than four sensors, it is possible that the HSD or TSD device can be procured with seven sensors such that the data can be analyzed using Method IV proposed by Zang et al. (2003) for pavement management. The specifications for procuring the device have been included in Appendix M.

REFERENCES

- Andr´en, P. and C. A. Lenngren (2000a, March 7–8). Evaluating pavement layer properties with a high-speed rolling deflectometer. In A. K. Mal (Ed.), *Nondestructive Evaluation of Aging Aircraft, Airports and Aerospace Hardware IV Proceedings*, Volume 3994, Newport Beach, CA, USA, pp. 192–200. SPIE—The International Society for Optical Engineering.
- Andr´en, P. and C. A. Lenngren (2000b, August 5–8). Evaluating subgrade properties with a highspeed rolling deflectometer. In M. S. Mamlouk (Ed.), *Pavement, Subgrade, Unbound Materials ,and Nondestructive Testing — Proceedings of Sessions of Geo-Denver 2000*, Number 98 in Geotechnical Special Publication, Denver, CO, USA, pp. 17–30.
- Andr´en, P. and C. A. Lenngren (2004). Rolling Wheel Deflectometer/FWD Correlation Study, Unpublished Report Obtained from Peter Andr´en of VTI aSwedish National Road and Transport Research Institute, Sweden
- Bay, James, A., Stokoe, Kenneth H., McNerney, Michael T., Suttisak, Soralump, Van Vleet, David A., and Rozycki, Dan K., 2000, "Evaluation of Runway Pavements at the Seattle-Tacoma International Airport Using Continuous Deflection Profiles Measured with the Rolling Dynamic Deflectometer, Transportation Research Board, 79th Annual Meeting, January 9-13.
- Briggs, R. C., Johnson, R. F., Stubstad, R. N., and Pierce, L., 1999, "A Comparison of the Rolling Weight Deflectometer with the Falling Weight Deflectometer," Nondestructive Testing of Pavements and Backcalculation of Moduli: Third Volume, ASTM STP 1375, S. D. Tayabji and E. O. Lukanen, Eds., American Society for Testing and Materials, West Conshohocken, PA.
- Hall, Jim W., and Steele, Douglas A., (2004), Rolling Wheel Deflectometer (RWD) Demonstration and Comparison to Other Devices in Texas, ERES Consultants, February.
- Harr, M., and N. Ng-A-Qui, 1977, "Noncontact, Nondestructive Determination of Pavement Deflection Under Moving Loads," FAA-RD-77-127, U.S. Department of Transportation, Washington D.C.
- Hildebrand, Gregers, and Rasmussen, Søren, 2002, Development of a High Speed Deflectograph, Road Directorate, Denmark, 2002
- Krarup, J., Rasmussen, S., Aagaard, L., and Hjorth, P.G., (2006), "Output from the Greenwood Traffic Speed Deflectometer," To be Presented at 22nd ARRB Group Conference, Canberra, Australia.
- Murphy, Michael Ray, 1998, A Mechanistic-Empirical Approach to Characterizing Subgrade Support and Pavement Structural Condition for Network Level Applications, Doctoral Dissertation, University of Texas at Austin, pp 289 – 333.
- Simonin J.M., Lièvre D., Rasmussen S. and Hildebrand G. (2005). Assessment of the Danish High Speed Deflectograph in France. 7th International Conference on the Bearing Capacity of Roads, Railways and Airfields, 27-29 June, Trondheim-Norway.
- Zhang, Zhanmin, Manuel, Lance, Damnjanovic, Ivan, and Li, Zheng, 2003, Development of a New Methodology for Characterizing Pavement Structural Condition for Network-Level Applications, Report FHWA/TX-04/0-4322-1.

APPENDIX A THEORY OF OPERATION, AND FIELD EVALUATION RESULTS OF AIRFIELD ROLLING WEIGHT DEFLECTOMETER (ARWD)

A.1 Theory of Operation

The ARWD uses optical triangulation with four non-contact optical sensors mounted on a beam of a trailer (Harr, 1977). The ARWD has one sensor placed near the load wheel and three sensors ahead of it inline with the first sensor and presumably beyond the deflection basin (Figure A.1). Distances to the pavement surface are measured by the first three sensors and then again a short while later with the second, third and fourth sensors. The mechanism is depicted in Figure A.1 where the sensors are denoted as A, B, C, and D. The measurements are so timed that they are spatially coincident.

The device works by calculating the changes in slope. In Figure A.1, A-B is the difference between the slope of the beam and the slope of the pavement, the slopes being measured across the points P1 and P2. Similarly, B-C is the difference between the beam and pavement slopes across the points P2 and P3. The difference between these two slopes, (A-B) - (B-C) = A-2B+C, is the change in pavement slope across the three points and is independent of the beam height or angle. A short while later, the load wheel has moved to the point P3 where another set of measurements is taken using the sensors labeled B, C, and D. This second set of measurements is referred to as B', C', and D'. If

$$h = A - 2B + C \tag{A.1}$$

$$h' = B' - 2C' + D' \tag{A.2}$$

Then it can be deduced that the

$$Deflection = h - h' \tag{A.3}$$

This method of measurement assumes that the sensors pass sequentially over identical areas of pavement, sensors do not move with respect to each other, and speed is accurately measured. The ARWD has an odometer with a stated error of within 2%.

The sensors are spaced 9 ft (2.74 m) apart based on the idea that the deflection basin in most pavements at highway speeds is generally less than 9 ft (2.74m) in radius. This implies that the beam on which the sensors are mounted must be greater than 27 ft (8.22 m) long. However, the deflections of the beam tend to cause significant errors which get magnified in the computations. To overcome these limitations, the ARWD uses a laser beam that passes inside the physical beam as a reference to measure the deflection of the physical beam and makes corrections for this deflection in the computations. This overcomes the problem of thermal expansion and vibrational bending of the beam.

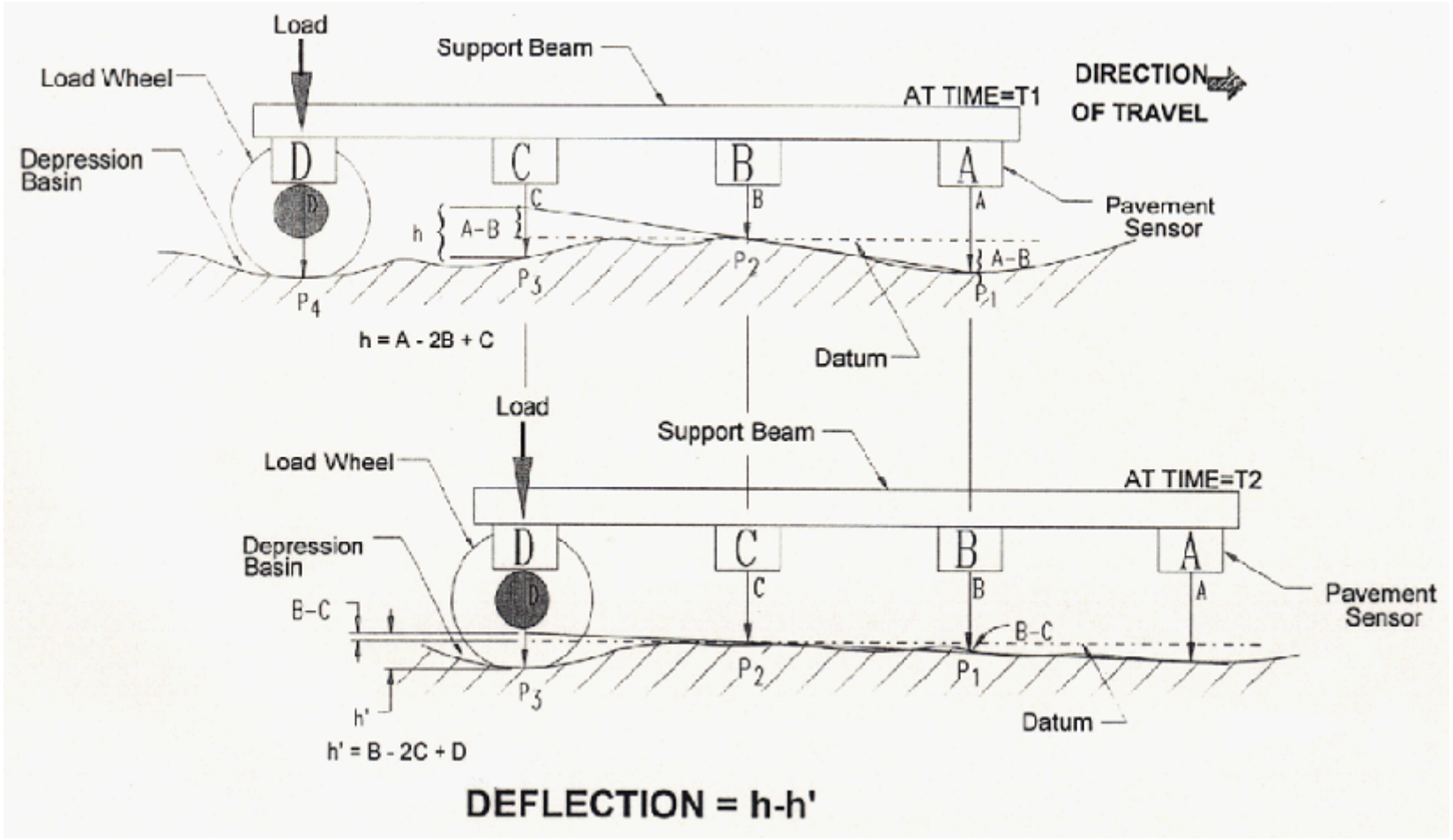

FIGURE A.1 Schematic of ARWD Deflection Measurement Mechanism (Briggs et al., 1999)

In addition to compensating for the deflections of the mounting beam, the ARWD is designed taking into account the highly textured nature of pavement surfaces. A vertical accelerometer measures the vertical acceleration of the load which determines the actual load applied to the pavement during each measurement. Additionally, the ARWD also measures the pavement temperature using an infrared pyrometer.

A.2 Field Evaluation Results

To investigate the applicability of this device, the Washington State DOT conducted a test in 1997 to compare the deflection measurements of the ARWD with a Dynatest FWD. The test was conducted on a stretch of SR-18 that consisted of 6.6 in. (167 mm) of asphalt concrete over 16 in. (400 mm) of crushed stone base on an embankment subgrade. The roadway had been heavily trafficked for a year after construction with no visible surface distress. The ARWD was traveling at a speed of 20 mph (35 km/h) and a deflection measurement was taken at every 9 ft (3 m). Since the individual deflections showed considerable random error, the deflections over a distance of approximately 90 ft (25 m) (i.e., 20 readings) were averaged. The test section was about 1,000 ft (300 m) long, and the first 300 ft (100 m) and the last 100 ft (30 m) were used for acceleration and turning. This amounts to a frequency of data collection of 0.3 Hz. The results of evaluation, based on the average of 20 deflections, are presented in Figure A.2. A trend similar to the one observed with the FWD deflections measured at an offset of 9 in. was observed, with some anomalies.

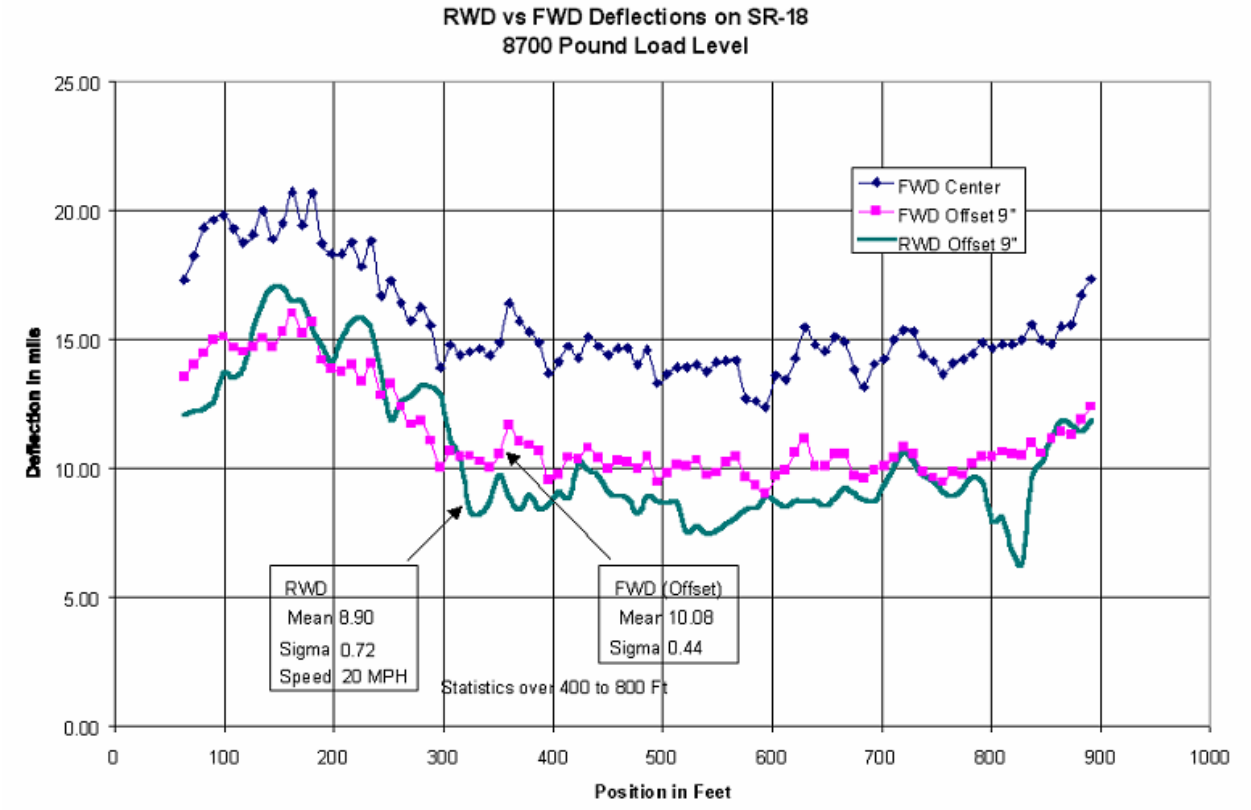

FIGURE A.2 ARWD and FWD Deflection Comparison (Briggs et. al., 1999)

APPENDIX B THEORY OF OPERATION, AND FIELD EVALUATION RESULTS OF ROLLING DYNAMIC TESTER (RDT)

B.1 Theory of Operation

The Swedish National Road Administration and Swedish National Road and Transport Research Institute have developed a Road Deflection Tester (RDT). The RDT consists of a Scania R143 truck that has been retrofitted with two arrays of laser range finders, each consisting of 20 sensors arranged in a line transverse to the direction of travel.

The first array of laser range finders is positioned 8.2 ft (2.5 m) behind the front wheels and the second array is placed 1.6 ft (0.5 m) behind the rear wheels as illustrated in Figure B.1. Thus, the distance between the two arrays is approximately 13.1 ft (4 m). The first array measures the transverse deflection profile outside the deflection basin while the second measures the deflection profile near the center of the deflection basin. The truck has two weights of 882 lb (400 kg) that can be moved back and forth. During testing, these weights are moved to the rear of the truck while weights are moved to the front of the truck during transportation for better distribution of weights. The engine of the truck is also placed in the rear and together with the weights; this produces a force of 8 to 14 kips (40 to 70 kN) in the rear axle. The information about laser system is included from Andr´en et. al. (2000a) and readers are advised to see the referenced paper for better explanation of the system.

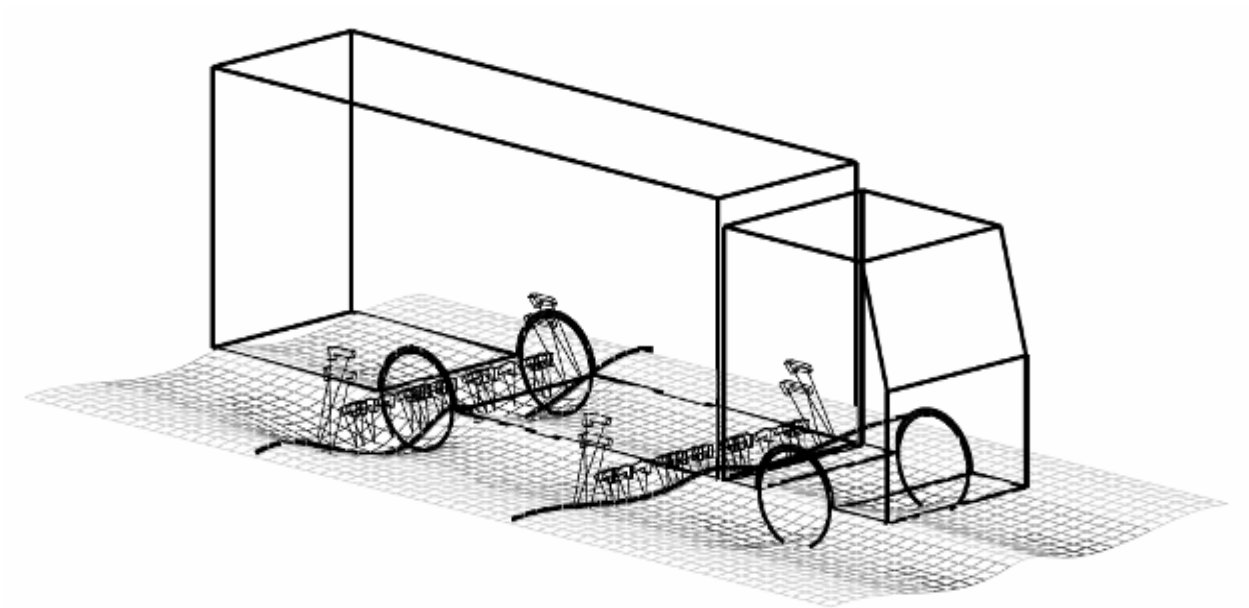

FIGURE B.1 Schematic of Sensor and Wheel Arrangement in the RDT (Andr´en and Lenngren, 2000a)

The Laser Range Finders (LRFs) are of four different types of Selcom OptocatorTM 2008. Depending on their positions on the truck different stand-off (the distance from the aperture to

the center of the measuring range) and measuring range are needed. An incremental wheel pulse transducer is mounted on the left front wheel for accurate traveled distance. Force transducers and accelerometers are mounted on the left and right sides of the rear axle. An optical speedometer for both longitudinal and transversal speed and a rate gyroscope are mounted near the front axle. These sensors, working in concert, gives quite detailed data on how the truck behaves when operating. Currently, this information is not used actively during data processing, but is helpful for examining unexpected results. The sampling hardware operates at a frequency of about 32 kHz, but data are normally collected at 1 kHz. With a 1 kHz sampling frequency and a speed of 70 km/h samples are stored every 20 millimeters. The laser sensors are calibrated using a combination of gauge set and liquid surface calibration.

The authors investigated two ways of analyzing collected data. The first method involves calculating the area under the transverse deflection profile. The second method involves calculating baseline values using the three sensors on either side of each wheel. Both methods are further explained in the following paragraphs.

In the first method, the distance measurements from the outer sensors (for example, the sensors labeled #02 and #17 shown in Figure B.2) are subtracted from the values measured by the other sensors to obtain the front and rear profiles. The front profile is subtracted from the rear profile to obtain the deflection profile. The area enclosed between this deflection profile and the horizontal datum is what the authors refer to as deflection area, as illustrated in Figure B.3

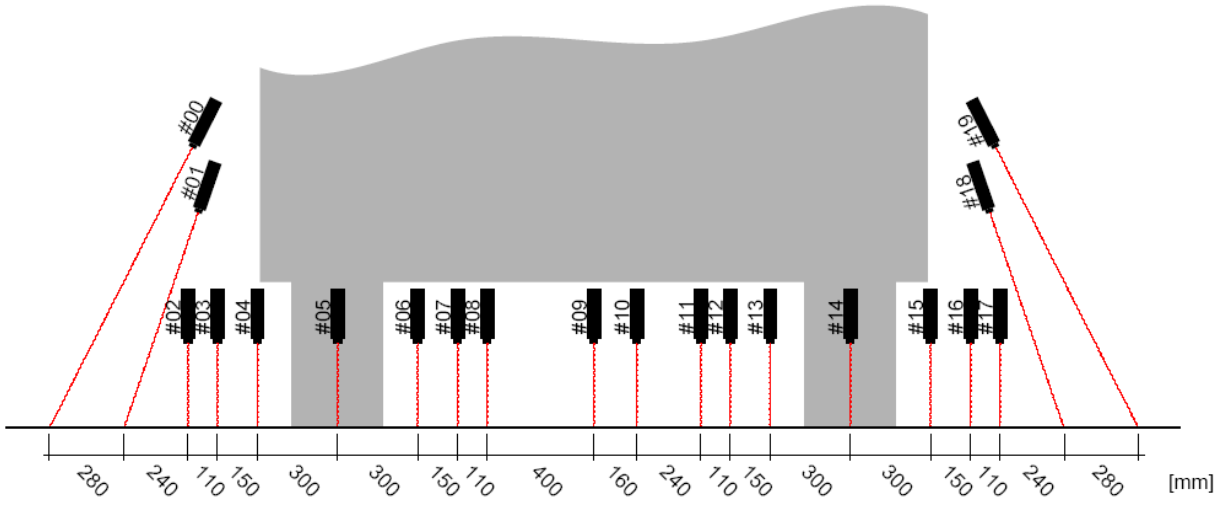

FIGURE B.2 Schematic of Sensor Arrangement on the Swedish RDT (Andr´en and Lenngren, 2000a)

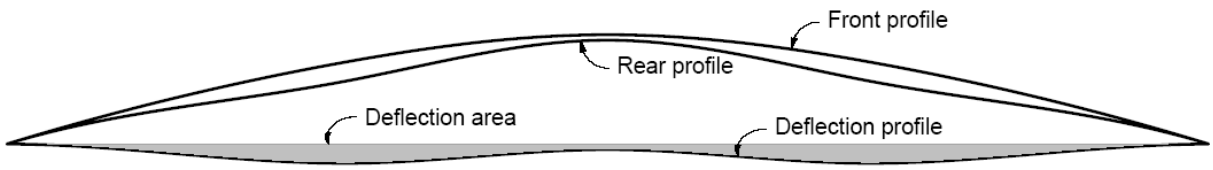

FIGURE B.3 Computation of Deflection Area (Andr´en and Lenngren, 2000a)

In the second method, the deflection profile is calculated as in the first method. Then the deflection at the center of the load wheel relative to a pair of sensors on each side of the wheel is calculated. This is called a baseline value and three such values can be computed for each wheel corresponding to the three sensors on each side of the load wheel, immediately next to the wheel. This is illustrated in Figure B.4 where the baseline values B56L and B30R are depicted.

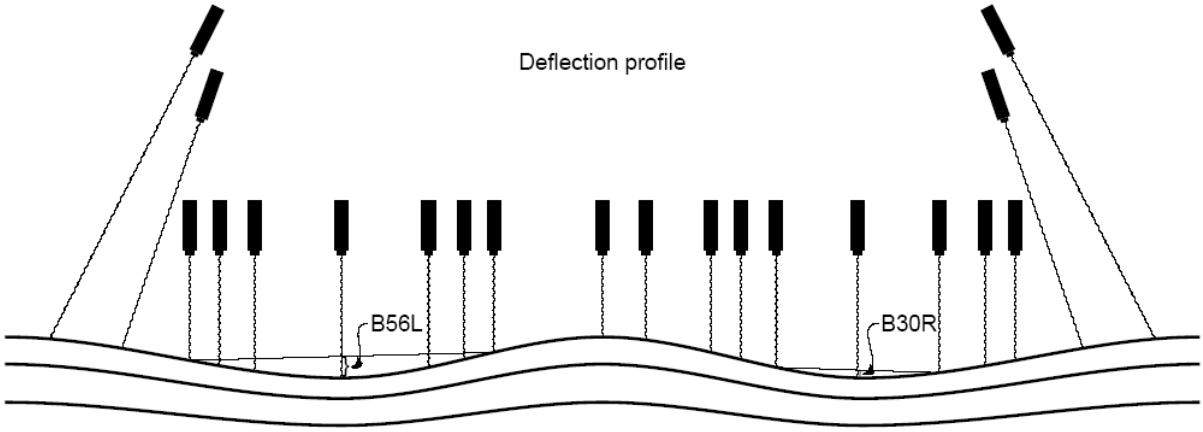

FIGURE B.4 Computation of the Baseline Values (Andr´en and Lenngren, 2000a)

B.2 Field Evaluation Results

Various RDT field evaluations have been conducted and the results of the evaluations are reported by Andr´en and Lenngren (2004, 2000a, and 2000b). Typically, results from each test sections were analyzed to identify the following:

- Repeatability of the device was identified by performing trial runs three times on the same road sections and in the end an average value is reported.
- Influence of speed (19, 31, 44, and 56 miles/h or 30, 50, 70, and 90 km/h) on the measured deflection area and baseline values. The tests at lower speeds were performed on two lane highways while tests at higher speeds were performed on freeways.
- The influence of applied wheel load on baseline values.
- Comparison of the deflection area and baseline deflection with the subgrade stiffness (backcalculated from FWD measurements). Although initial evaluations were performed using baseline values, Andr´en and Lenngren (2004) suggested not using it because data from only six sensors (three in the front array and three in the rear one) of the twenty is used.

A typical trial test result for 177 Vannacka – Hajom (rural low volume two lane) road tested at 19 miles/hr (30 km/h) is shown in Figure B.5. The test results are for the data obtained near the left wheel of RDT. The figure shows that the applied load levels varied between 10 to 13.5 kips (45 to 60 kN) along a length of 17, 400 ft (5,300 m) of tested section indicating good repeatability.

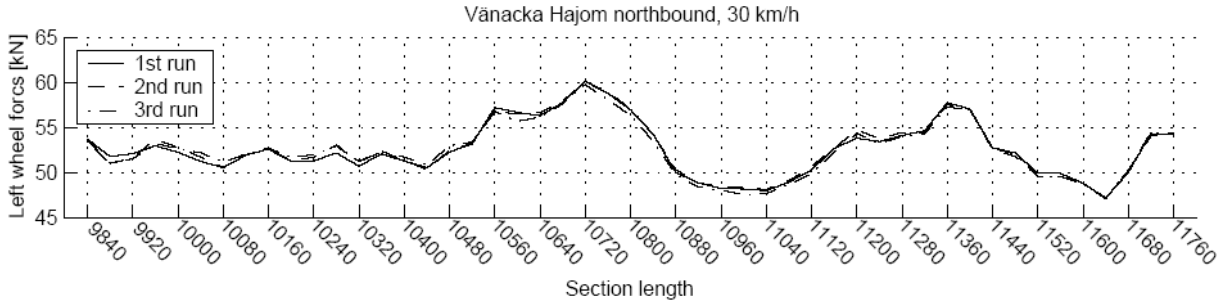

FIGURE B.5 Trial Run Test Results at a Speed of 19 miles/hr (Andr´en and Lenngren, 2000a)

Andr´en and Lenngren (2004) reported results of the study performed on three sections; however, results from only two sites are discussed here for the sake of brevity. At each site FWD tests at 11.2 kips (50 kN) load levels were also performed to identify static deflection levels and layer properties. The first site is located on old Stockholm-Copenhagen road built fifty years ago. The surface layer consisted of asphalt concrete (AC) and the base layer consisted of cement treated base (CTB). Based on FWD test results, the estimated modulus of AC, CTB, and subgrade layers to be 640 ksi (4,500 MPa), 2,300 ksi (16,000 MPa), and 15 ksi (100 MPa), respectively. The second site consisted of AC layer and unbound base layer. Based on FWD test results, the estimated modulus of AC, base, and subgrade layers to be 1,570 ksi (11,000 MPa), 9 ksi (65 MPa), and 20 ksi (135 MPa), respectively.

The transverse RDT deflection profile obtained from two sites is shown in Figures B.6 and B.7. Since CTB is stronger in comparison to unbound base material, the deflection profile shown in Figure B.6 does not show the influence of wheel (bending of the surface) as compared to the data shown in Figure B.7 for unbound layer. Although the difference in deflection near wheels at two sites is 10% (9.8 mils versus 10.8 in.; 0.25 mm versus 0.275 mm), the difference to the outermost surface is roughly two times (3.9 versus 6.9 mils; 0.1 mm versus 0.175 mm) indicating that deflection measurements just below the wheels may not provide much information about pavement conditions

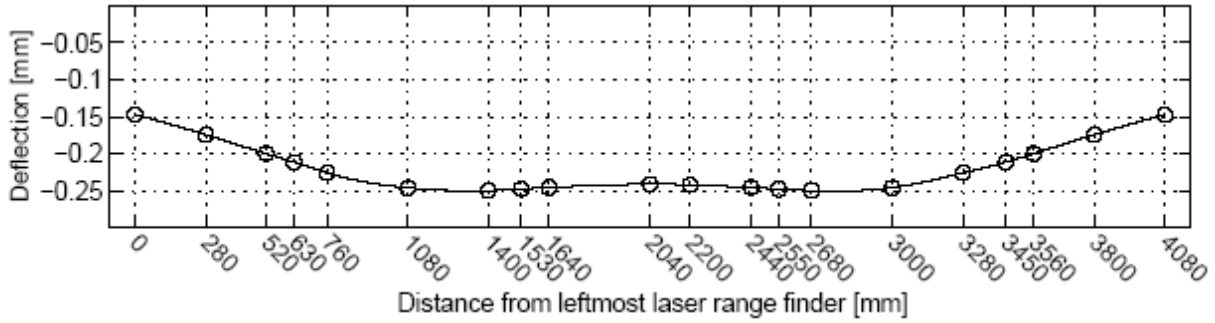

FIGURE B.6 Transverse Deflection Profile for Site 1 (Andr´en and Lenngren, 2004)

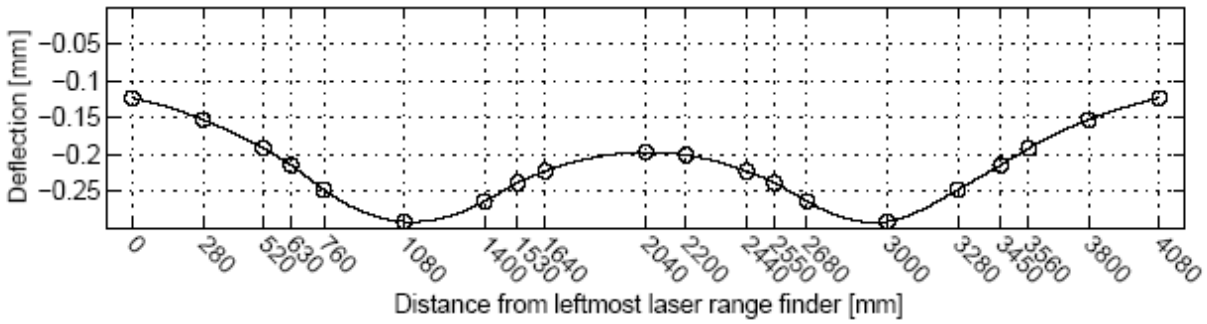

FIGURE B.7 Transverse Deflection Profile for Site 2 (Andr´en and Lenngren, 2004)

The test results from the two sites are presented in Figures B.8 through B.10. In Figure B.8, the deflection area of RDT is compared with the FWD center deflection for Site 1 consisting of CBT. Overall, the deflection area follows the FWD center deflection with few exceptions. For example, FWD center deflection, at a distance of 300 ft (100 m), is lower than deflection area obtained from RDT but it is higher at a distance of 2,700 ft (900 m). In addition, the influence of speed is also significant at these distances as well indicating further investigation might be needed. In terms of subgrade stiffness (Figure B.9), the deflection area follows subgrade stiffness pattern very closely except at few sections. For instance, a spike in subgrade stiffness is observed at 1,000 ft (300 m) while deflection ratio data does not exhibit the spike at that location.

For Site 2, the relationship between deflection ratio and subgrade stiffness is presented in Figure B.10. The data shows that deflection area is similar for 44 and 56 mph (70 and 90 km/hour) speed but it varied when tested at a speed of 30 mph (50 km/hour) especially around 1,150 and 1,500 ft (350 and 450 m) distance. The subgrade stiffness also followed closely deflection area pattern with few exceptions, as shown in Figure B.10.

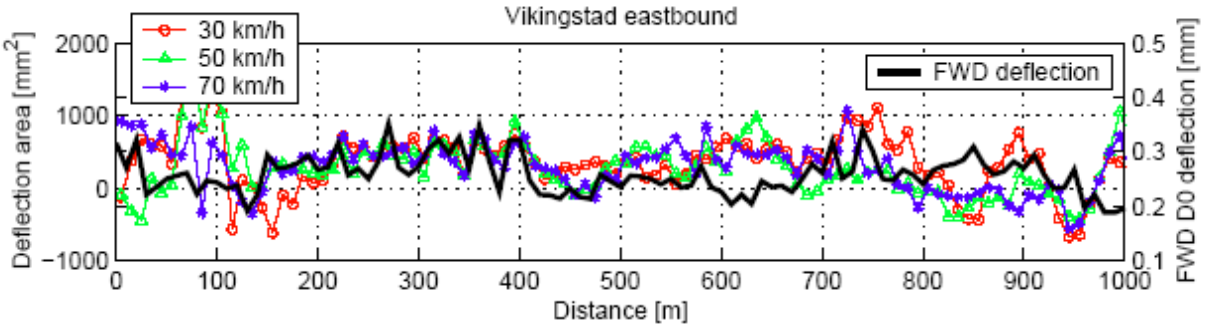

FIGURE B.8 Comparison between FWD Center Deflection and Deflection Area for Site 1 (Andr´en and Lenngren, 2004)

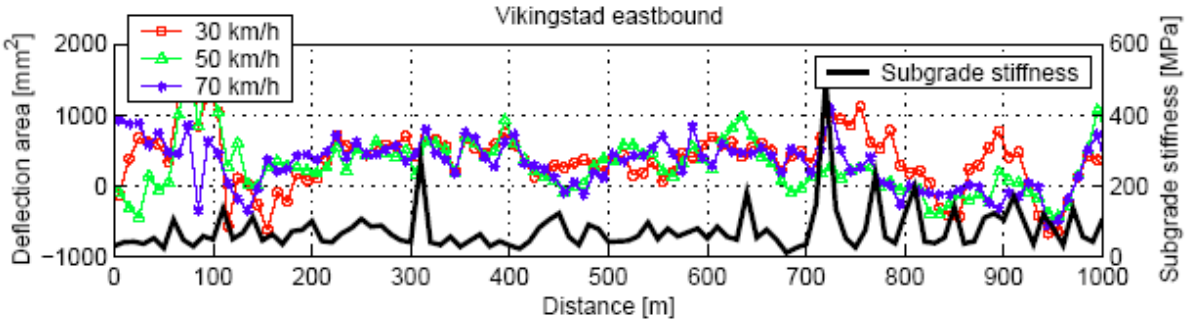

FIGURE B.9 Relation Between Subgrade Stiffness and Deflection Area for Site 1 (Andr´en and Lenngren, 2004)

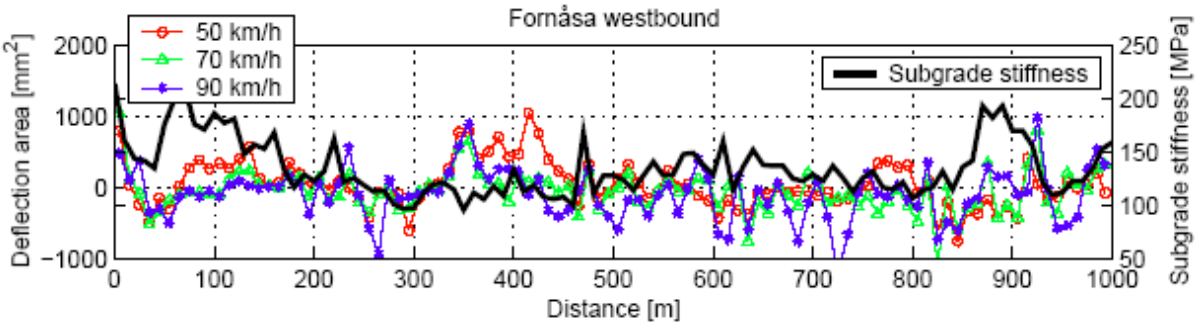

FIGURE B.10 Relation Between Subgrade Stiffness and Deflection Area for Site 2 (Andr´en and Lenngren, 2004)

APPENDIX C THEORY OF OPERATION, AND FIELD EVALUATION RESULTS OF ROLLING DYNAMIC DEFLECTOMETER (RDD)

C.1 Theory of Operation

The RDD is a truck-mounted device consisting of a servo-hydraulic loading system and force and deflection measurement systems. The schematic of RDD device is shown in Figure C.1a and C.1b. The hydraulic actuator drives a 7500-lb (3400-kg) mass up and down, generating vertical dynamic forces up to 34.7 kips (308 kN) peak-to-peak at frequencies from 5 to 100 Hz. These vertical dynamic forces are transferred down the stilt structure to a loading frame, which is supported by two loading rollers. The two loading rollers apply the dynamic (and static) forces to the pavement. The loading wheels consist of a solid aluminum rim coated with hard urethane and measure 18 in. (460 mm) in diameter and are 5 in. (127 mm) wide. The loading rollers are held in contact with the pavement by means of a static hold- down force, which is generated by hydraulic actuators reacting against the mass of the truck. The vertical downward force is applied to the load frame through four air springs. The combined static and dynamic forces applied to the pavement are measured with four load cells between the loading frame and the loading rollers, as shown in Figure C.1b.

Vertical pavement deflections generated by the dynamic force are measured with up to four rolling deflection sensors. These sensors consist of a lightweight, rigid, three-wheeled cart supporting a vertically-sensitive velocity transducer (geophone) with a 2-Hz resonant frequency. The rolling deflection sensors are pulled along with the truck by cables attached to an isolated frame. The rolling sensors can be positioned in any number of configurations. A plan view of the configuration used for the testing at Seattle –Tacoma International Airport is shown in Figure C.1c. In this configuration, three rolling deflection sensors are positioned along a line, so that they are equidistant from the center of the two loaded areas (two loading rollers). The in-line sensor is positioned at the midpoint between the loading rollers, which is a radial distance of 1.93 ft (588 mm) from the center of each loaded area. The first leading sensor is positioned directly in front of the in-line sensor a radial distance of 5 ft (1524 mm) from the center of each loaded area. The second leading sensor is on the same line as the other two sensors a radial distance of 3 ft (914 mm) from the center of each loaded area. The sensors are isolated from the truck by cables attached to an isolated frame.

Tests are typically performed by applying a sinusoidal dynamic force to the pavement while the RDD slowly drives along the pavement. Testing speeds of 0.6 to 1.5 ft/s (0.2 to 0.5 m/s) are typically used. As the RDD moves over the pavement, the deflections induced by the dynamic force are measured with the rolling sensors.

Deflections measured with the in-line sensor are a good indicator of the overall stiffness of the pavement system. The outputs of all sensors can be used to determine the shape of the induced

deflection basin. The basin shape is a function of the stiffness of the various pavement layers. The deflections measured with the leading sensors provide a very good indication of the load transfer efficiency of joints in rigid pavements.

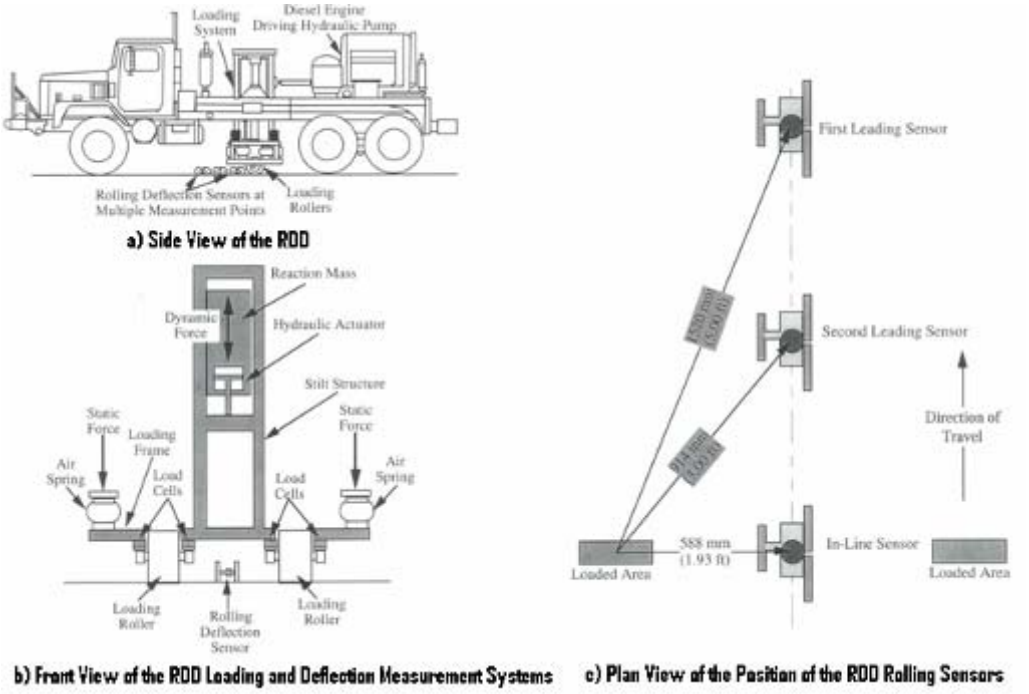

FIGURE C.1 Schematic of RDD and Sensor Location (Bay et. al. 2000)

C.2 Field Evaluation Results

Bay et. al. (2000) tested the RDD at the Seattle-Tacoma International Airport in Seattle, Washington. They measured the profiles along runways 16R-34L and 16L-34R and several taxiways using a peak to peak dynamic force of 25 kips (111 kN) at a frequency of 32 Hz with a static hold down force of 25 kips (111 kN). The RDD was moving at a speed of 1 ft/s (0.3 m/s).

Runway 16R-34L was 9425 ft (2073 m) long and 150 ft (45.7 m) wide rigid jointed Portland Cement Concrete pavement consisting of 18.75 ft wide and 20.0 ft long (5.72 m wide and 6.10 m long) slabs. The deflection profiles were measured along the lanes shown in Figure C.2. The deflection profile measured along lane 5 is plotted in Figures C.3 and C.4. Two transverse profiles are plotted in Figures C.5 and C.6, measured at distances of 995 ft (303 m) from the south end of runway 16R-34L and at the adjacent mid slab region directly north of the transverse joint.

Deflection profiles measured with all three sensors are plotted in Figure C.7. This figure illustrates that the RDD is capable of measuring the load transfer across joints as the deflections in the sensors decrease as they cross the joint. A deflection profile illustrating good load transfer is shown in Figure C.8 where it is seen that the deflections in the sensors do not change suddenly as they traverse a joint.

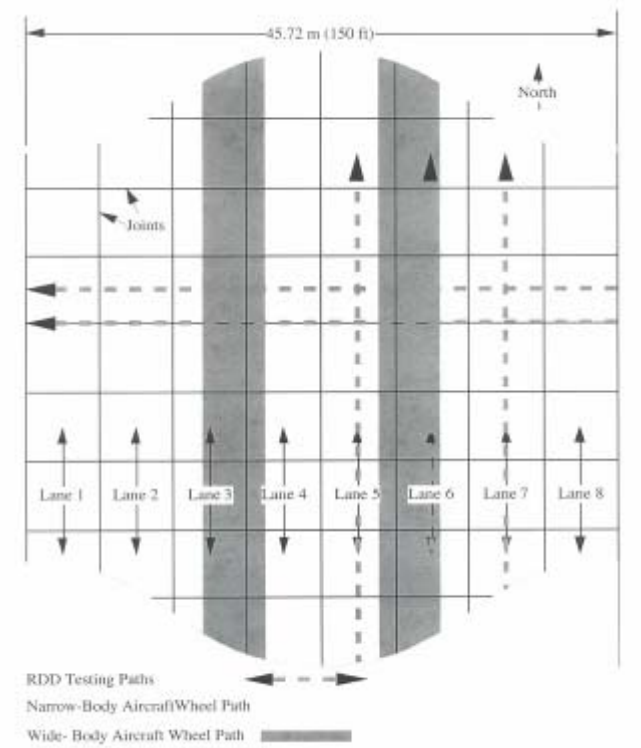

FIGURE C.2 Illustration of Lanes Tested by RDD (Bay et. al. 2000)

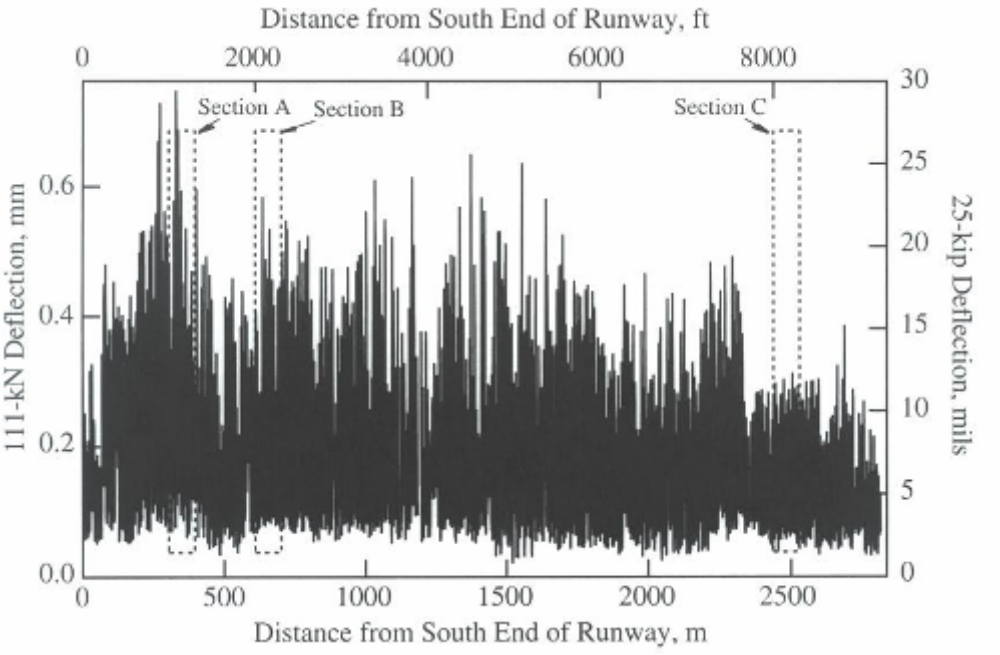

FIGURE C.3 Deflection Profile Along Lane 5 (Bay et. al. 2000)

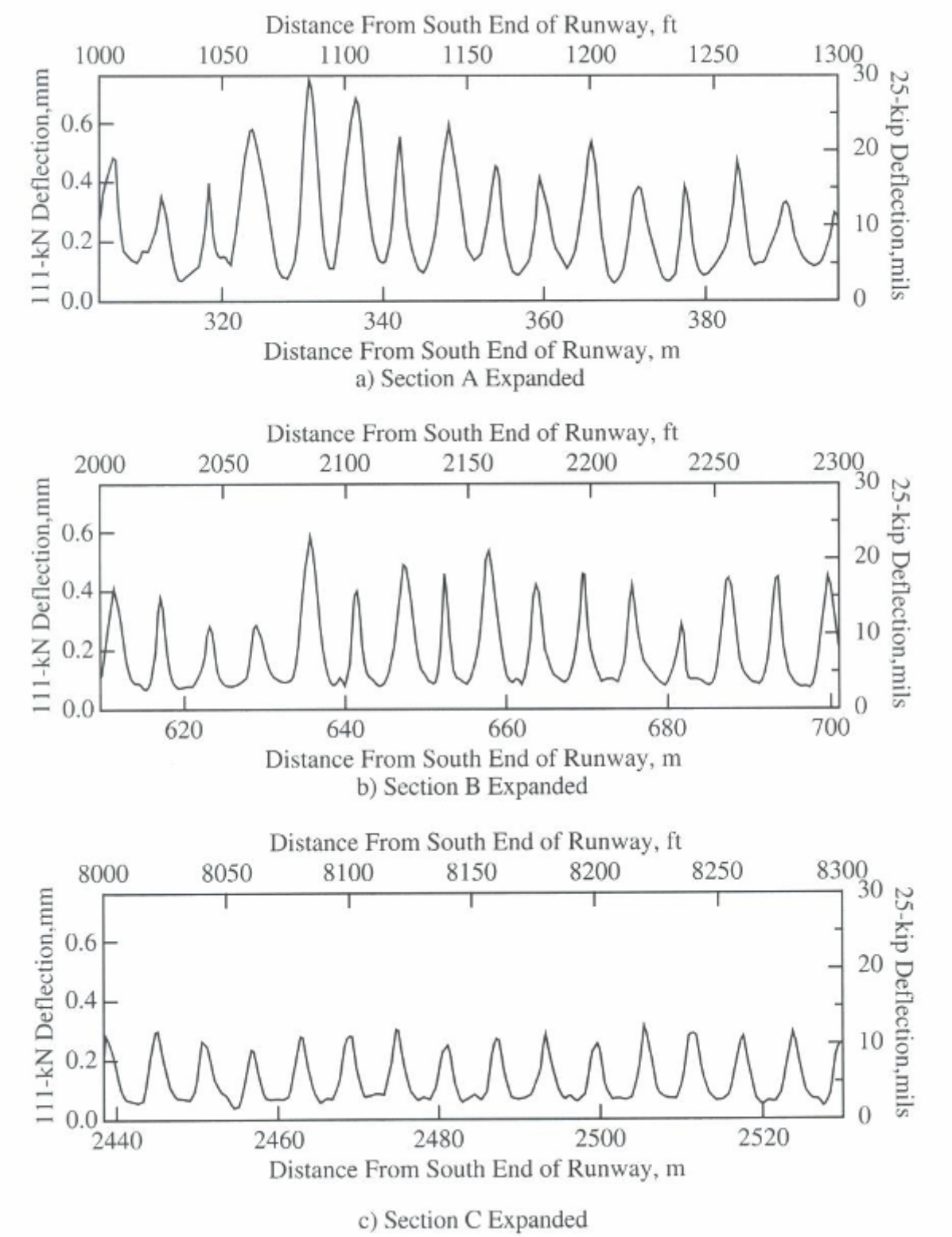

FIGURE C.4 Section Details from Longitudinal Deflection Profile (Bay et. al. 2000)

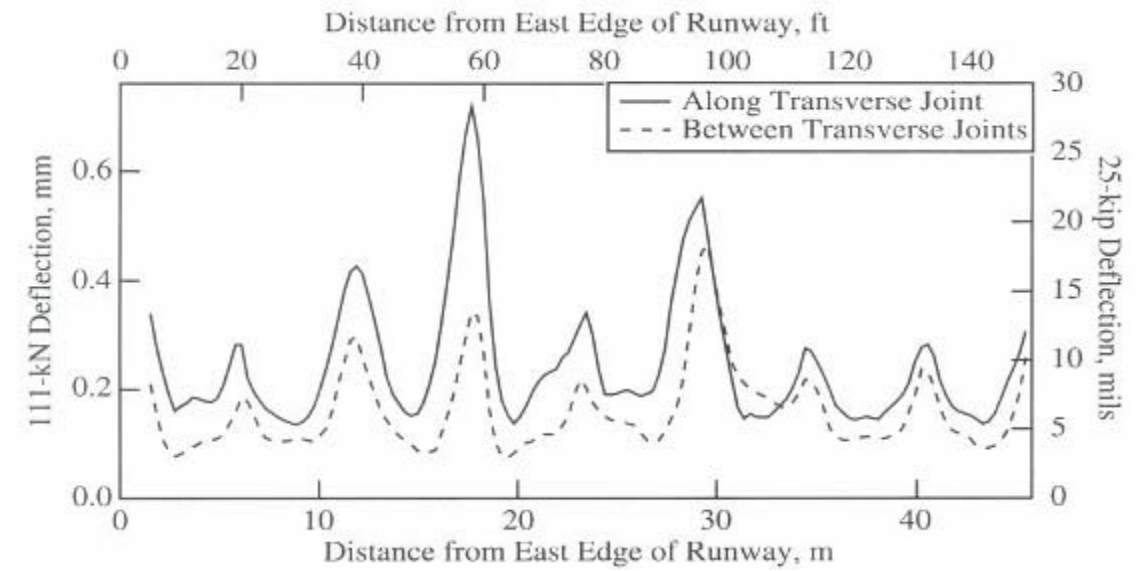

FIGURE C.5 Transverse Deflection Profile Using All Three Sensors (Bay et. al. 2000)

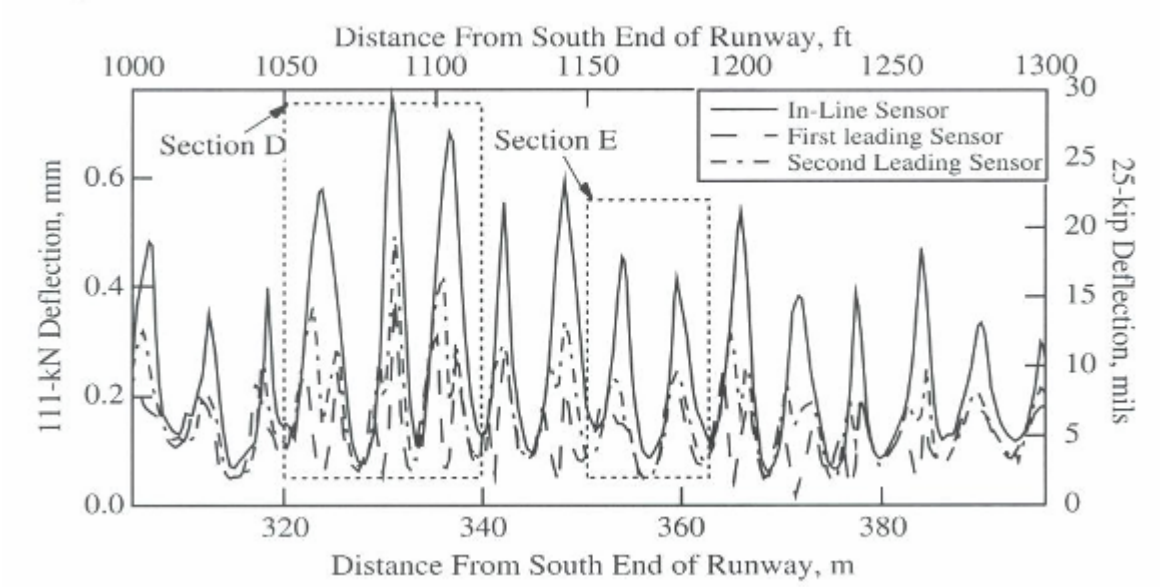

FIGURE C.6 Transverse Deflection Profile Using All Three Sensors (Bay et. al. 2000)

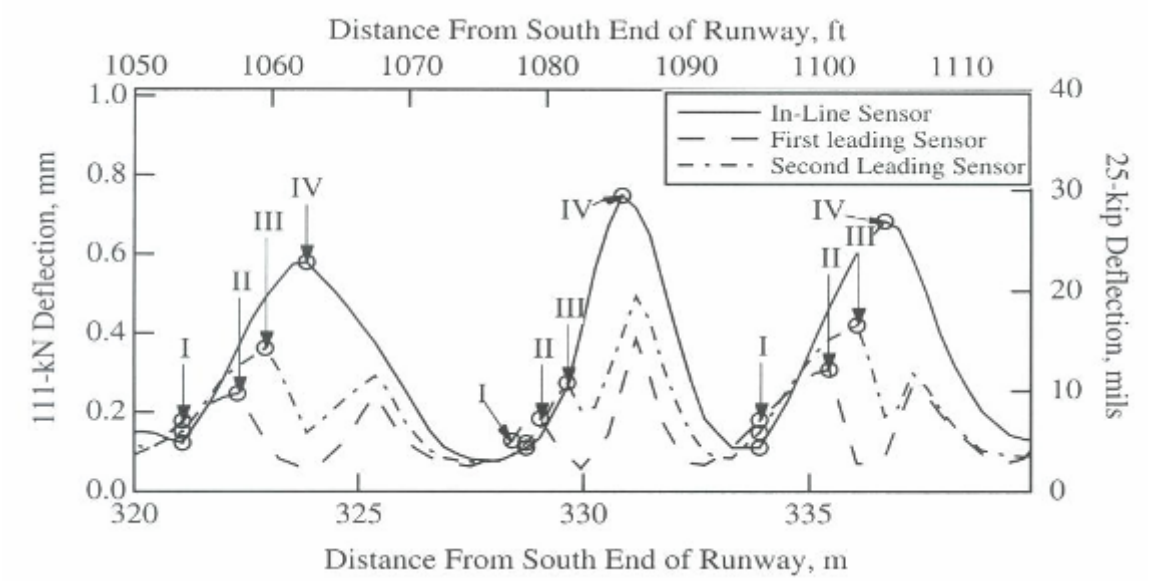

FIGURE C.7 Deflection Profile Illustrating Poor Load Transfer Across Joints (Bay et. al. 2000)

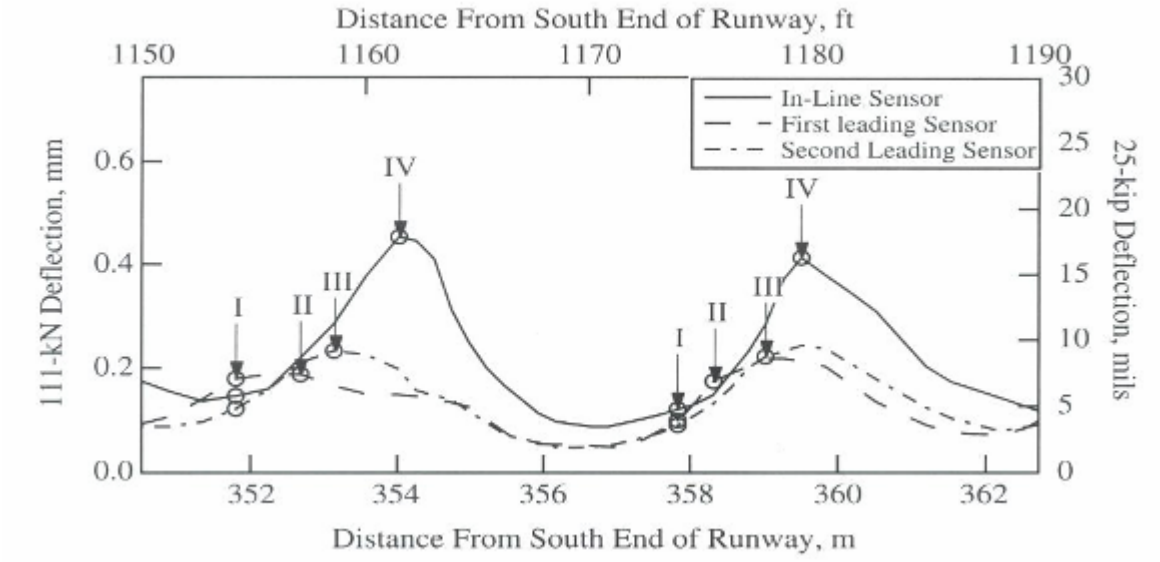

FIGURE C.8 Transverse Deflection Profile Showing Good Load Transfer (Bay et. al. 2000)

Runway 16L-34R was 11,900 ft (3627 m) long and consisted of 6 in (150 mm) thick rigid PCC pavement with extensions of thicknesses up to 12 in (300 mm) and AC overlays varying from 30 in (760 mm) to 14 in (350 mm). The AC overlay is generally greater on the east side of the runway. A deflection profile measured 10 ft (3.05 m) east of the centerline of the runway with the in-line sensor is presented in Figure C.9. It can be seen that the deflections on the extension are greater because the extension has an overall thinner section.

Three typical transverse profiles for this runway are shown in Figure C.10. The profiles correctly show more deflection in the central part of the runway which has been more heavily trafficked as compared to the lightly trafficked edges.

The RDD is able to distinguish between the weaker and stronger sections of the runway as well as give an indication of the load transfer across joints.

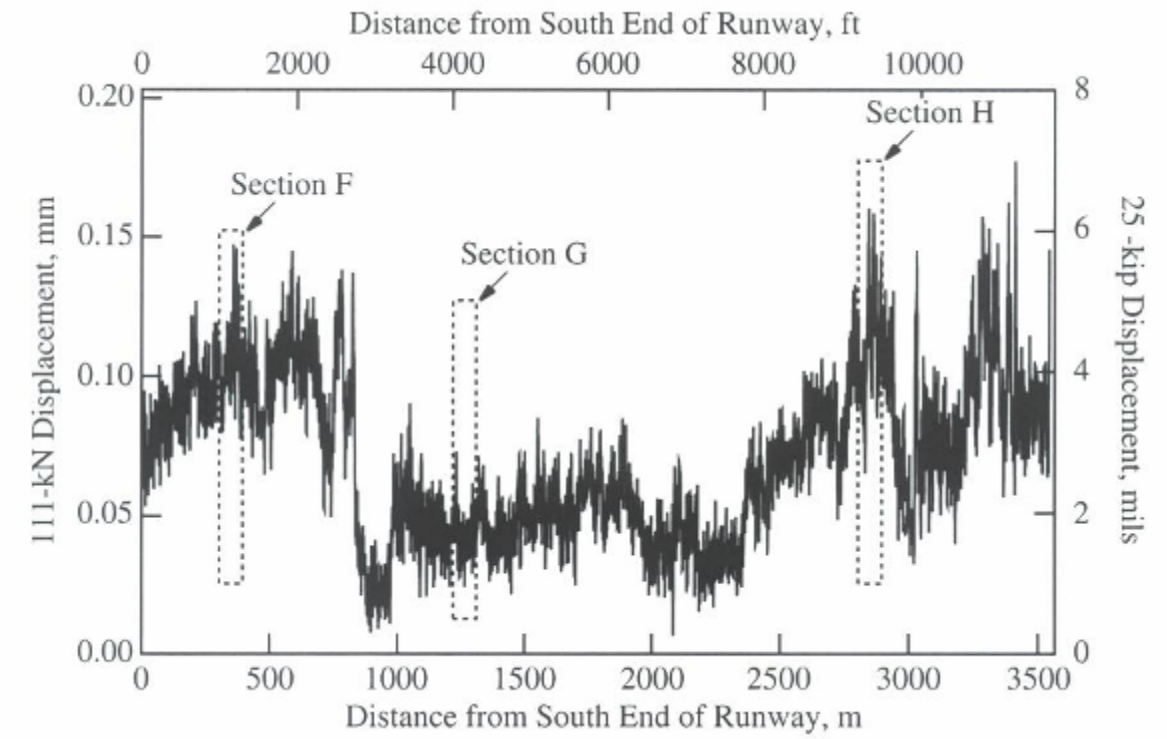

FIGURE C.9 Deflection Profile of Runway 16L-34R (Bay et. al. 2000)

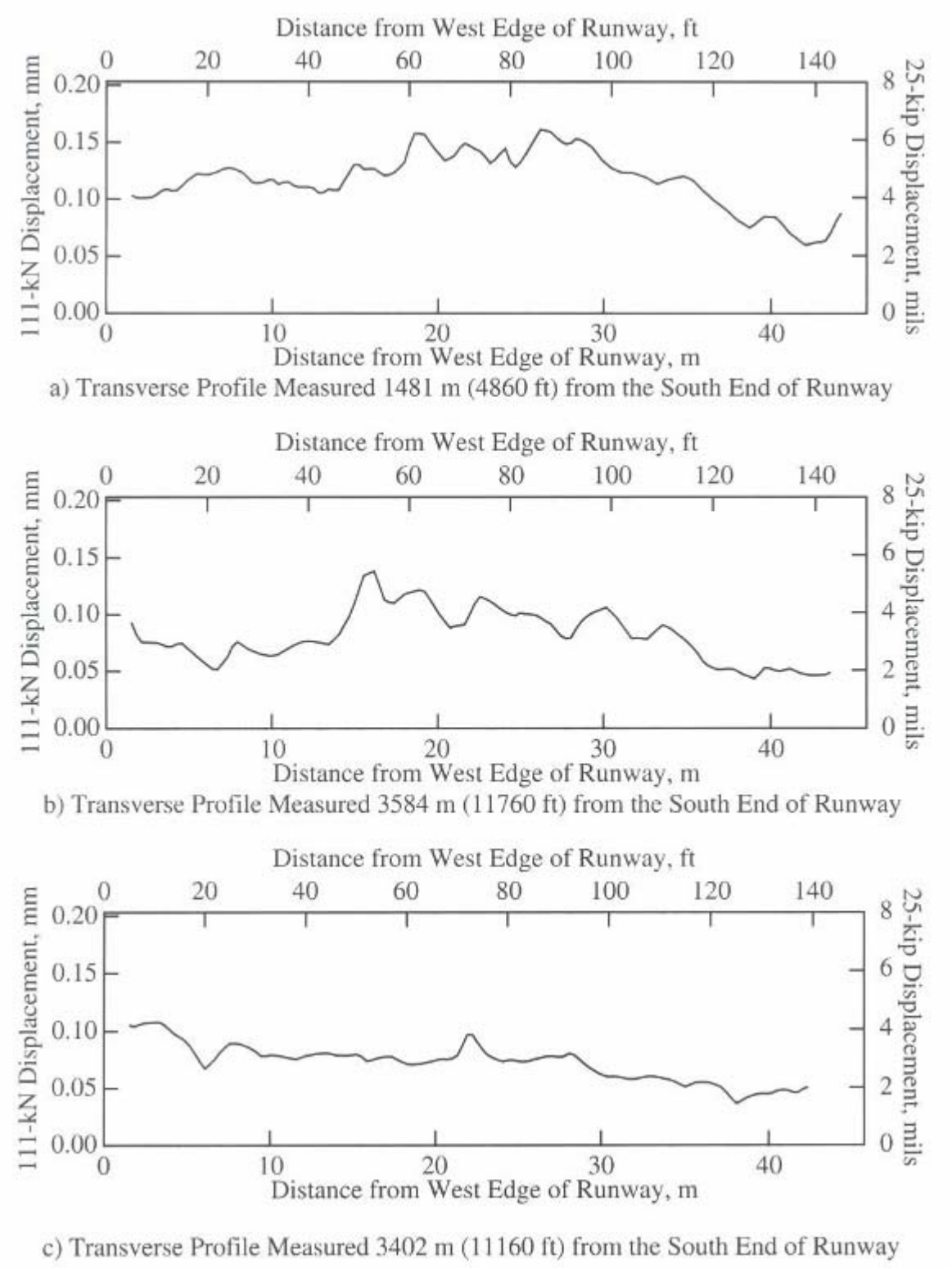

FIGURE C.10 Three Transverse Profiles for Runway 16L-34R (Bay et. al. 2000)

APPENDIX D THEORY OF OPERATION, AND FIELD EVALUATION RESULTS OF HIGH SPEED DEFLECTOMETER (HSD)

D.1 Theory of Operation

The Danish device, known as a High Speed Deflectograph (HSD), uses two laser sensors based on the Doppler technique to measure the deflection velocity of the road surface. One sensor measures the undeflected shape and the other measures the deflected shape. The difference of these two values is the deflection of the pavement. The load is applied through a load wheel that applies a load of magnitude of 11,000 lb (50 kN) and is monitored using a servo system. The motion of the sensors is monitored using inertial systems. The HSD trailer, shown in Figure D.1, can be towed at speeds up to 50 mph (80 km/h).

FIGURE D. 1 Danish HSD Trailer Showing Beam and Sensor Arrangement (Hildebrand, et. al. 2002)

The Doppler technique is based on the fact that the wavelength of any energy dispersion registered by a moving observer will be phase shifted by a factor (v/c) as described by Equation D.1.

$$F_{Doppler} = -F_{Source} \cdot \frac{V}{c} \tag{D.1}$$

Where v is the relative velocity between source and receiver, c is the wave propagation speed, $F_{Doppler}$ is the frequency shift at the receiver and F_{Source} is the emitted frequency. This principle is illustrated in Figure D.2 which shows that the wavelength of the emitted wave is reduced if the object is approaching and increased if the object is receding.

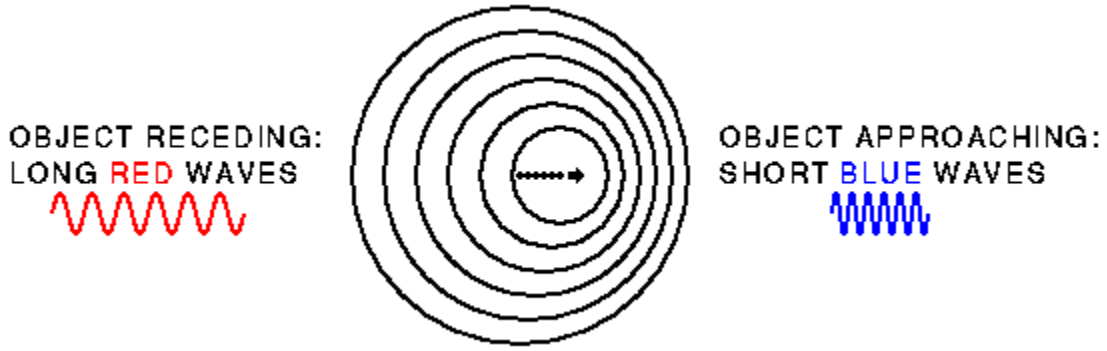

FIGURE D. 2 Doppler Principle (Hildebrand, et. al. 2002)

The application of this principle in the HSD is illustrated in the schematic in Figure D.3. Laser rays from the sensors strike the road surface and the sensors measure the velocity in the direction of the laser rays. The sensors are mounted on a rigid beam in front of the right wheel as shown in Figure D.3 and also visible in Figure D.1. They measure the velocity of deflection due to the load applied by the wheel.

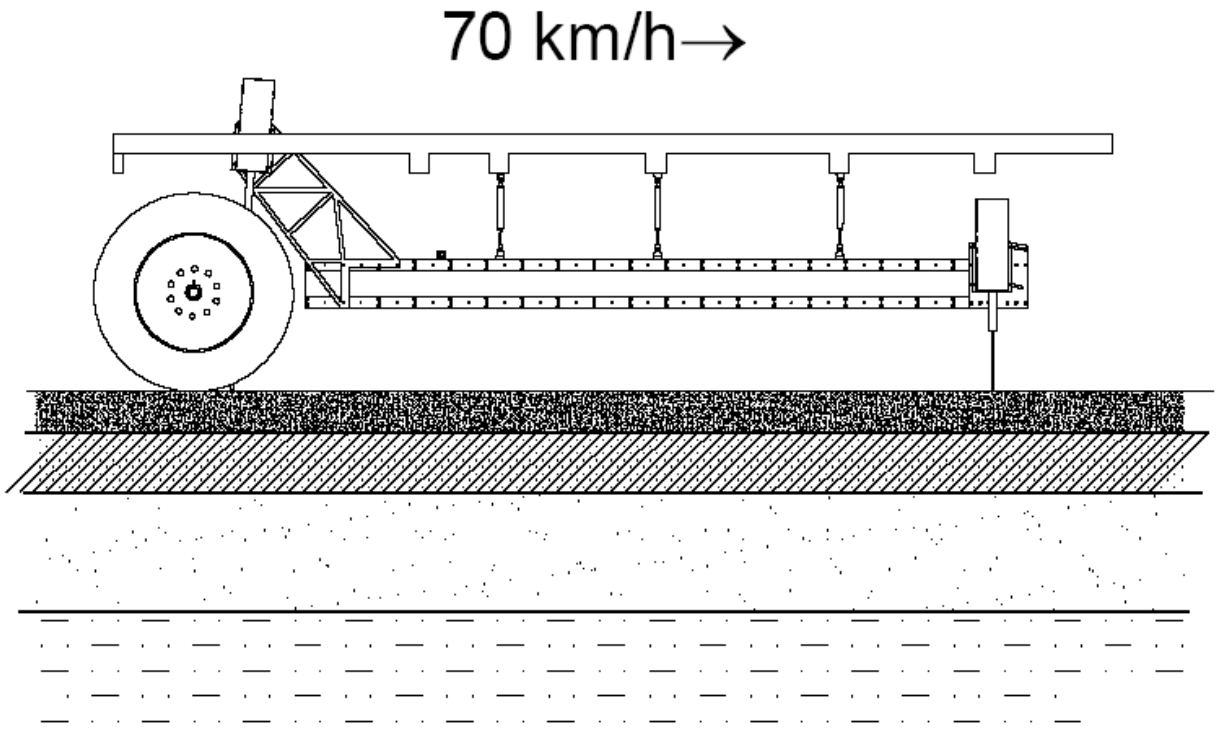

FIGURE D. 3 Schematic of the Sensor and Beam Arrangement in the HSD (Hildebrand, et. al., 2002)

Three accelerometers and three gyro sensors measure the velocity of the sensors and their angle of incidence with respect to the road. Using this data, the measured velocity is adjusted to account for the motion of the sensors and their angle of incidence with respect to road. The Doppler sensor movements are limited and controlled by a servo system mounted on the beam which assures that the sensors are focused at all times. The servo system is controlled by two distance measuring lasers at the ends of the beam. The adjustments are made using Equations D.2 and D.3 which apply to sensor measuring deflected shape and the reference sensor respectively.

$$V_{DS} = V_D + V_K \sin \alpha_{DS} \tag{D.2}$$

$$V_{RS} = V_K \sin \alpha_{RS} \tag{D.3}$$

Here V_{DS} is the measured velocity, V_D is the deflection velocity, V_K is the driving speed and α_{DS} is the angle of incident of the light from the sensor on the road where an angle of zero corresponds to perpendicular incident. In the second equation, V_{RS} is the velocity measured by the reference sensor, V_K is the driving speed and α_{RS} is the angle of incident of the light from the reference sensor on the road.

The HSD needs to be calibrated before use. The purpose of this calibration is to determine the difference between α_{DS} and α_{RS}. For this purpose, much of the load is removed from the trailer and then measurements are conducted on a very stiff road. It is then assumed that the deflection velocity being zero, the difference between V_{DS} and V_{RS} is solely due to the difference between α_{DS} and α_{RS}. The difference is then assumed to remain constant as the sensors are mounted on a stiff beam.

The HSD includes software for data acquisition and analysis. It is claimed that additional sensors can be added to the HSD to yield more than one deflection values which will give more detailed information about the shape of the deflection basin and make it possible to use standard techniques to analyze the data that has been acquired.

D.2 Field Evaluation Results

Hildebrand, et. al. (2002) tested the HSD on Motorway M30 between Maribo and Rødbyhavn in Denmark. This motorway has two lanes in each direction and consists of 9 in. to 11 in. (230 mm to 280 mm) asphalt concrete on top of more than 3.3 ft (1 m) of base and subbase materials composed of cement concrete, gravel and sand, with a subgrade of moraine clay. The measurements were conducted at speeds of 45 to 50 mph (70 to 80 km/h). Samples were collected at a frequency of 1000 Hz which corresponds to one sample every 0.8 in (20 mm) at a driving speed of 45 mph (72 km/h). A moving average of 500 samples is used for the deflection value.

The graph in Figure D.4 shows the repeatability of the deflection velocities when measured on the same road. The graph show good repeatability and the shift may have been caused by a difference in driving speed.

To compare the results of the HSD with the FWD, Equation D.4 was used to compute a deflection velocity from FWD deflections and an assumed driving speed of 45 mph (72 km/h).

$$V_{dFWD} = V_{ds} \frac{d_{200} - d_{300}}{d_{\Delta}} \tag{D.4}$$

Here V_{dFWD} is the estimated deflection velocity, V_{ds} is driving speed, d_{200} is the maximum deflection in the position 8 in. (200 mm) from the center of the load, d_{300} is the maximum deflection in the position 12 in. (300 mm) from the center of the load and, d_{Δ} is the distance between d_{200} and d_{300} (= 4 in. or 100 mm). Figures D.5 and D.6 show the comparison between two HSD tests and deflection velocities computed from FWD data. The graphs show good correlation between the deflection velocities measured by the HSD and the deflection velocity computed from the FWD deflections.

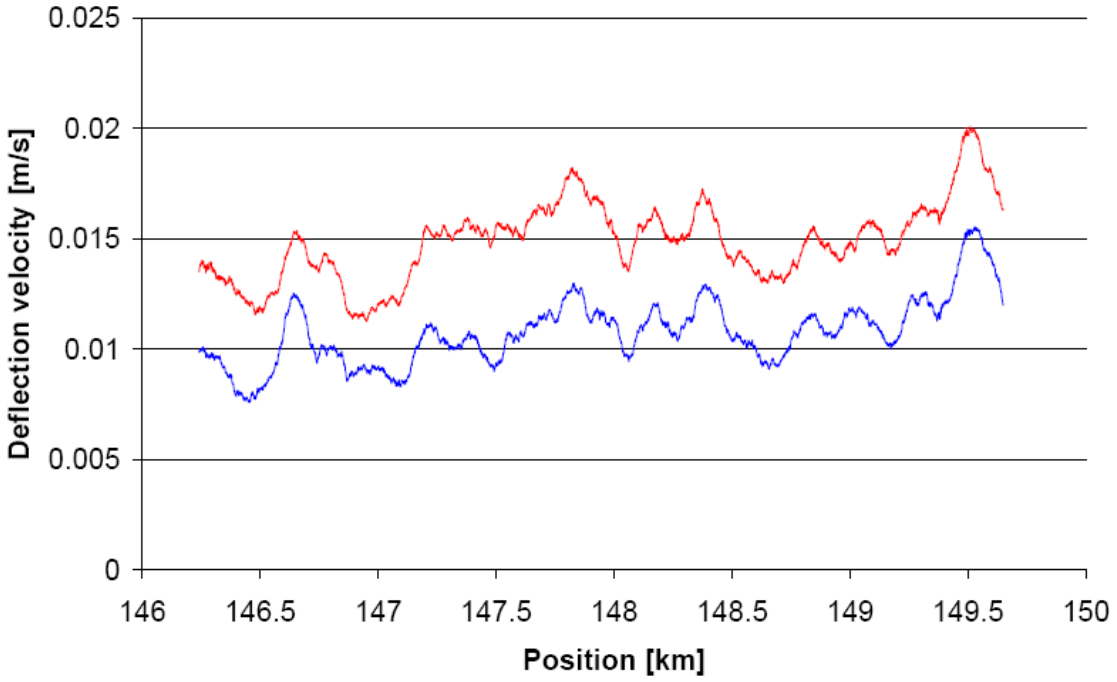

FIGURE D. 4 Repeatability of Deflection Velocities by the HSD (Hildebrand, et. al., 2002)

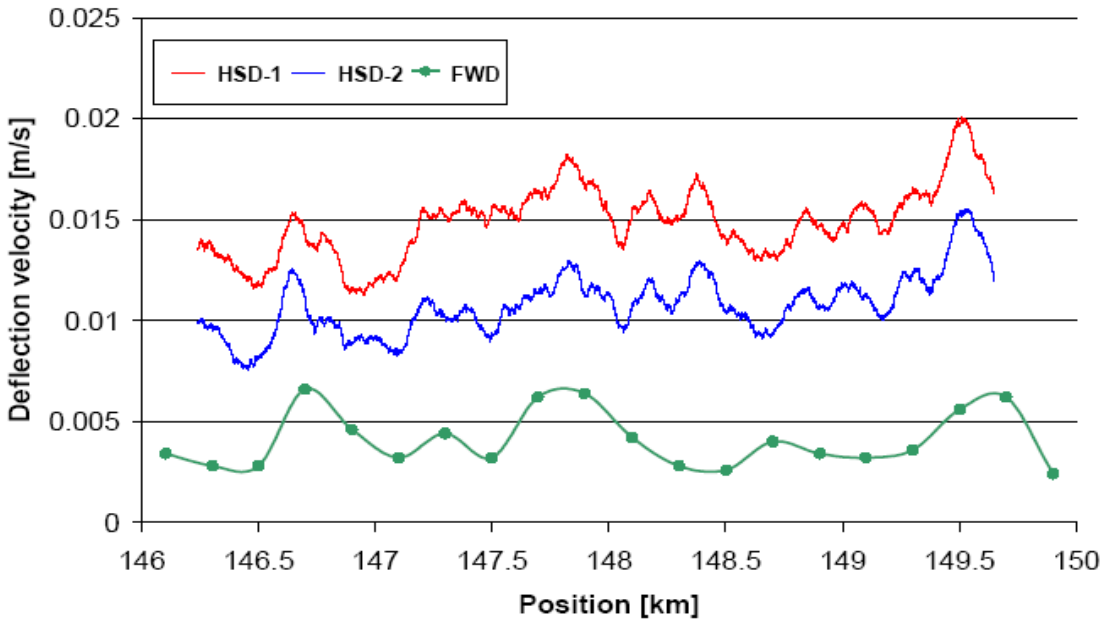

FIGURE D. 5 Comparison of Data From 2 HSD Tests and Deflection Velocities Computed From the FWD (Hildebrand, et. al., 2002)

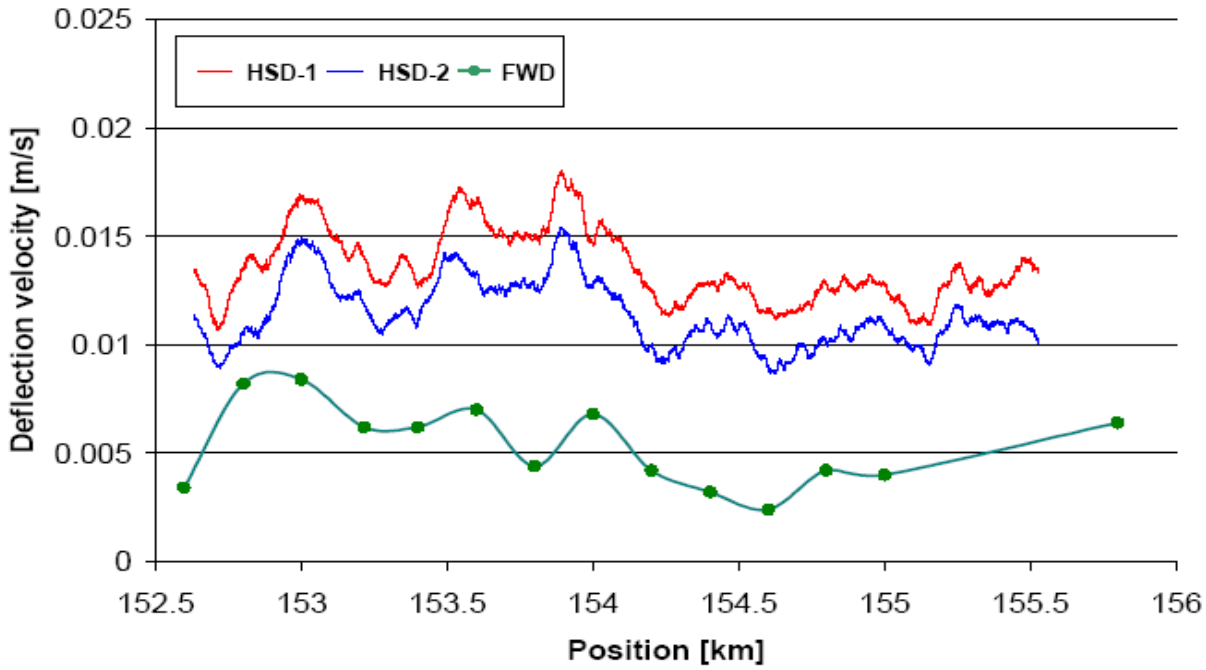

FIGURE D. 6 Comparison of HSD Data With Deflection Velocities Computed From the FWD (Hildebrand, et. al., 2002)

APPENDIX E QUESTIONNAIRE FOR CONTINUOUS TESTING EQUIPMENT

Availability and Cost

1. The device is

   (a) Prototype/Under development (b) Commercially available

2. If it is under development, what is the anticipated release date for a commercial version?

   _____

3. What is the anticipated cost of the device?

   $ _____

Device Functionality

4. The physical quantity(s) measured directly by the sensors is

   (a) Deflection (b) Velocity (c) Acceleration (d) Load

5. The types of sensors used in the device are:

   Load: _____ Deformation_____

6. The inherent accuracy of the deformation sensor is

   ± _____ mm or ± _____ mils

7. The inherent accuracy of the load sensor is

   ± _____ KN or ± _____ lbs

8. The accuracy of the device as a whole is

   ± _____ mm or ± _____ mils

9. What is the precision of the device?

   ± _____ mm or ± _____ mils

10. What is the resolution of the device?

± _____ mm or ± _____ mils

11. Does the device has GPS or similar device to identify test locations?

(a) Yes (b) No

12. If answer to the question 11 is no, how the location is identified?

_____

Device Operation

13. How many operators are required to operate the device?

(a) One (b) Two (c) More than two; please indicate _____

14. What is the level of training required for the operators?

(a) One month (b) Two months (c) Three months

(d) Other _____ months

15. What is the operational speed of the device?

_____ km/hr or _____ miles/hr

16. What is the operating cost of the device?

$ _____

17. Has a calibration process been developed for the device?

(a) Yes (b) No

18. How often calibration needs to be performed?

(a) Daily (b) Weekly (c) Monthly (d) Yearly (e) Every_____ miles or km

19. Can user perform the calibration?

(a) Yes (b) No

20. How long does it take to perform the calibration?

_____ days or hours

21. Does the device require proprietary software for processing the data?

(a) Yes **(b) No**

22. What is the output after processing?

(a) Deflections **(b) Layer thickness (es)** **(c) Layer moduli**

(d) Qualitative pavement condition

(e) Other; please specify _____

23. Is the output available in real time (immediately), or is post processing required at a central location?

(a) Real time (immediately) **(b) Post processing required**

24. If post processing is required, how long does it take?

_____ days/hours

25. What is the distance between successive readings?

_____ m or _____ ft

26. What is the typical applied load?

_____ KN or _____ lbs

27. Is it possible to vary the load?

(a) Yes **(b) No**

28. If yes, the load can be varied between

_____ KN/lb to _____ KN/lb in steps of _____KN/lb

Support and Service

29. Do you provide (or propose to provide) a warranty for the device?

(a) Yes **(b) No**

30. If yes, please indicate the term of the warranty

_____ months or years

31. Do you provide (or propose to provide) service contracts for service and support after the warranty period?

(a) Yes **(b) No**

32. If yes, please indicate the cost of a typical service contract

$ _____ /year

33. Can spare parts and replacements be ordered directly from you?

(a) Yes **(b) No**

Miscellaneous

34. Have you developed a specification sheet and schematic for the device?

(a) Yes (please enclose a copy) **(b) No**

35. The device is designed for

(a) Project level use **(b) Network level use**

36. The device is intended to

(a) Complement the FWD **(b) Replace the FWD**

39. Are there any reports available documenting results and comparison to FWD device?

(a) Yes (please enclose a copy of it) **(b) No**

THANK YOU

APPENDIX F TABLES FOR COMPUTATION OF SSI

F.1 Utility Factors (U_{FWD}) for Pavement Types 1, 2, 3, 4, and 5

Normalized SCI (mils)	Normalized W7 (mils)	U_{FWD}
0.01-9.99	0.01-1.20	1.00
	1.21-1.99	0.90
	2.00-99.99	0.80
10.00-15.99	0.01-1.20	0.80
	1.21-1.99	0.70
	2.00-99.99	0.55
16.00-20.99	0.01-1.20	0.60
	1.21-1.99	0.50
	2.00-99.99	0.40
21.00-25.99	0.01-1.20	0.40
	1.21-1.99	0.35
	2.00-99.99	0.30
26.00-29.99	0.01-1.20	0.30
	1.21-1.99	0.25
	2.00-99.99	0.20
30.00-99.99	0.01-1.20	0.20
	1.21-1.99	0.15
	2.00-99.99	0.10

F.2 Utility Factors (U_{FWD}) for Pavement Types 6, 7, 8, and 9

Normalized SCI (mils)	Normalized W7 (mils)	U_{FWD}
0.01-14.99	0.01-1.20	1.00
	1.21-1.99	0.90
	2.00-99.99	0.80
15.00-20.99	0.01-1.20	0.80
	1.21-1.99	0.70
	2.00-99.99	0.55
21.00-25.99	0.01-1.20	0.60
	1.21-1.99	0.50
	2.00-99.99	0.40
26.00-30.99	0.01-1.20	0.40
	1.21-1.99	0.35
	2.00-99.99	0.30
31.00-35.99	0.01-1.20	0.30
	1.21-1.99	0.25
	2.00-99.99	0.20
36.00-99.99	0.01-1.20	0.20
	1.21-1.99	0.15
	2.00-99.99	0.10

F.3 Utility Factors (U_{FWD}) for Pavement Type 10

Normalized SCI (mils)	Normalized W7 (mils)	U_{FWD}
0.01-19.99	0.01-1.20	1.00
	1.21-1.99	0.90
	2.00-99.99	0.80
20.00-25.99	0.01-1.20	0.80
	1.21-1.99	0.70
	2.00-99.99	0.55
26.00-30.99	0.01-1.20	0.60
	1.21-1.99	0.50
	2.00-99.99	0.40
31.00-35.99	0.01-1.20	0.40
	1.21-1.99	0.35
	2.00-99.99	0.30
36.00-39.99	0.01-1.20	0.30
	1.21-1.99	0.25
	2.00-99.99	0.20
40.00-99.99	0.01-1.20	0.20
	1.21-1.99	0.15
	2.00-99.99	0.10

The Rainfall Factor (RF) is based on the average annual rainfall and is obtained from Table B3

F.4 Rainfall Factor from Average Annual Rainfall

Average Annual Rainfall (inches)	Rainfall Factor (RF)
0.01 — 20.00	1.00
20.01 — 40.00	0.97
40.01 — 99.99	0.94

F.5 Traffic Factor Based on Pavement Type and 18 kip ESAL

Pavement Type	18-k ESAL (millions)	Traffic Factor (TF)
1	0.001-17.000	1.30
	17.001-27.000	1.15
	27.001-40.000	1.00
	40.001-54.000	0.85
	54.001-999.999	0.70
2	0.001-4.100	1.30
	4.101-8.300	1.15
	8.301-22.000	1.00
	22.001-43.000	0.85
	43.001-999.999	0.70
3	0.001-0.600	1.30
	0.601-7.300	1.15
	7.301-26.000	1.00
	26.001-27.000	0.85
	27.001-999.999	0.70
4	0.001-6.000	1.30
	6.001-11.000	1.15
	11.001-18.000	1.00
	18.001-26.000	0.85
	26.001-999.999	0.70
5	0.001-1.500	1.30
	1.501-3.100	1.15
	3.101-6.500	1.00
	6.501-21.000	0.85
	21.001-999.999	0.70

Pavement Type	18-k ESAL (millions)	Traffic Factor (TF)
6	0.001-0.500	1.30
	0.501-1.400	1.15
	1.401-2.700	1.00
	2.701-7.500	0.85
	7.501-999.999	0.70
7	0.001-1.700	1.30
	1.701-6.300	1.15
	6.301-22.000	1.00
	22.001-33.000	0.85
	33.001-999.999	0.70
8	0.001-1.700	1.30
	1.701-3.800	1.15
	3.801-12.500	1.00
	12.501-34.600	0.85
	34.601-999.999	0.70
9	0.001-0.260	1.30
	0.261-1.400	1.15
	1.401-3.200	1.00
	3.201-6.400	0.85
	6.401-999.999	0.70
10	0.001-0.090	1.30
	0.091-0.240	1.15
	0.241-0.790	1.00
	0.791-3.400	0.85
	3.401-999.999	0.70

APPENDIX G SSI RESULTS FROM DALLAS AREA DATA

G.1 SSI Score Compared With Deflection Data for Pavement Type 1

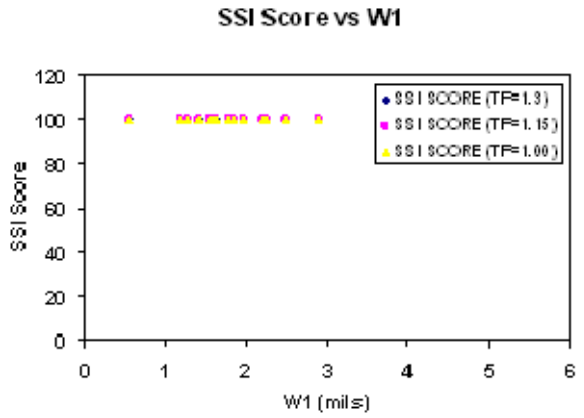

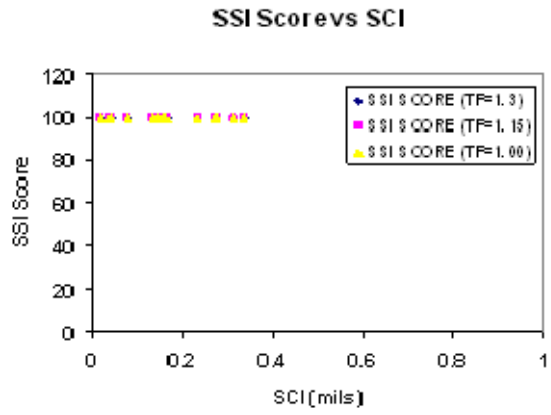

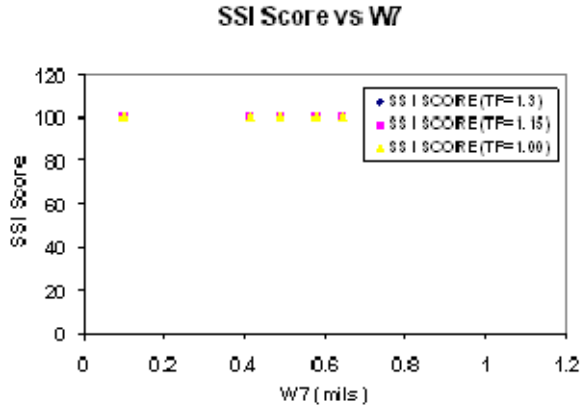

G.2 SSI Score Compared With Deflection Data for Pavement Type 5

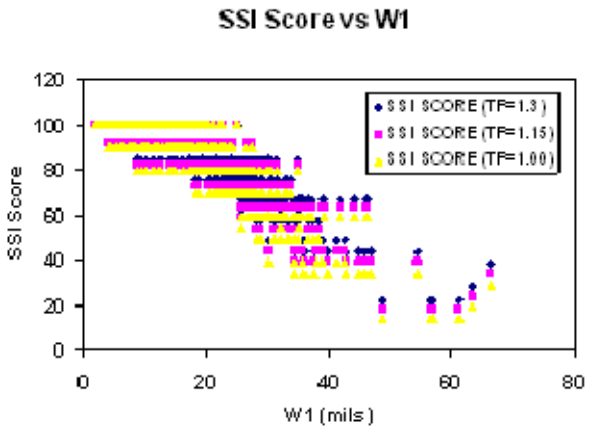

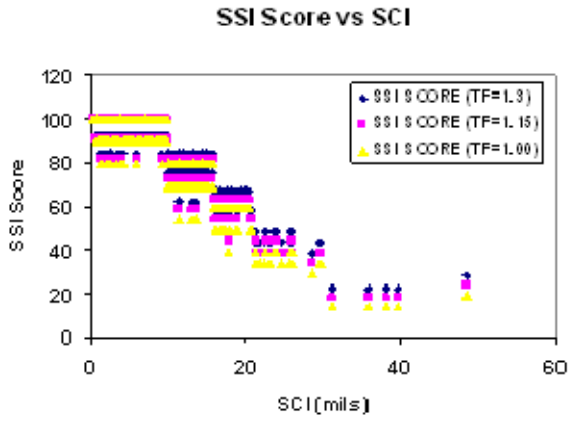

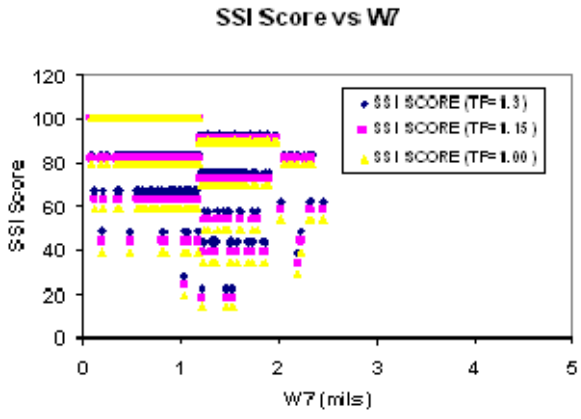

G.3 SSI Score Compared With Deflection Data for Pavement Type 6

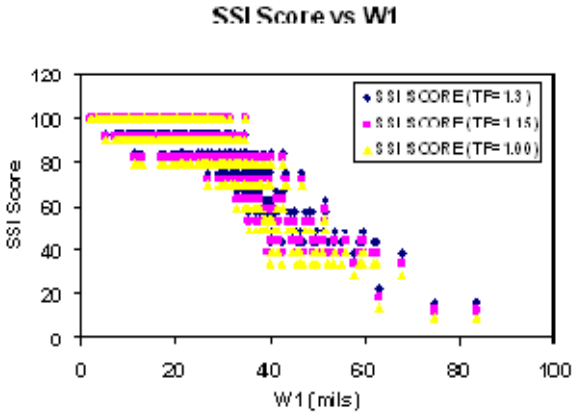

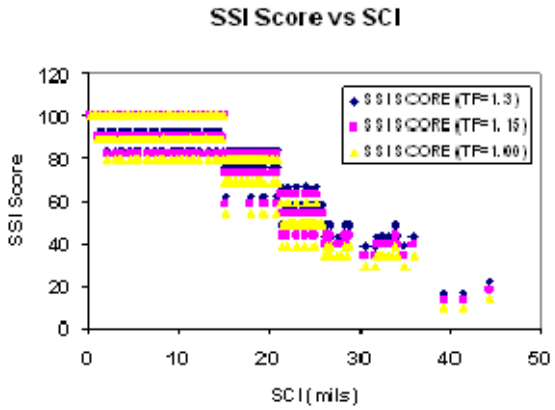

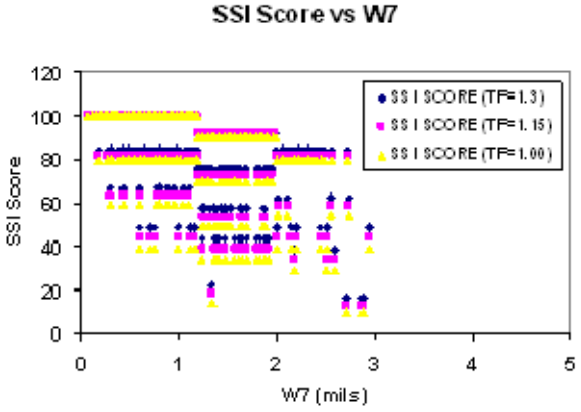

G.4 SSI Score Compared With Deflection Data for Pavement Type 8

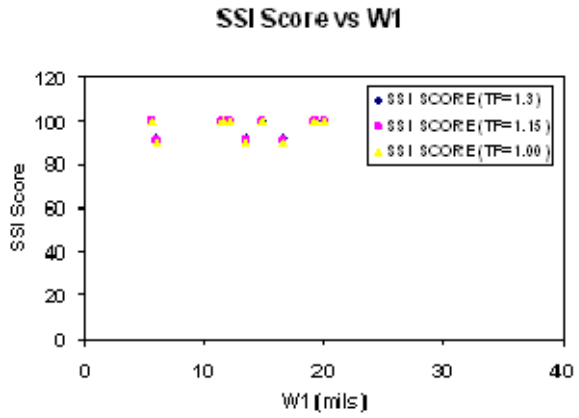

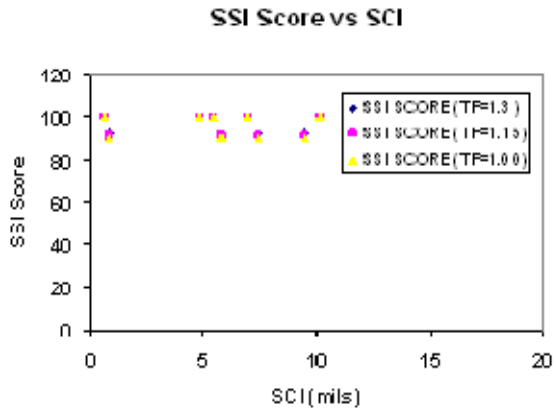

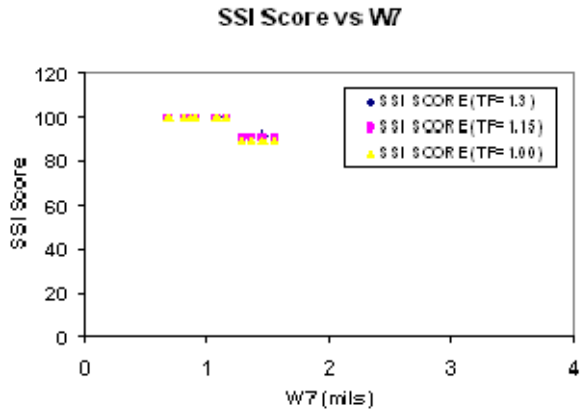

G.5 SSI Score Compared With Deflection Data for Pavement Type 10

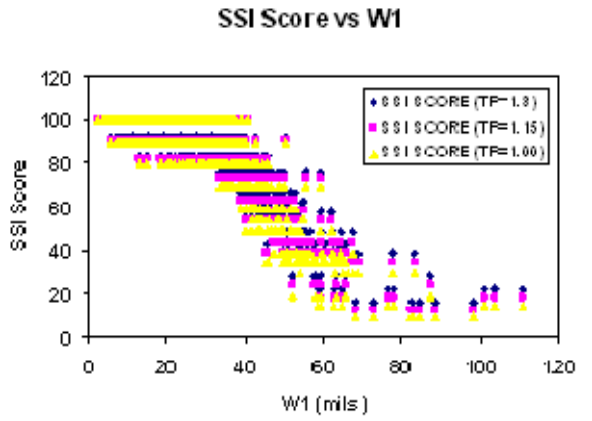

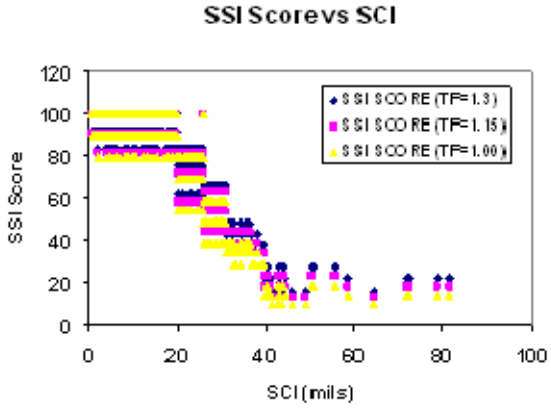

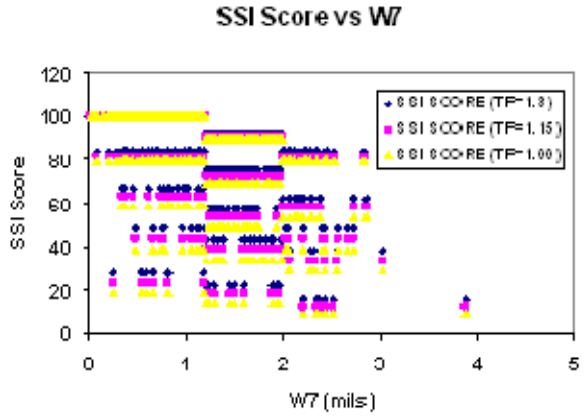

APPENDIX H SSI RESULTS FROM SIMULATED DATA

H.1 SSI Score Compared with W7

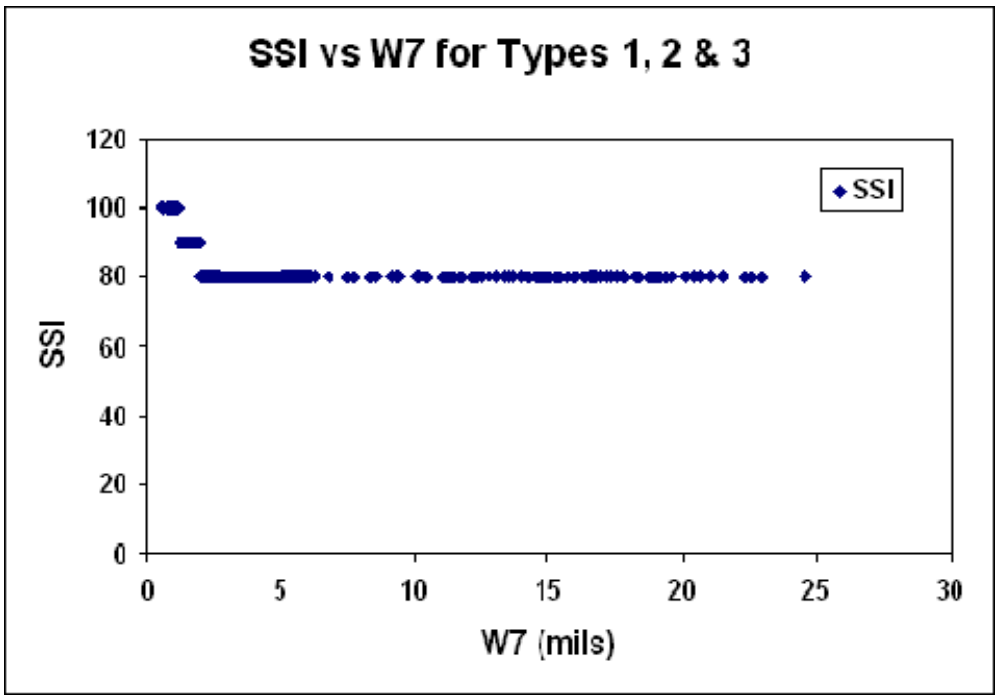

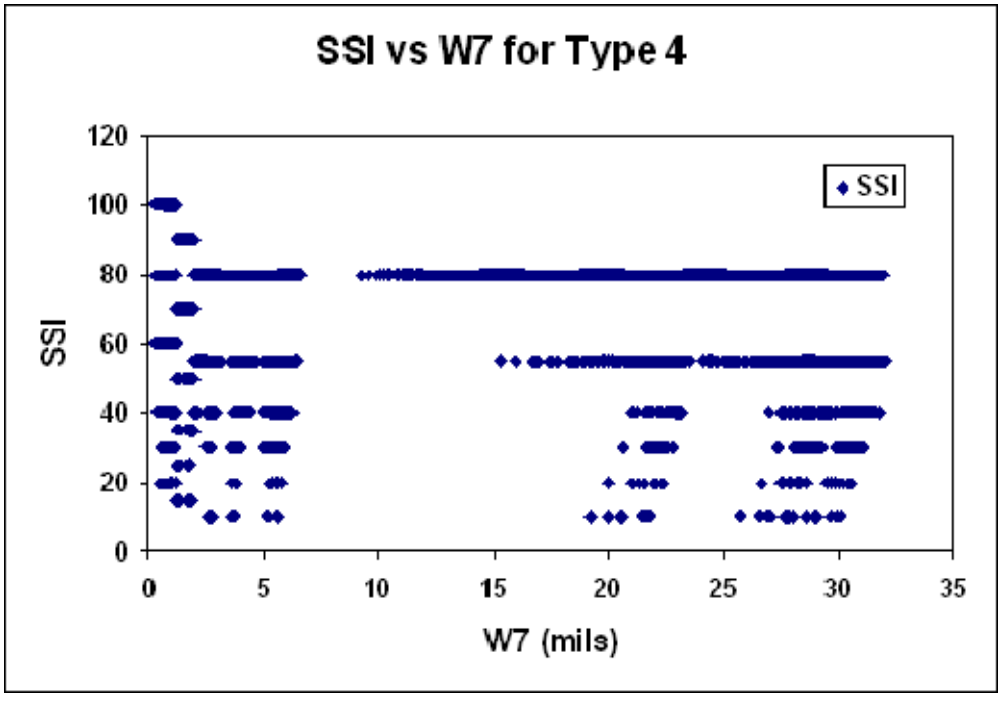

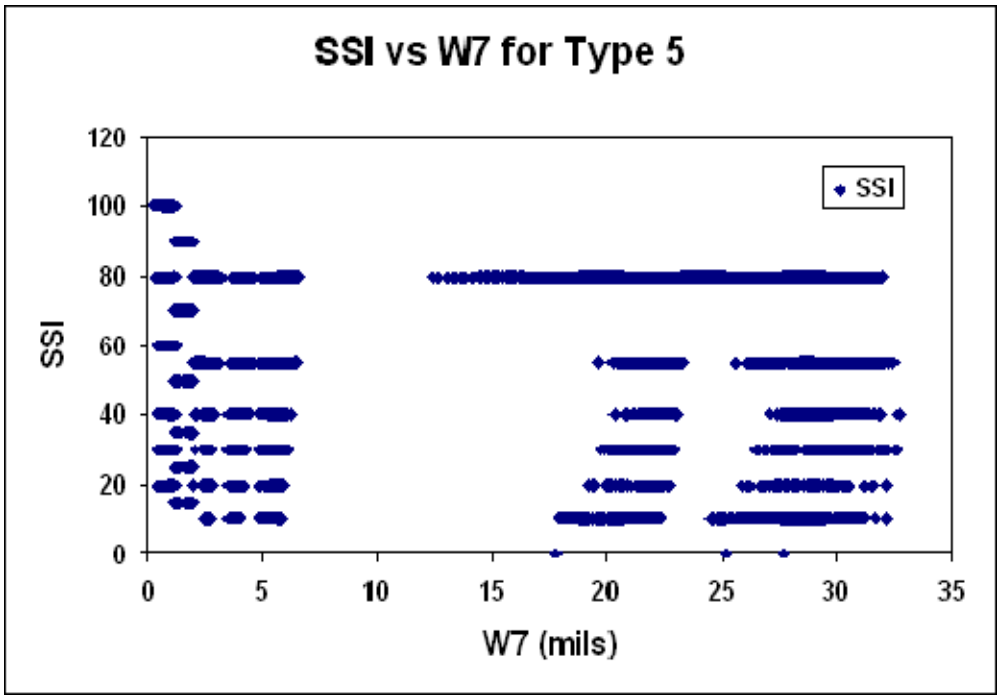
SSI vs W7 for Type 5
SSI
120
100
80
60
40
20
0
0
5
10
15
20
25
30
35
W7 (mils)
SSI

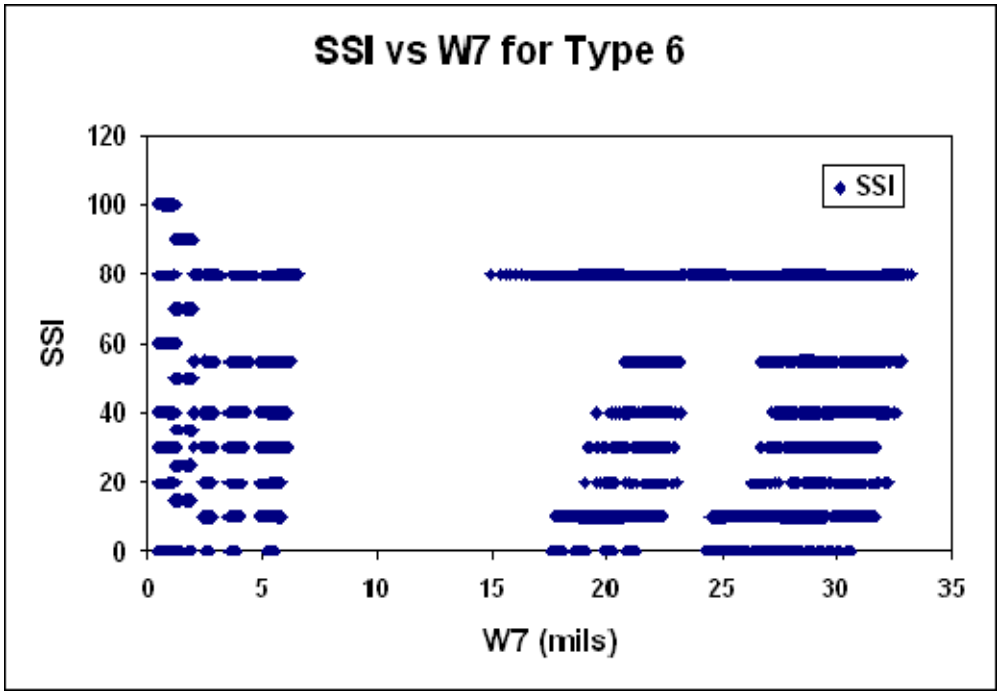
SSI vs W7 for Type 6
SSI
120
100
80
60
40
20
0
0
5
10
15
20
25
30
35
W7 (mils)
SSI

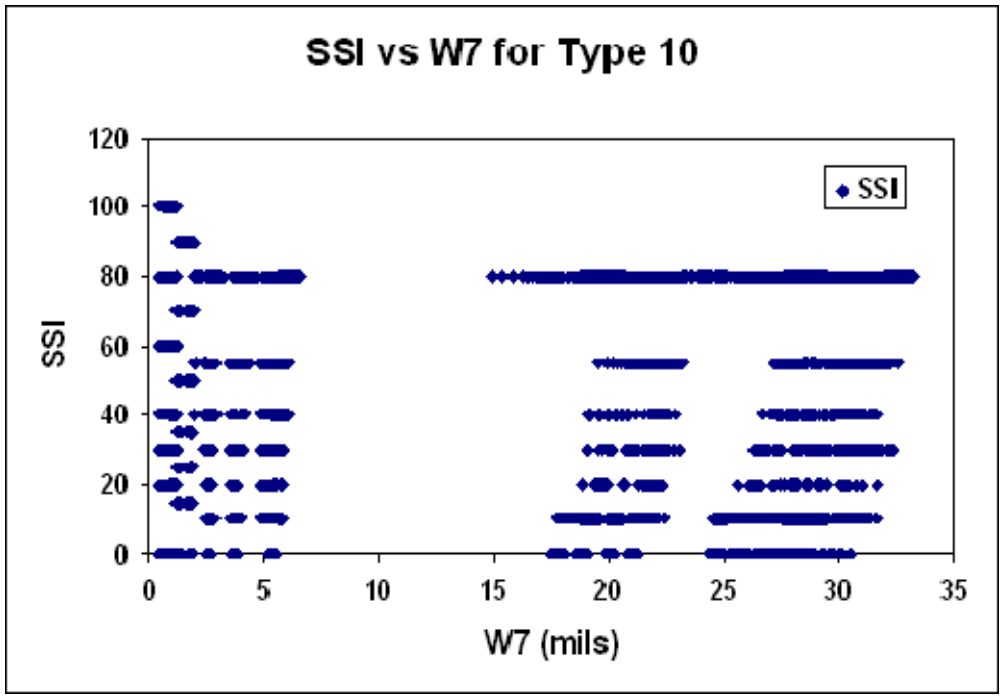
SSI vs W7 for Type 10
SSI
120
100
80
60
40
20
0
0
5
10
15
20
25
30
35
W7 (mils)
SSI

H.2 SSI Score Compared with SCI

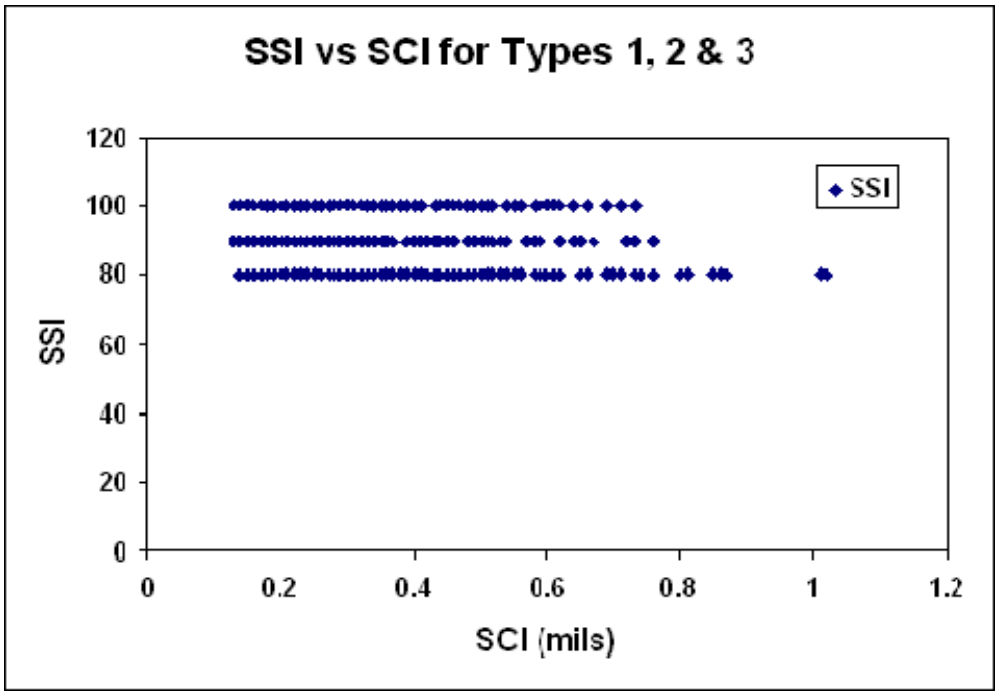

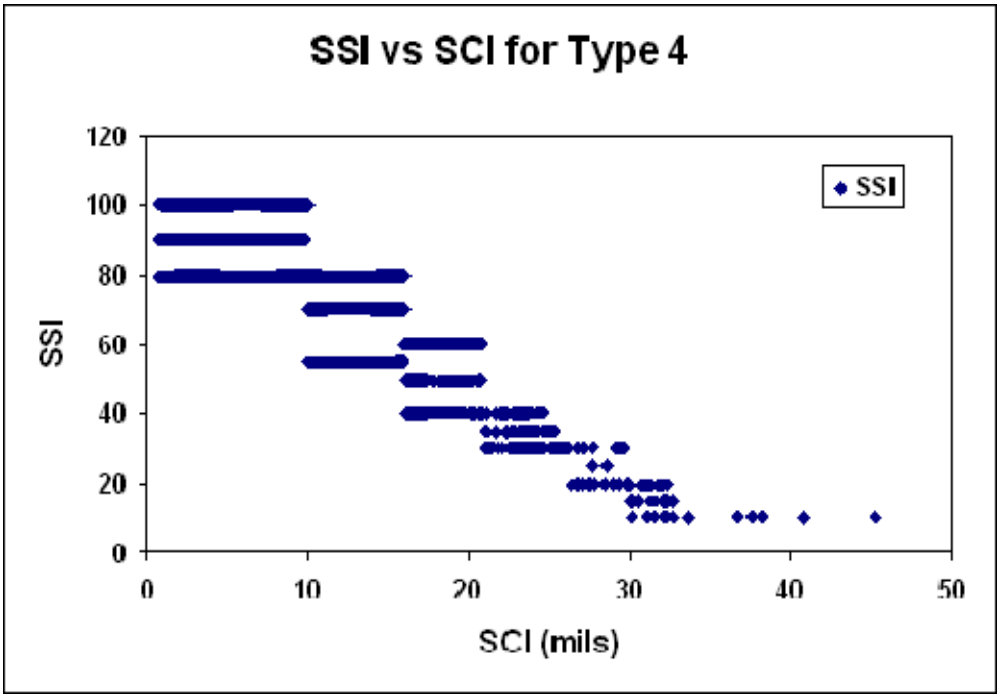

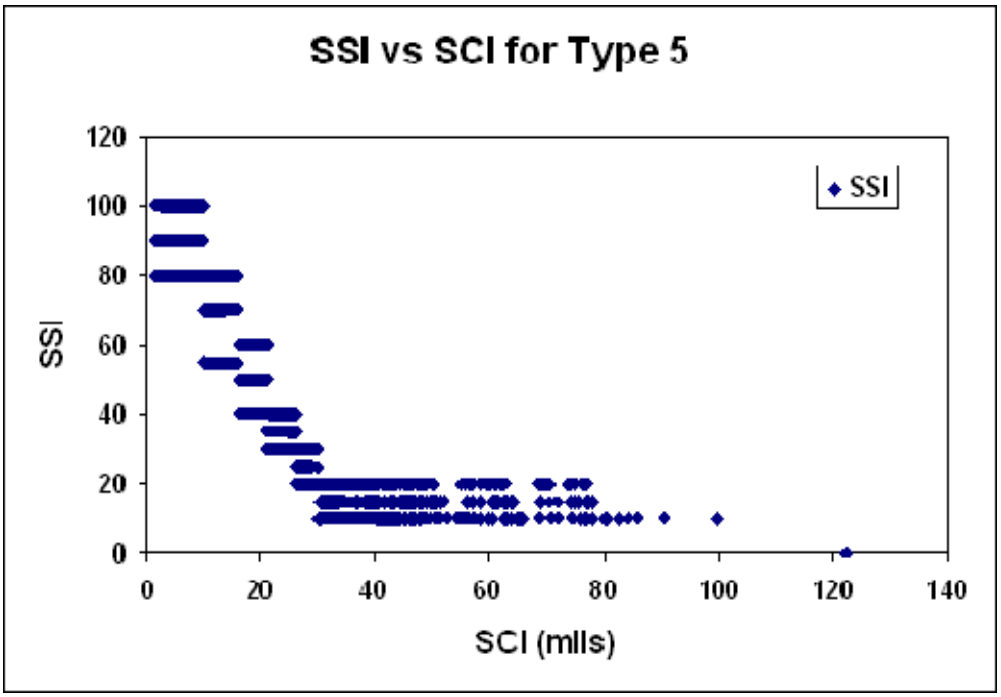
SSI vs SCI for Type 5
SSI
SCI (mils)
0
20
40
60
80
100
120
140
SSI

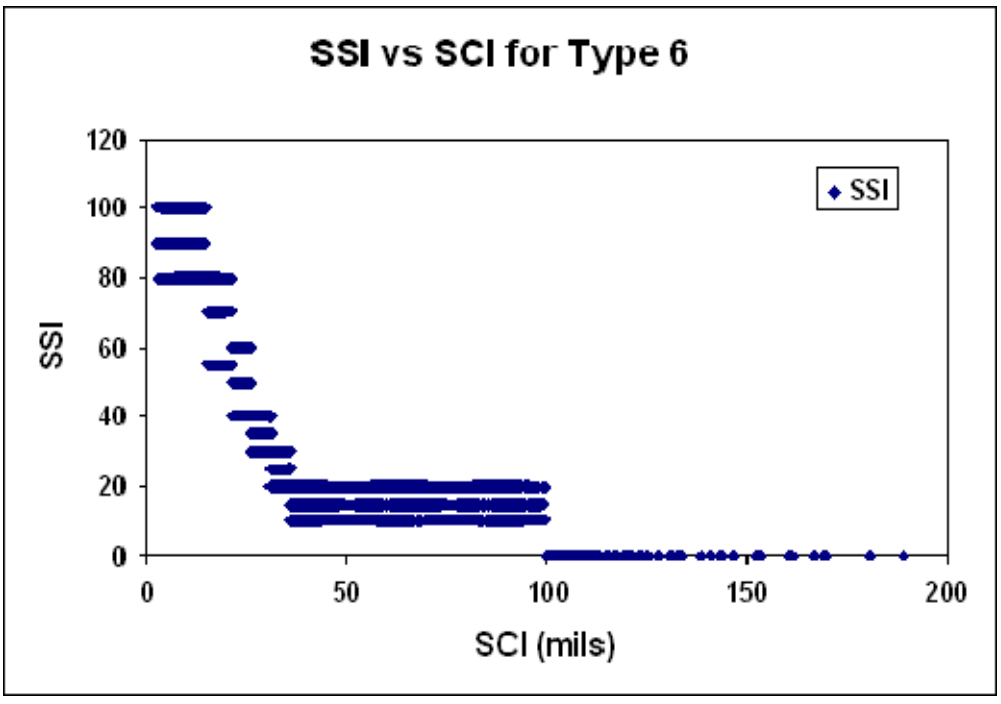
SSI vs SCI for Type 6
SSI
SCI (mils)
0
50
100
150
200
SSI

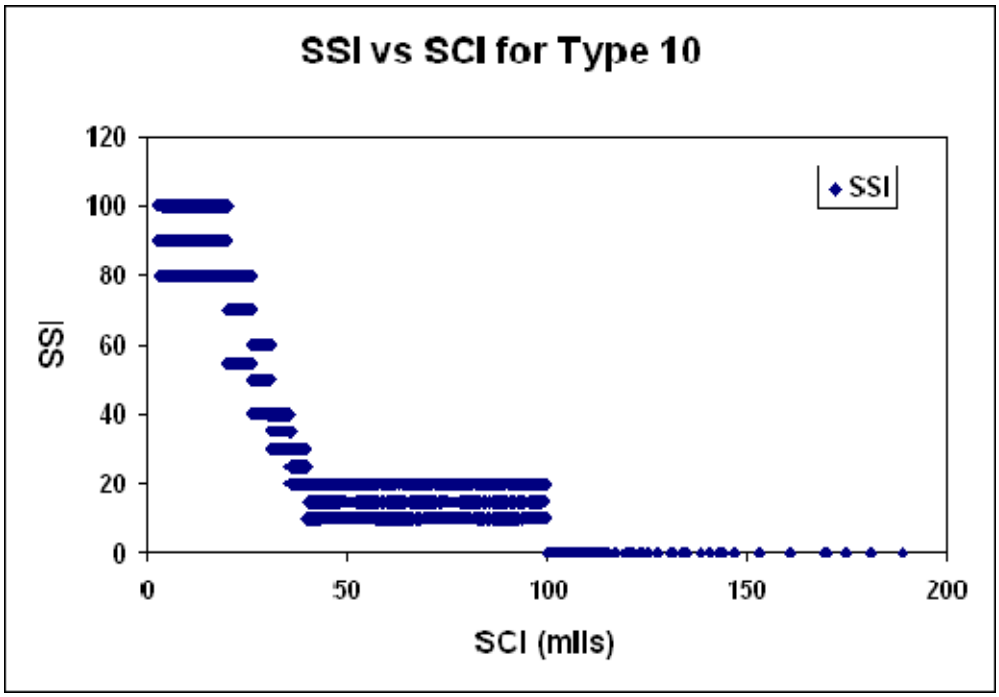
SSI vs SCI for Type 10
120
100
80
60
40
20
0
SSI
0
50
100
150
200
SCI (mils)
SSI

APPENDIX I RESULTS OF INITIAL INVESTIGATION OF MORE THAN ONE SENSOR

I.1 Method I

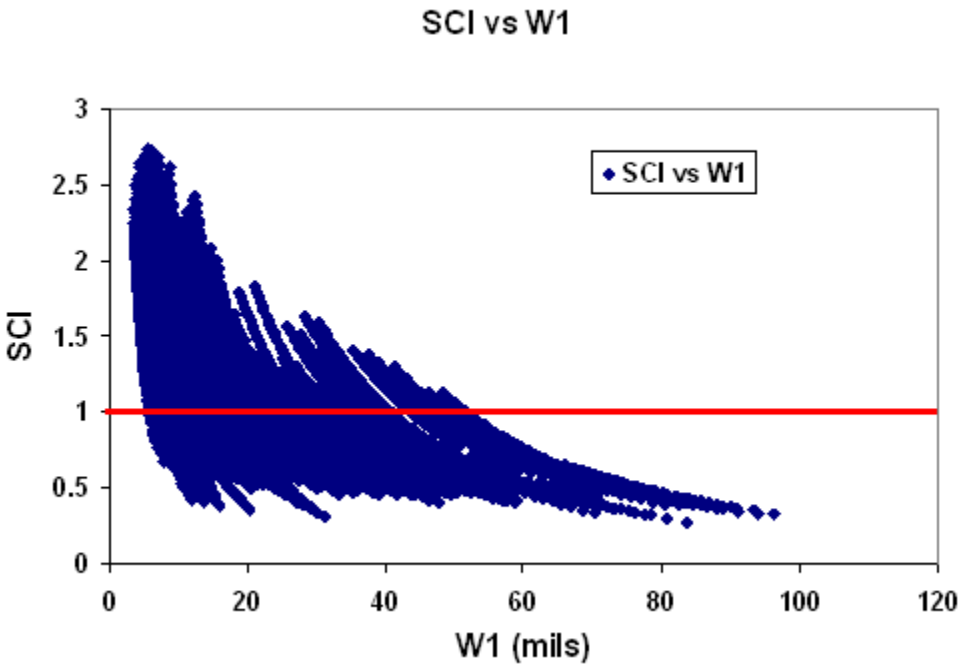

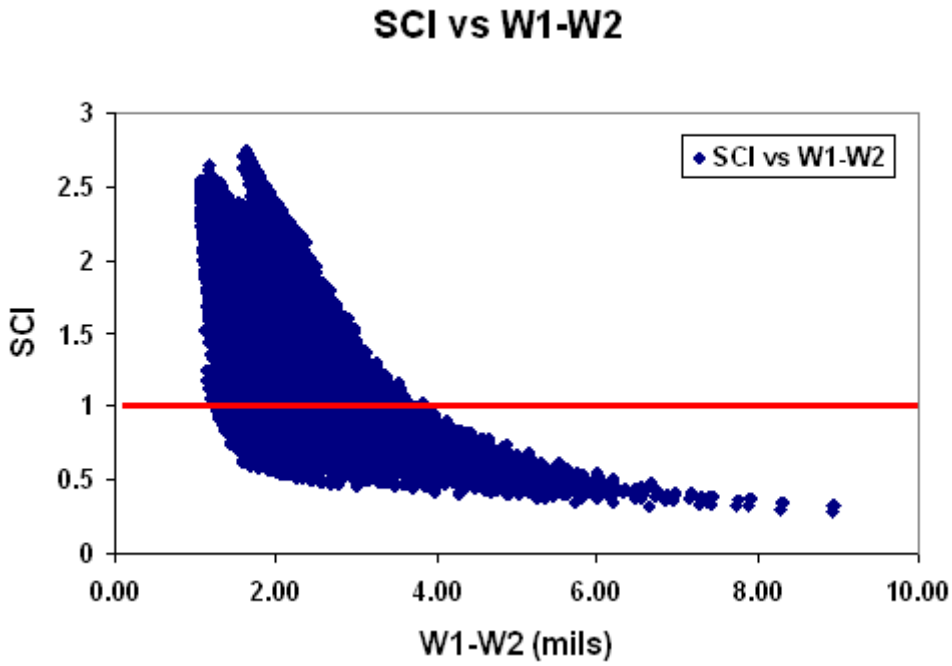
SCI vs W1-W2
SCI vs W1-W2
SCI
W1-W2 (mils)
0
0.5
1
1.5
2
2.5
3
0.00
2.00
4.00
6.00
8.00
10.00

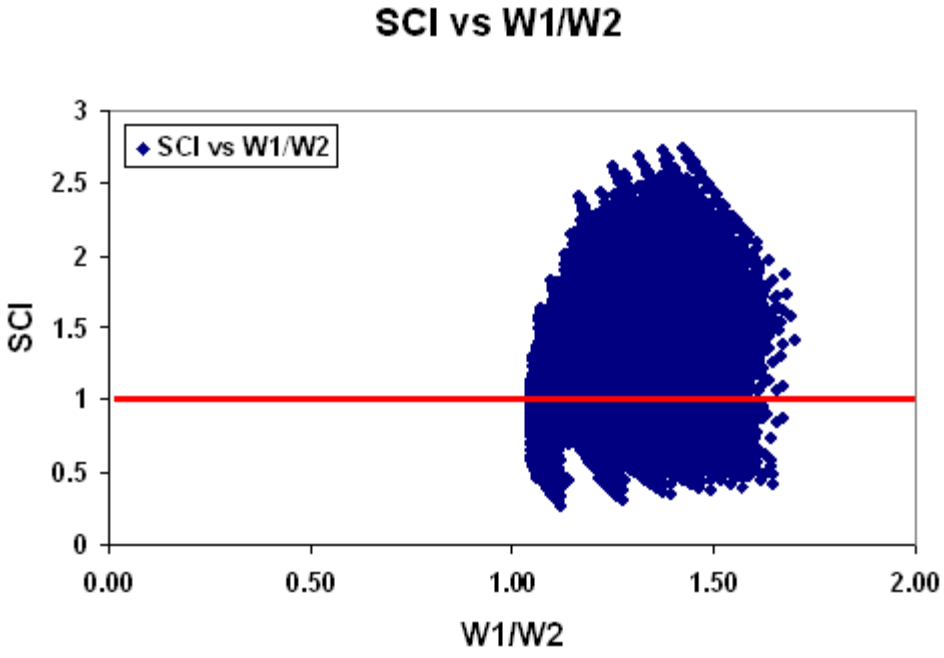
SCI vs W1/W2
SCI vs W1/W2
SCI
W1/W2
0
0.5
1
1.5
2
2.5
3
0.00
0.50
1.00
1.50
2.00

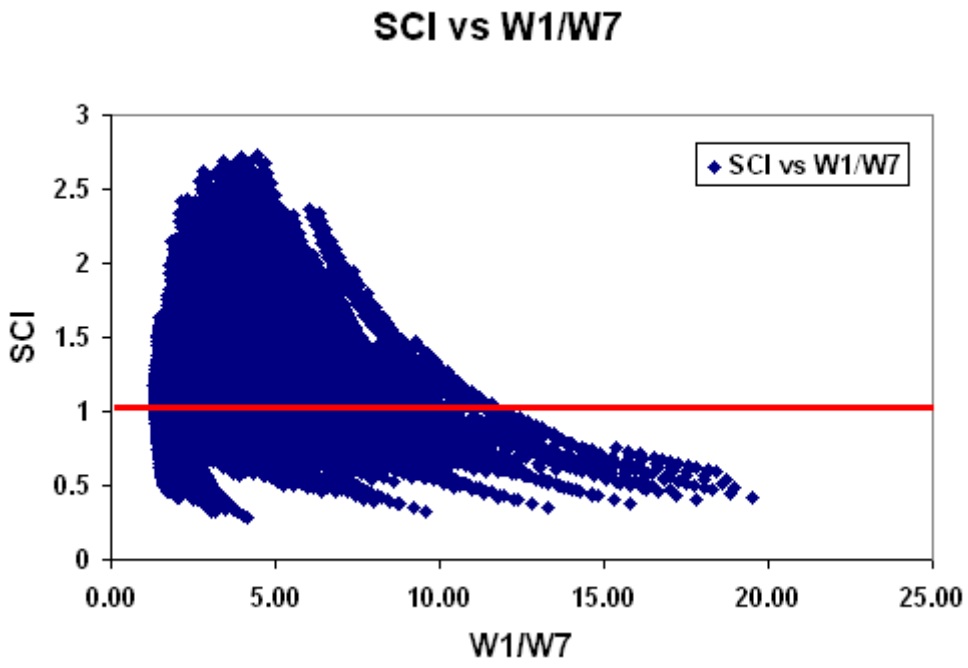
SCI vs W1/W7
SCI vs W1/W7
SCI
W1/W7
3
2.5
2
1.5
1
0.5
0
0.00
5.00
10.00
15.00
20.00
25.00

I.2 Method II

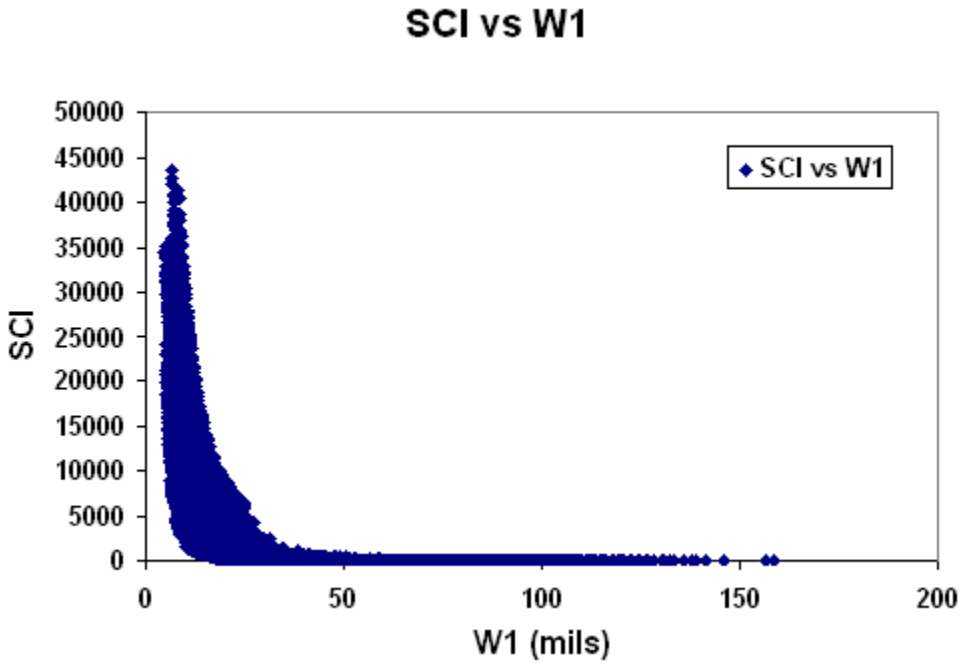
SCI vs W1
SCI vs W1
SCI
W1 (mils)
50000
45000
40000
35000
30000
25000
20000
15000
10000
5000
0
0
50
100
150
200

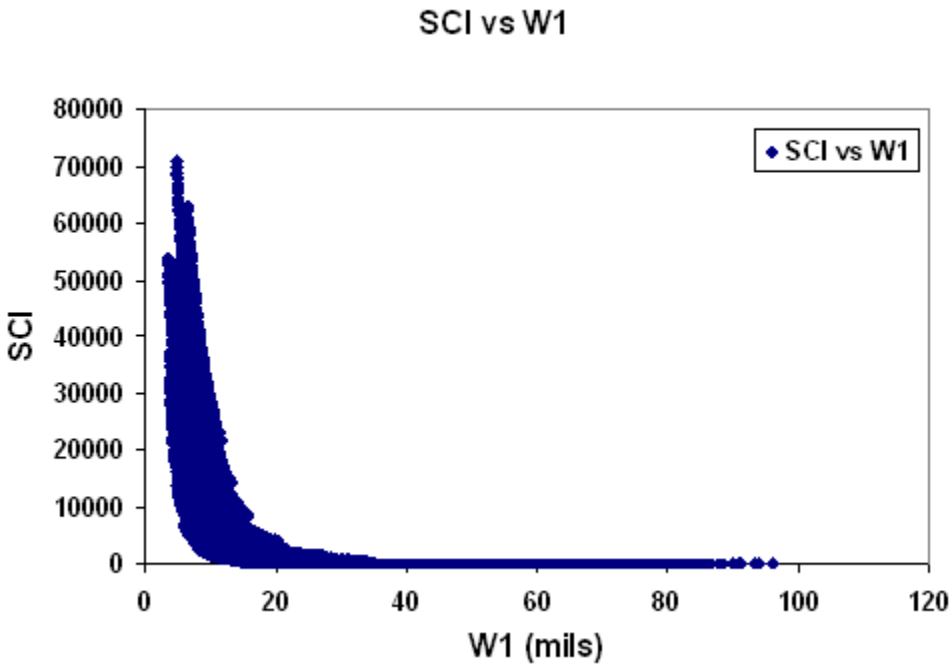
SCI vs W1
SCI vs W1
80000
70000
60000
50000
40000
30000
20000
10000
0
SCI
0
20
40
60
80
100
120
W1 (mils)

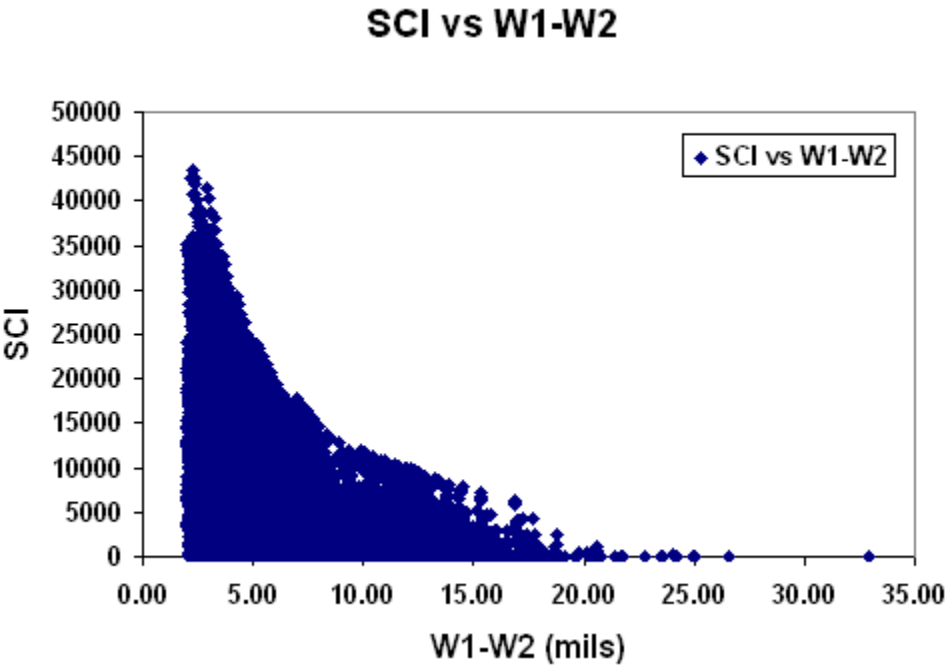
SCI vs W1-W2
SCI vs W1-W2
50000
45000
40000
35000
30000
25000
20000
15000
10000
5000
0
SCI
0.00
5.00
10.00
15.00
20.00
25.00
30.00
35.00
W1-W2 (mils)

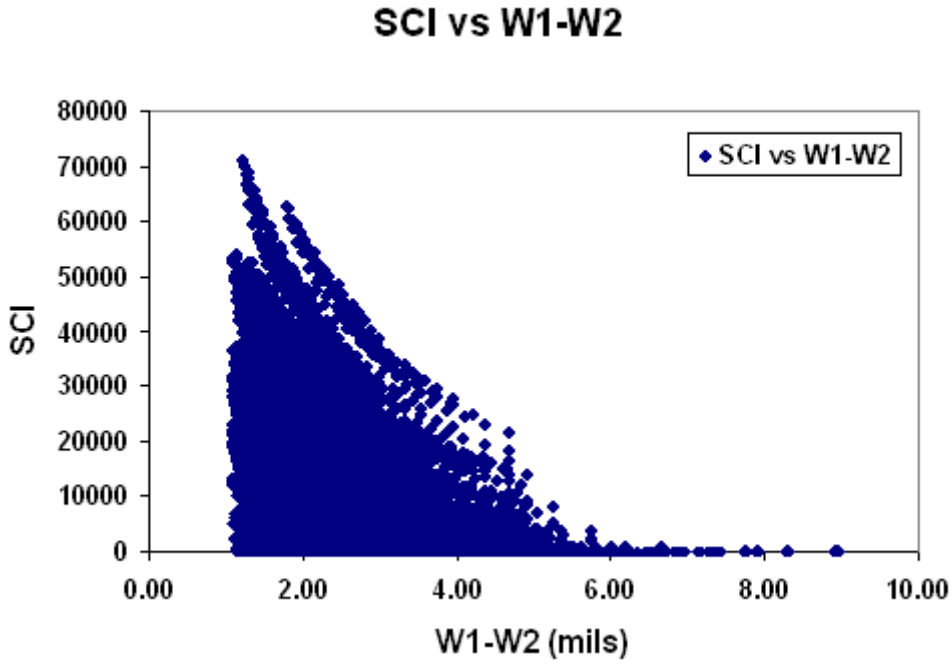
SCI vs W1-W2
SCI vs W1-W2
80000
70000
60000
50000
40000
30000
20000
10000
0
SCI
0.00
2.00
4.00
6.00
8.00
10.00
W1-W2 (mils)

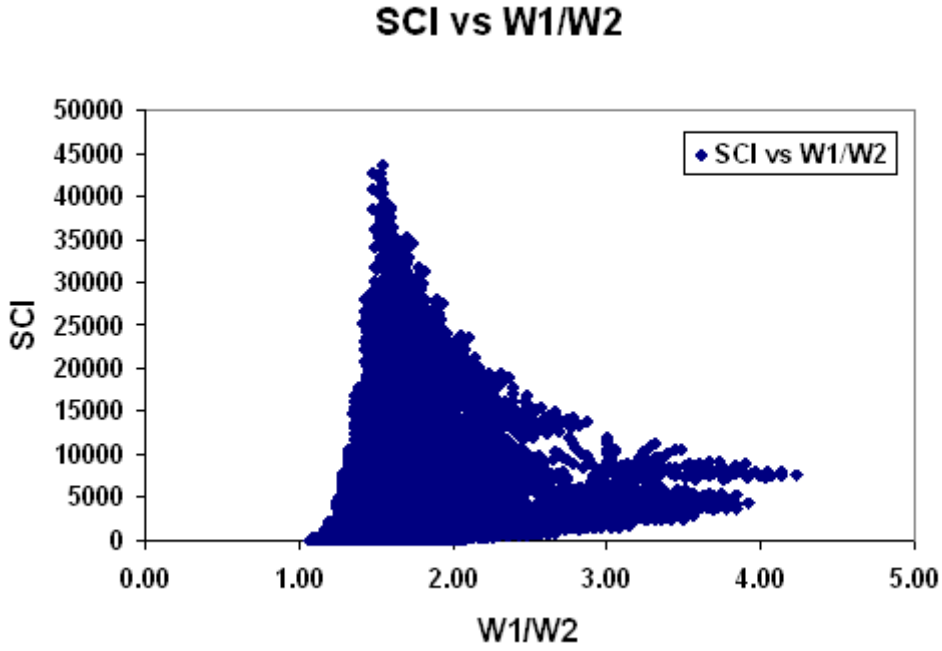
SCI vs W1/W2
SCI vs W1/W2
50000
45000
40000
35000
30000
25000
20000
15000
10000
5000
0
SCI
0.00
1.00
2.00
3.00
4.00
5.00
W1/W2

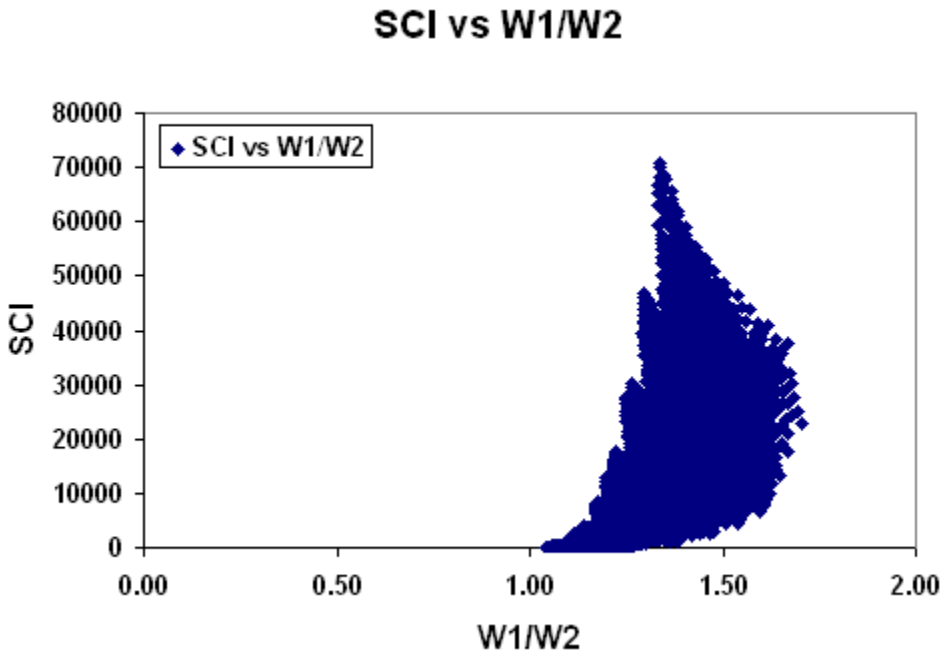
SCI vs W1/W2
SCI vs W1/W2
80000
70000
60000
50000
40000
30000
20000
10000
0
SCI
0.00
0.50
1.00
1.50
2.00
W1/W2

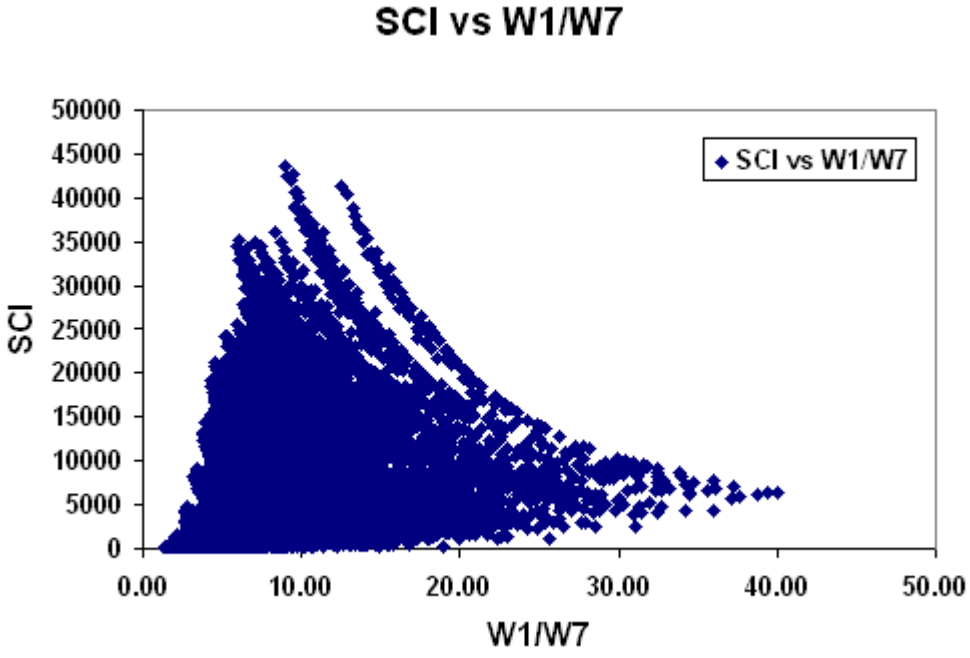
SCI vs W1/W7
SCI vs W1/W7
50000
45000
40000
35000
30000
25000
20000
15000
10000
5000
0
SCI
0.00
10.00
20.00
30.00
40.00
50.00
W1/W7

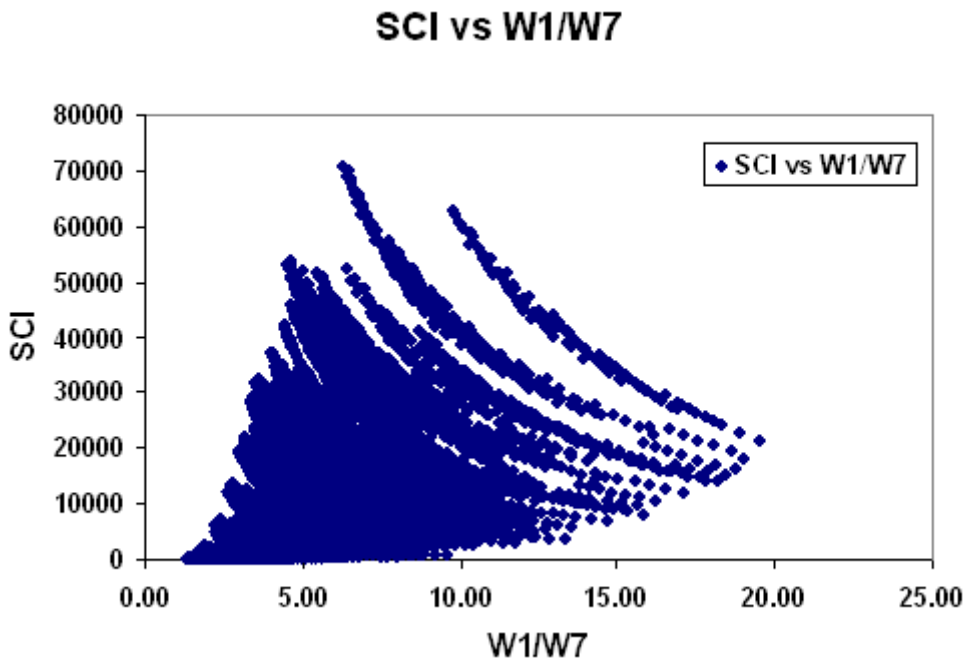

I.3 Method III

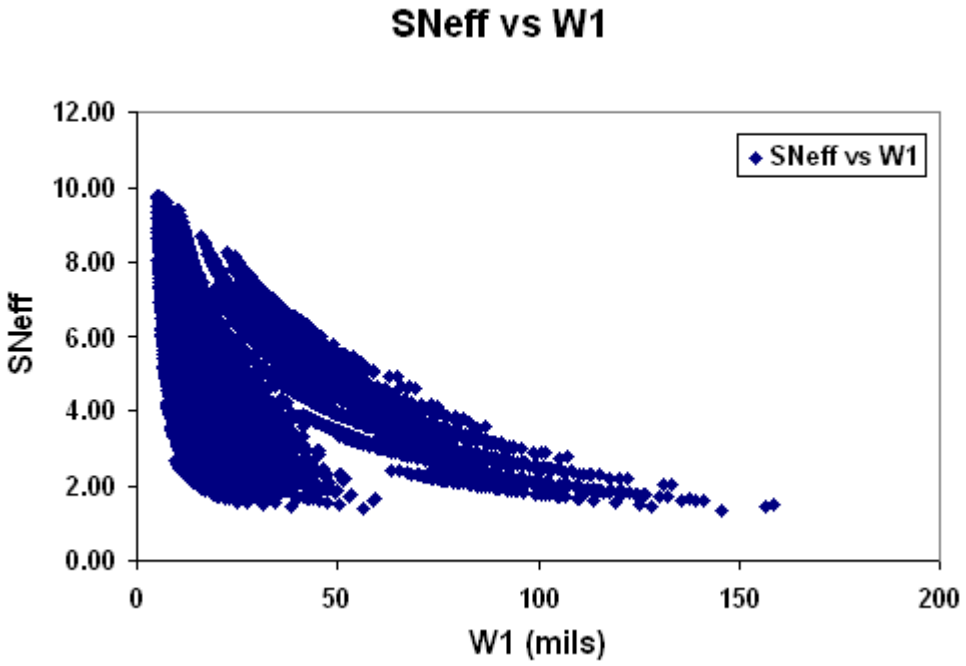

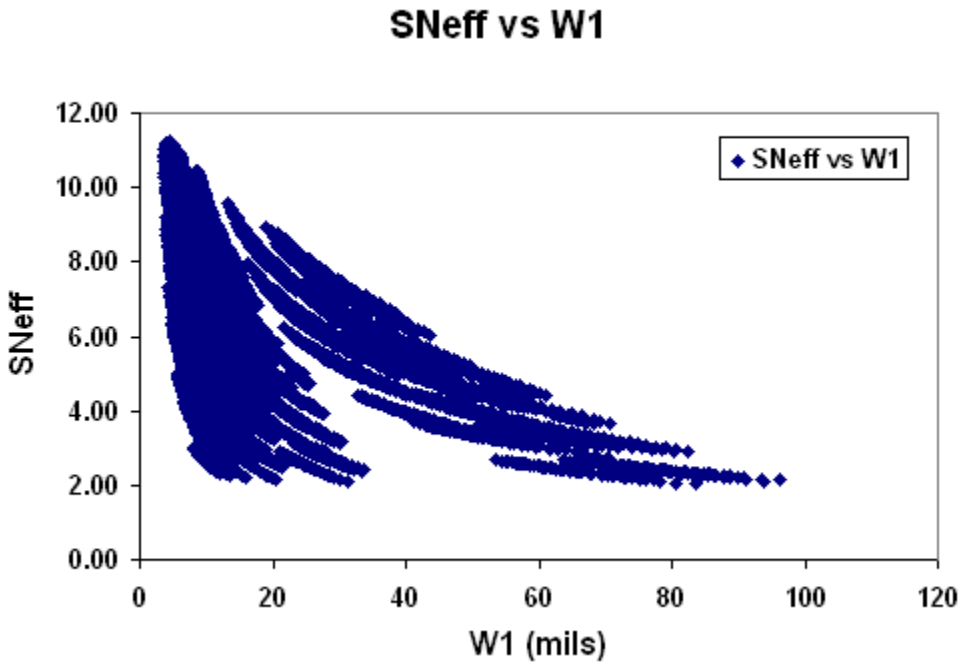
SNeff vs W1
SNeff vs W1
12.00
10.00
8.00
6.00
4.00
2.00
0.00
SNeff
0
20
40
60
80
100
120
W1 (mils)

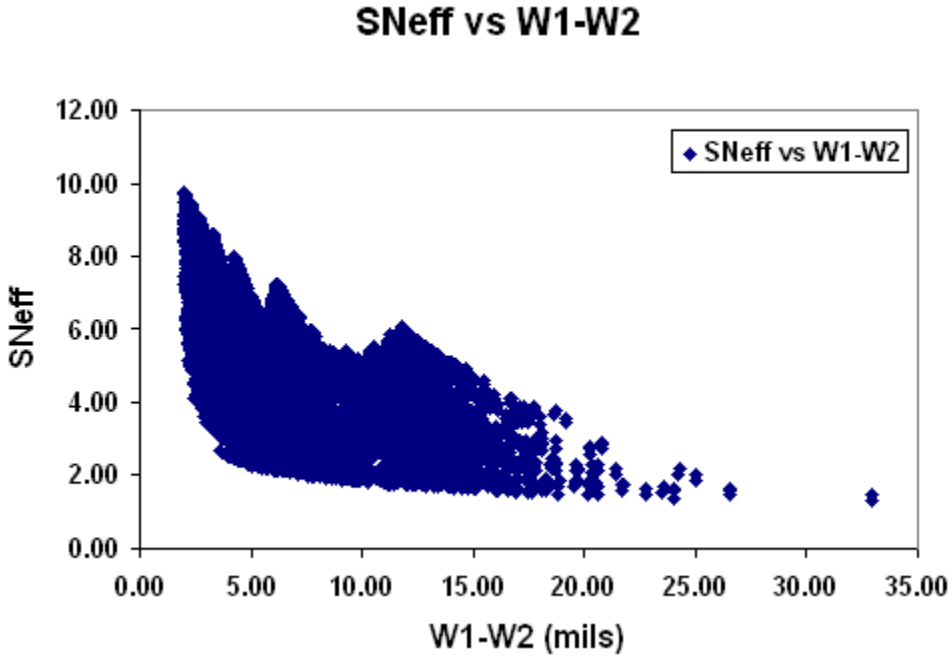
SNeff vs W1-W2
SNeff vs W1-W2
12.00
10.00
8.00
6.00
4.00
2.00
0.00
SNeff
0.00
5.00
10.00
15.00
20.00
25.00
30.00
35.00
W1-W2 (mils)

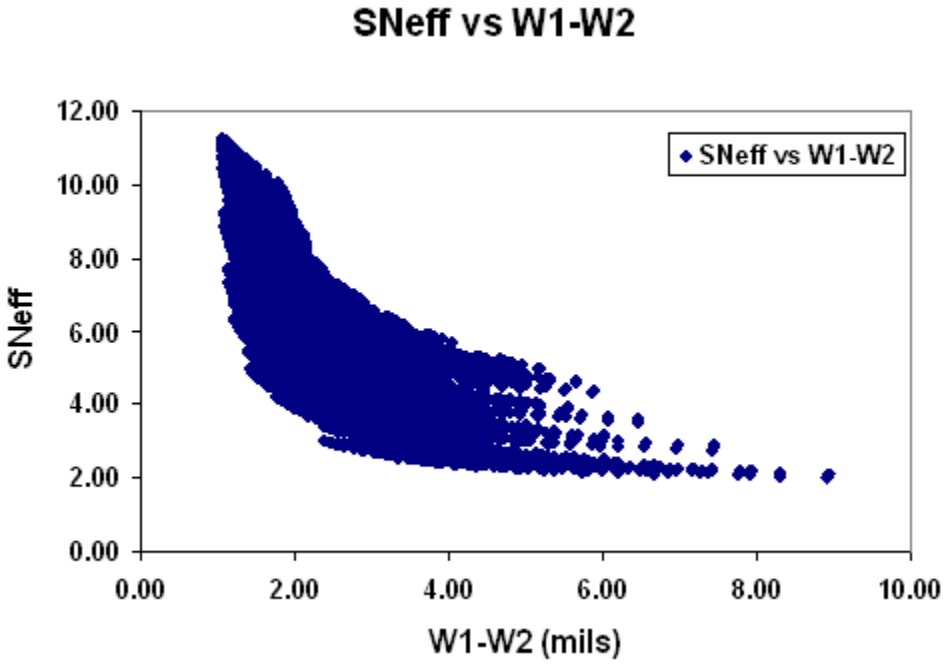
SNeff vs W1-W2
SNeff vs W1-W2
SNeff
12.00
10.00
8.00
6.00
4.00
2.00
0.00
0.00
2.00
4.00
6.00
8.00
10.00
W1-W2 (mils)

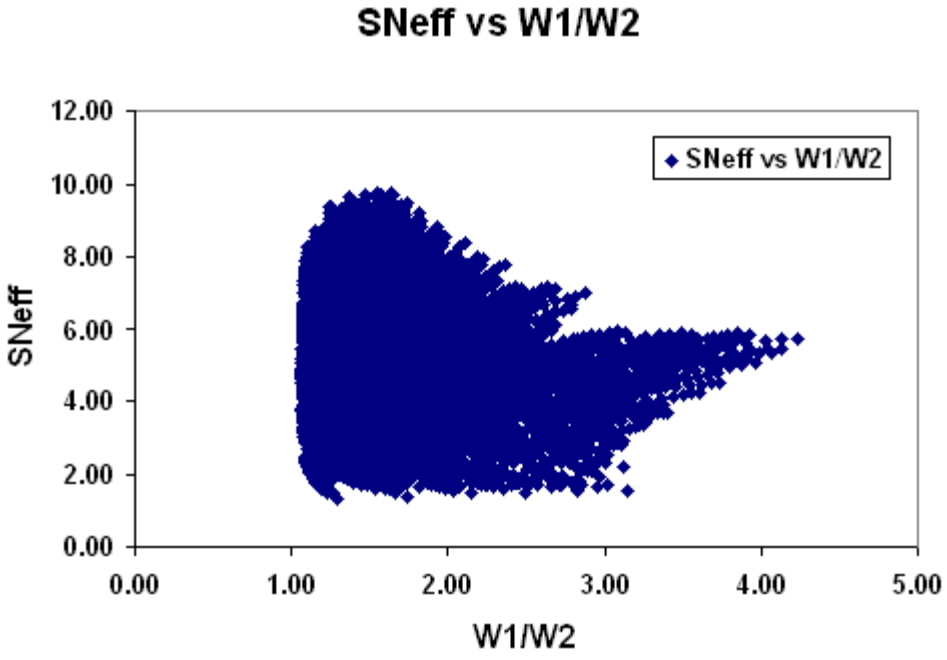
SNeff vs W1/W2
SNeff vs W1/W2
SNeff
12.00
10.00
8.00
6.00
4.00
2.00
0.00
0.00
1.00
2.00
3.00
4.00
5.00
W1/W2

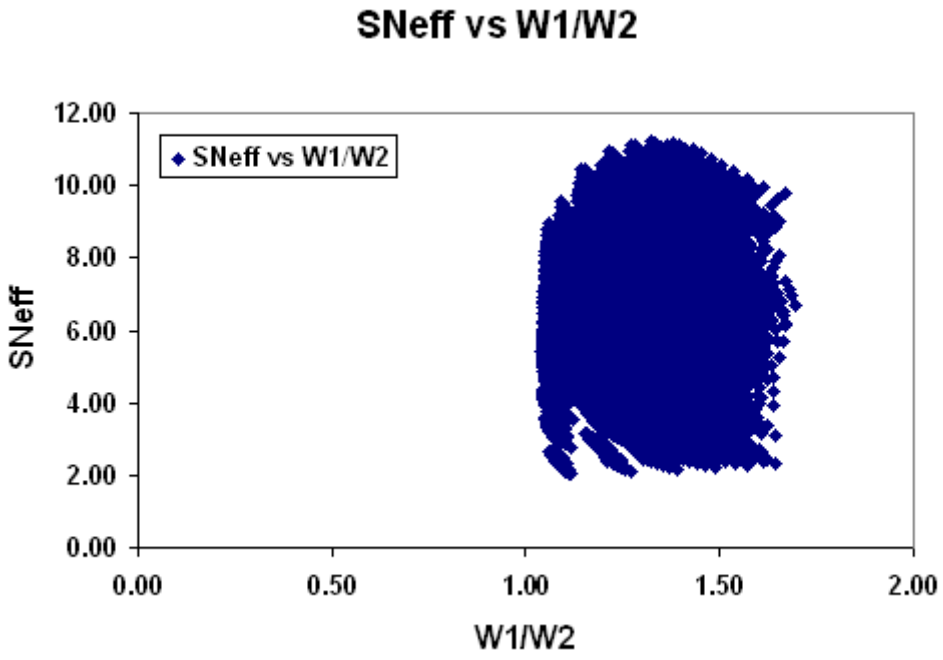
SNeff vs W1/W2
SNeff vs W1/W2
12.00
10.00
8.00
6.00
4.00
2.00
0.00
SNeff
0.00
0.50
1.00
1.50
2.00
W1/W2

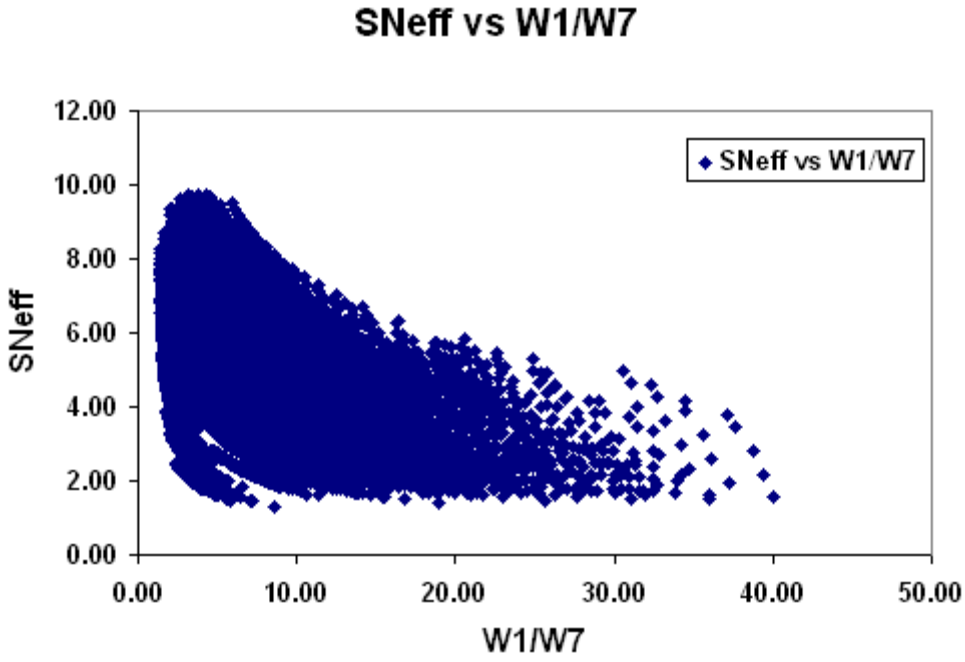
SNeff vs W1/W7
SNeff vs W1/W7
12.00
10.00
8.00
6.00
4.00
2.00
0.00
SNeff
0.00
10.00
20.00
30.00
40.00
50.00
W1/W7

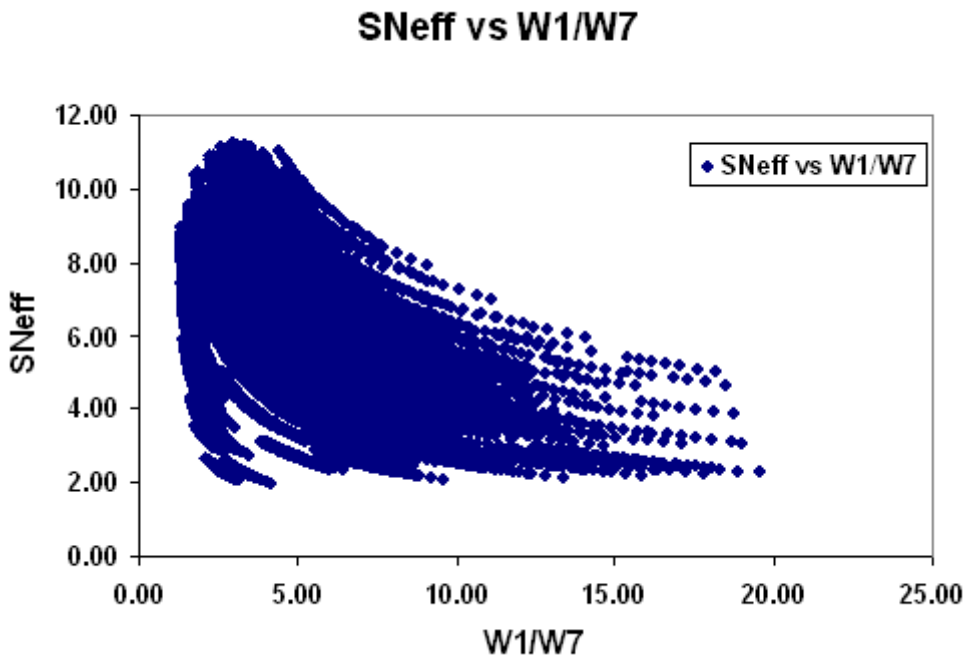
SNeff vs W1/W7
SNeff vs W1/W7
SNeff
W1/W7
12.00
10.00
8.00
6.00
4.00
2.00
0.00
0.00
5.00
10.00
15.00
20.00
25.00

I.4 Method IV

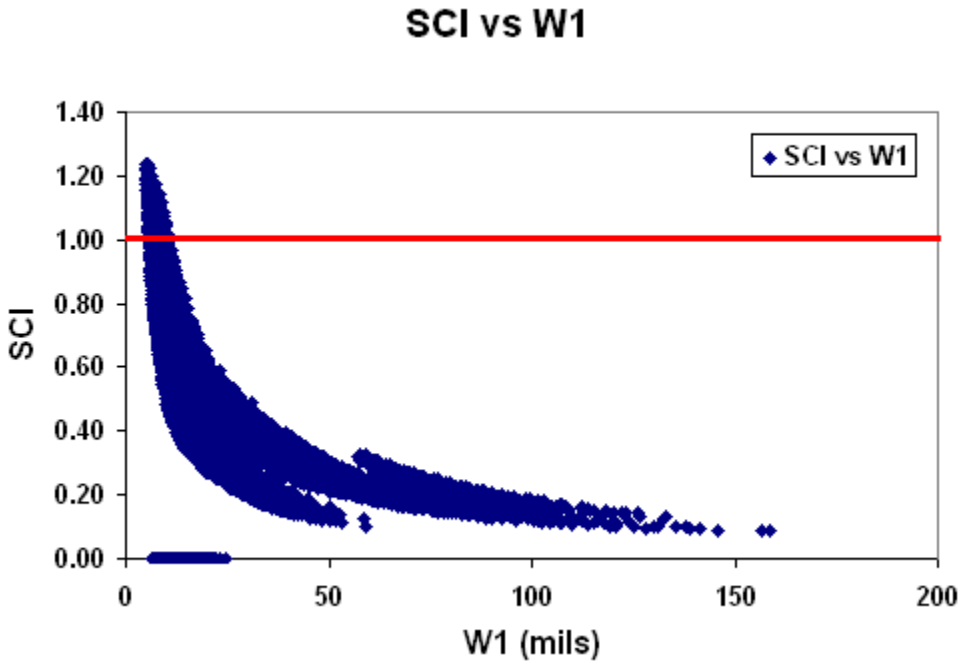
SCI vs W1
SCI vs W1
SCI
W1 (mils)
1.40
1.20
1.00
0.80
0.60
0.40
0.20
0.00
0
50
100
150
200

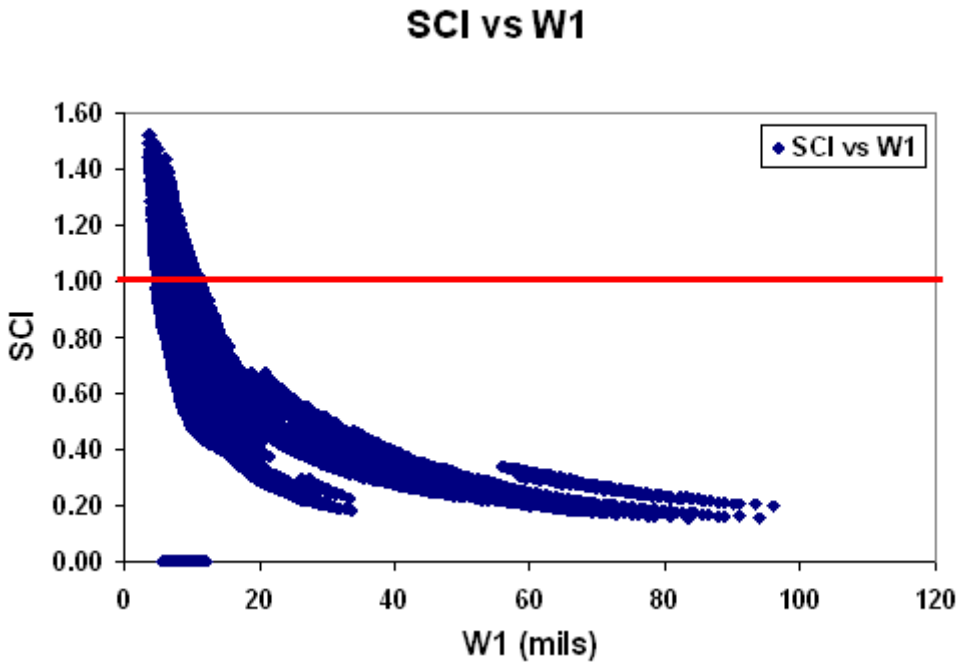
SCI vs W1
SCI vs W1
1.60
1.40
1.20
1.00
0.80
0.60
0.40
0.20
0.00
SCI
0
20
40
60
80
100
120
W1 (mils)

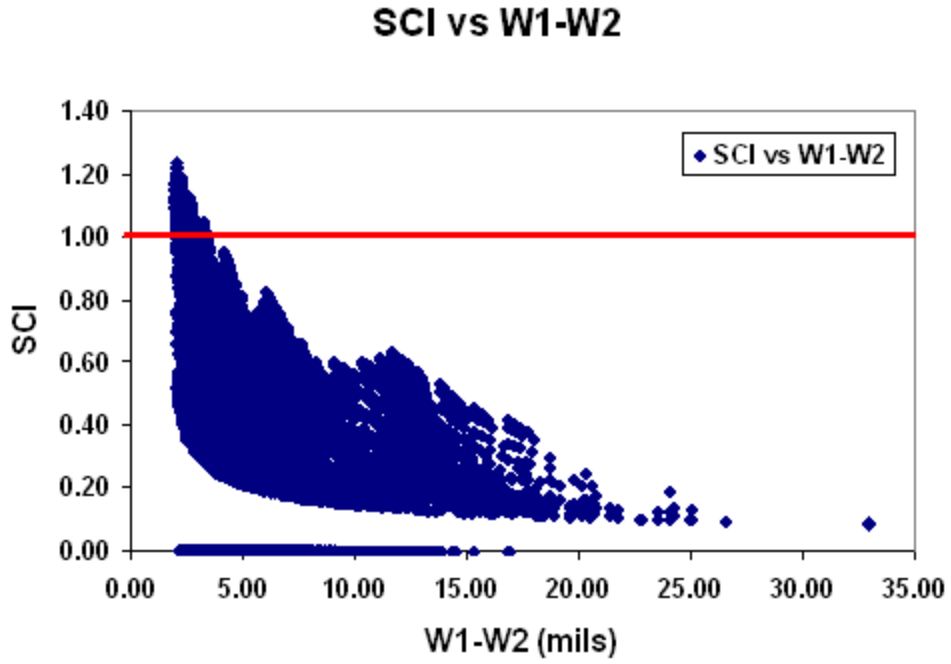
SCI vs W1-W2
SCI vs W1-W2
1.40
1.20
1.00
0.80
0.60
0.40
0.20
0.00
SCI
0.00
5.00
10.00
15.00
20.00
25.00
30.00
35.00
W1-W2 (mils)

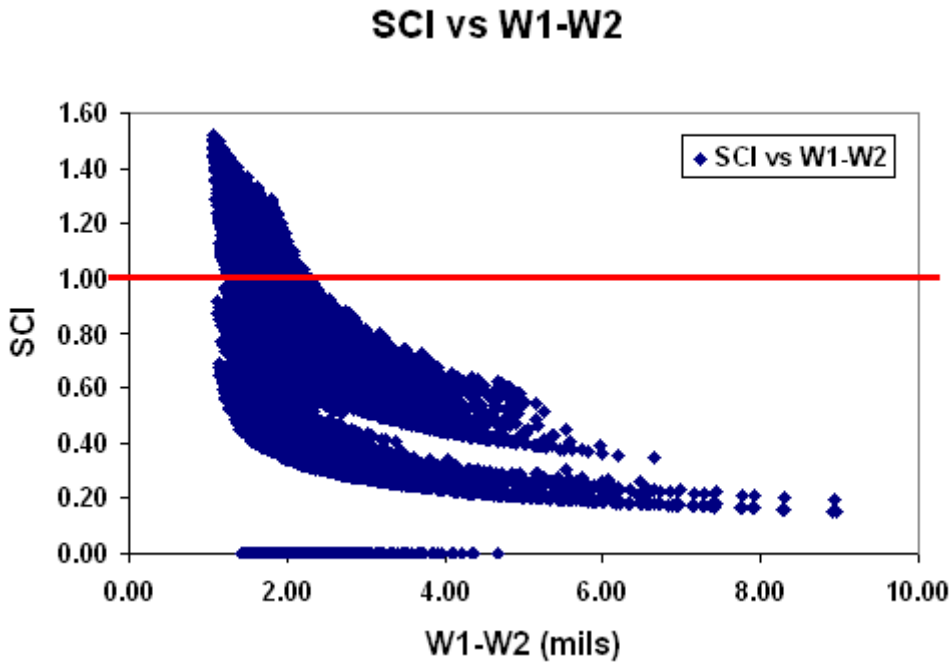
SCI vs W1-W2
SCI vs W1-W2
SCI
1.60
1.40
1.20
1.00
0.80
0.60
0.40
0.20
0.00
0.00
2.00
4.00
6.00
8.00
10.00
W1-W2 (mils)

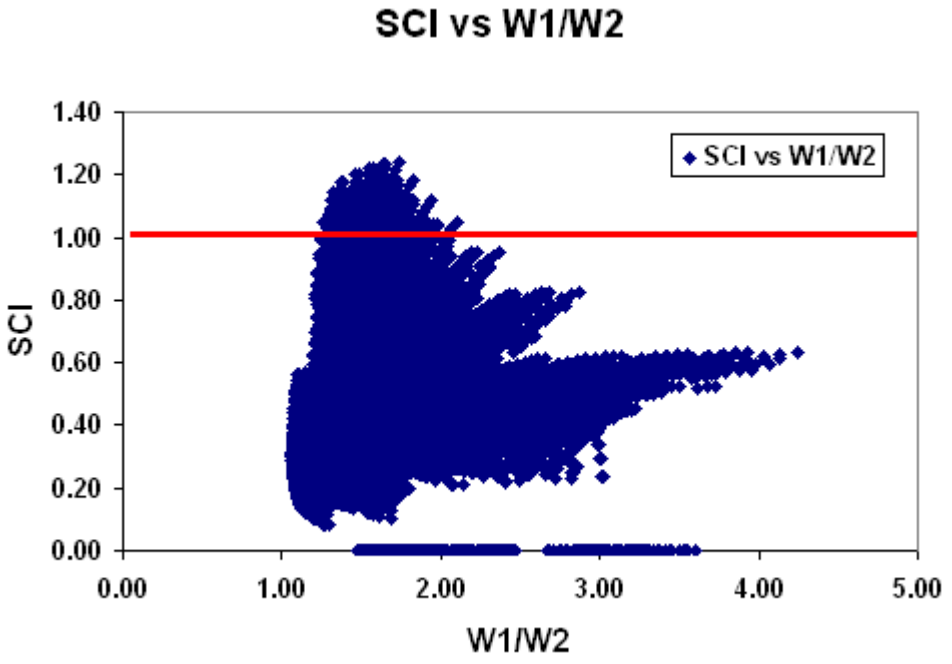
SCI vs W1/W2
SCI vs W1/W2
SCI
1.40
1.20
1.00
0.80
0.60
0.40
0.20
0.00
0.00
1.00
2.00
3.00
4.00
5.00
W1/W2

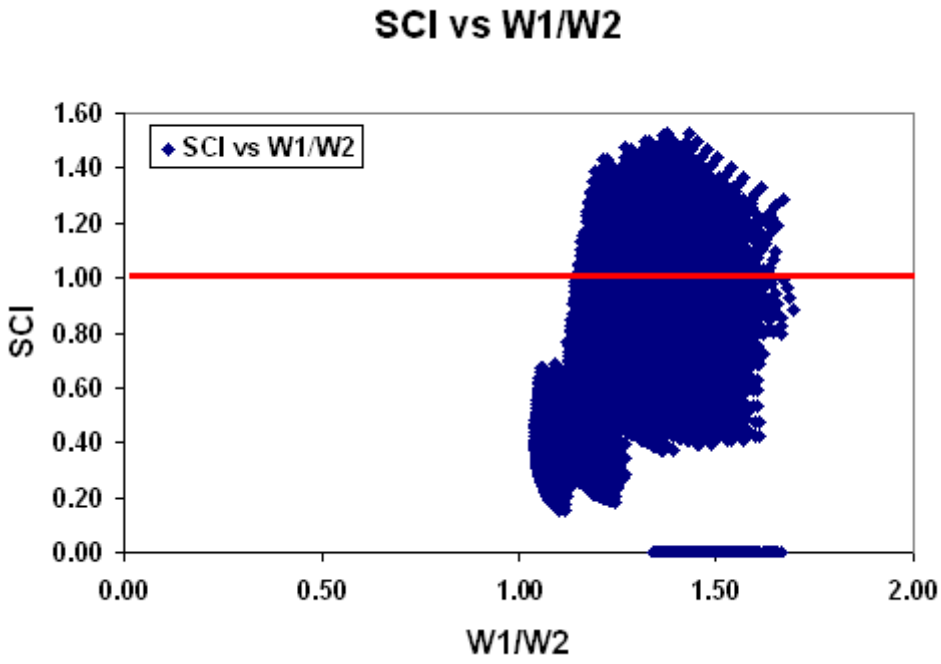
SCI vs W1/W2
SCI vs W1/W2
1.60
1.40
1.20
1.00
0.80
0.60
0.40
0.20
0.00
SCI
0.00
0.50
1.00
1.50
2.00
W1/W2

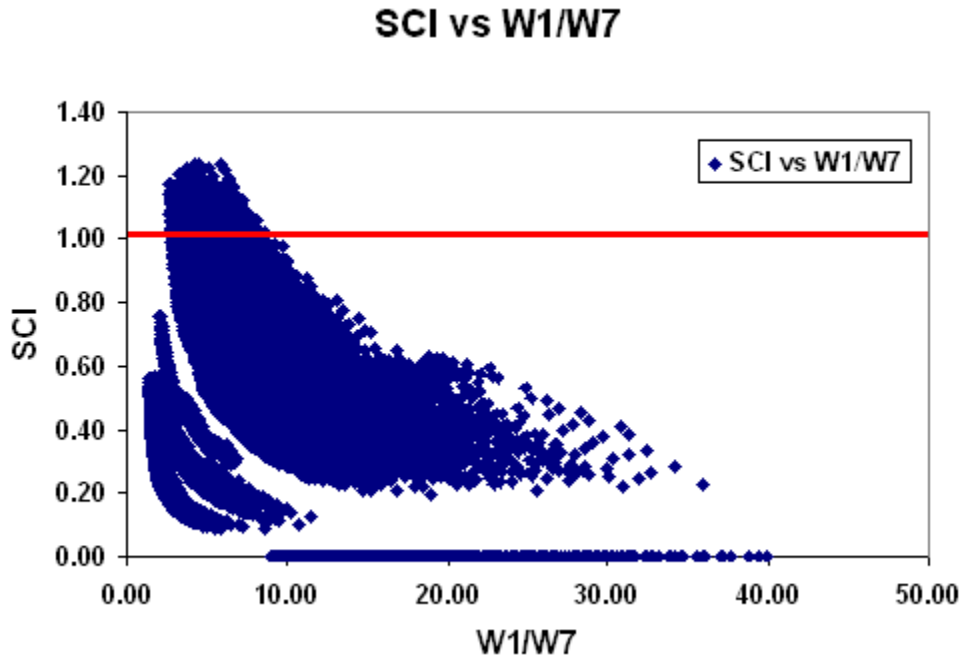
SCI vs W1/W7
SCI vs W1/W7
1.40
1.20
1.00
0.80
0.60
0.40
0.20
0.00
SCI
0.00
10.00
20.00
30.00
40.00
50.00
W1/W7

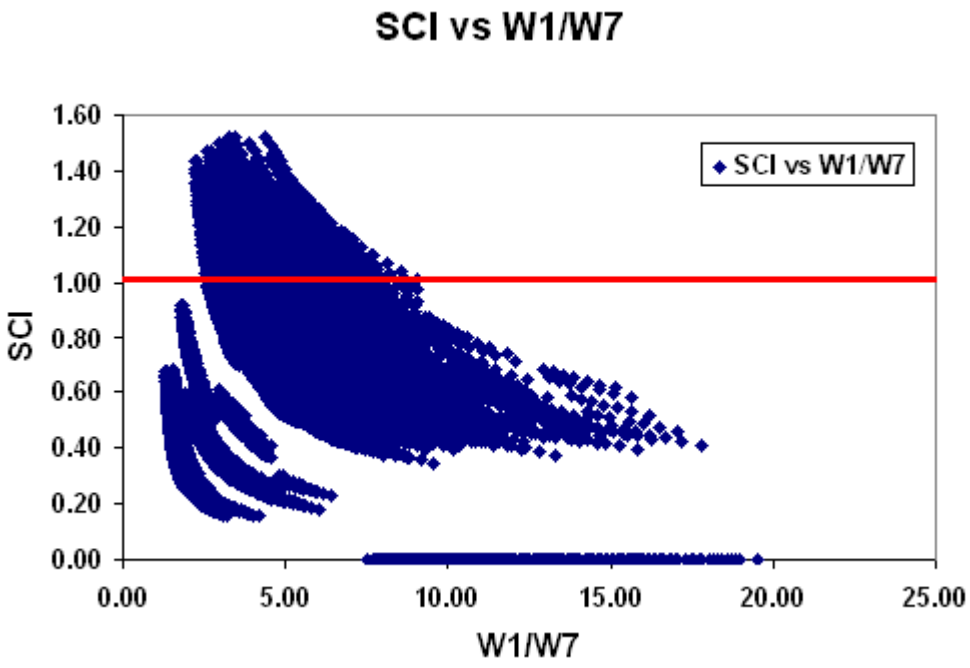
SCI vs W1/W7
SCI vs W1/W7
SCI
W1/W7
1.60
1.40
1.20
1.00
0.80
0.60
0.40
0.20
0.00
0.00
5.00
10.00
15.00
20.00
25.00

I.5 Method V

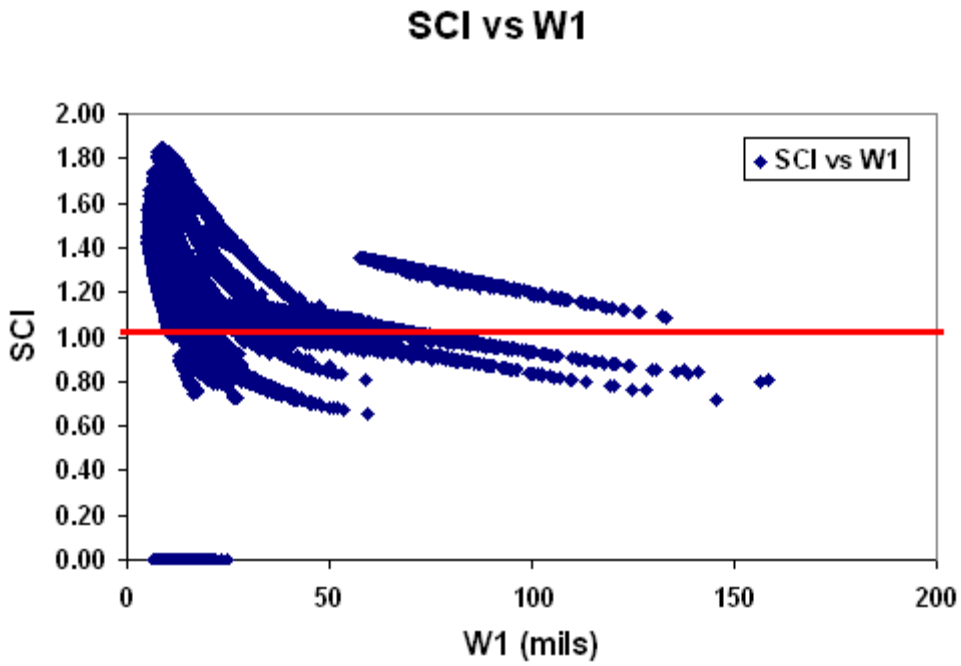
SCI vs W1
SCI vs W1
SCI
W1 (mils)
2.00
1.80
1.60
1.40
1.20
1.00
0.80
0.60
0.40
0.20
0.00
0
50
100
150
200

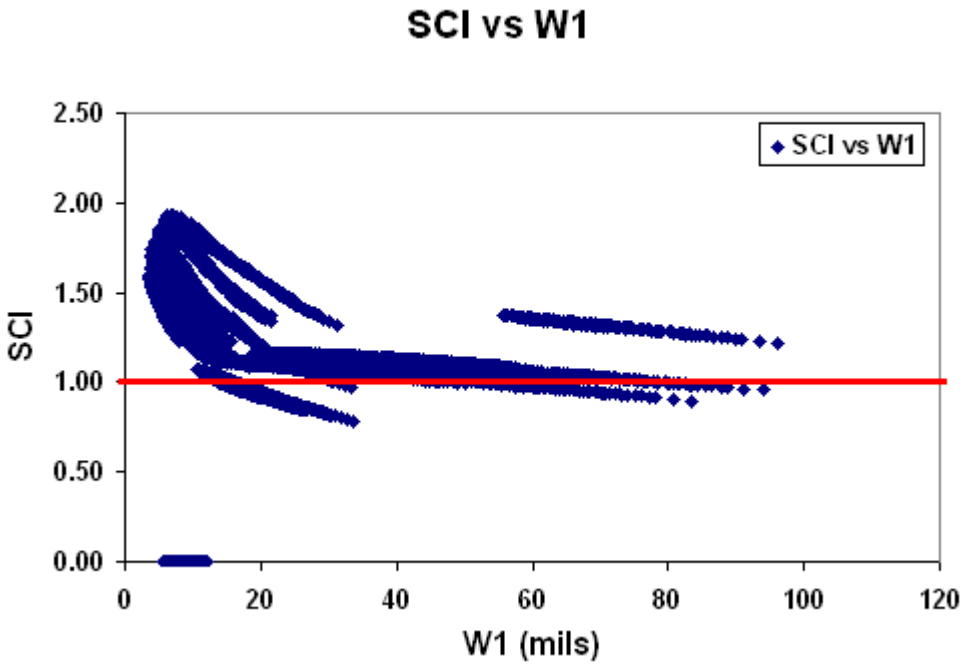
SCI vs W1
SCI vs W1
SCI
W1 (mils)
2.50
2.00
1.50
1.00
0.50
0.00
0
20
40
60
80
100
120

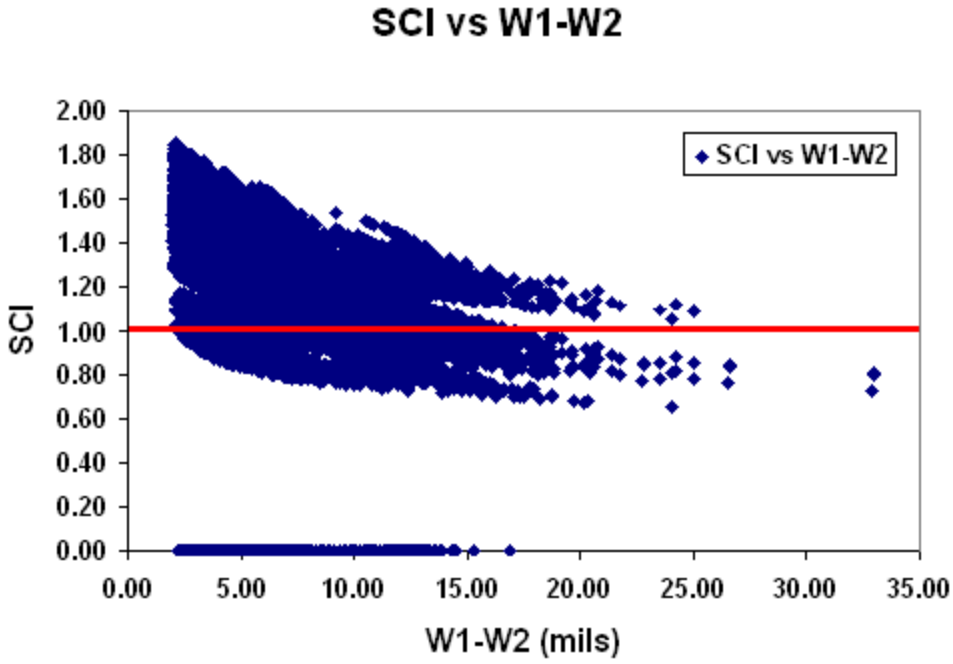
SCI vs W1-W2
SCI vs W1-W2
SCI
W1-W2 (mils)
2.00
1.80
1.60
1.40
1.20
1.00
0.80
0.60
0.40
0.20
0.00
0.00
5.00
10.00
15.00
20.00
25.00
30.00
35.00

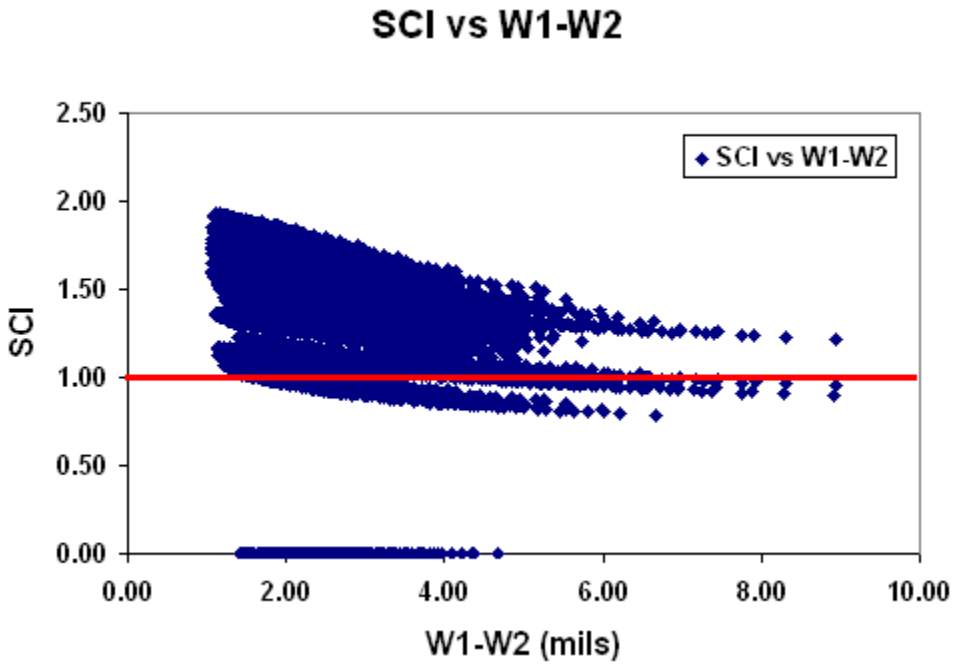
SCI vs W1-W2
SCI vs W1-W2
SCI
2.50
2.00
1.50
1.00
0.50
0.00
0.00
2.00
4.00
6.00
8.00
10.00
W1-W2 (mils)

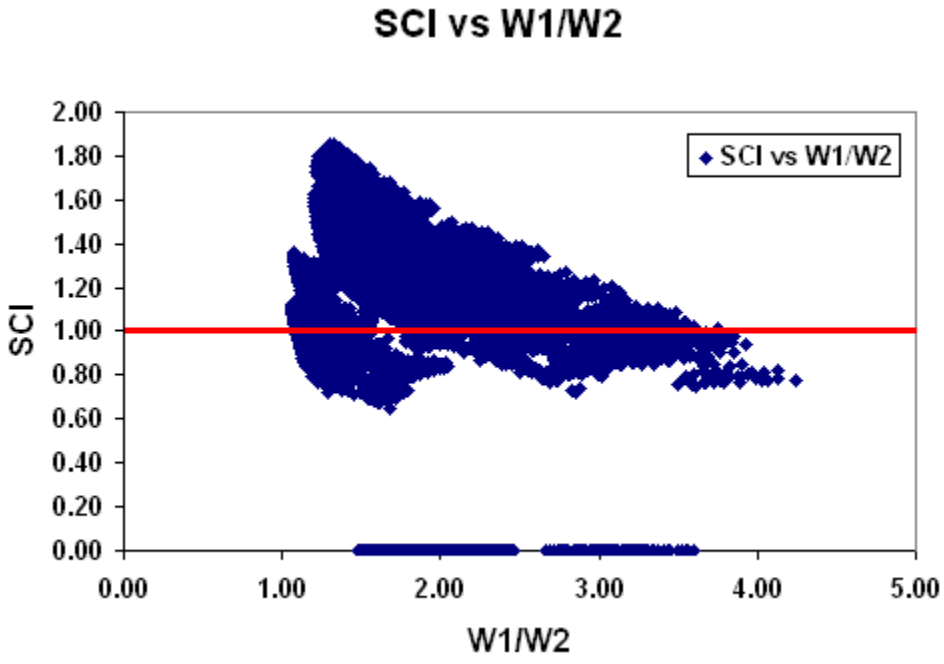
SCI vs W1/W2
SCI vs W1/W2
SCI
2.00
1.80
1.60
1.40
1.20
1.00
0.80
0.60
0.40
0.20
0.00
0.00
1.00
2.00
3.00
4.00
5.00
W1/W2

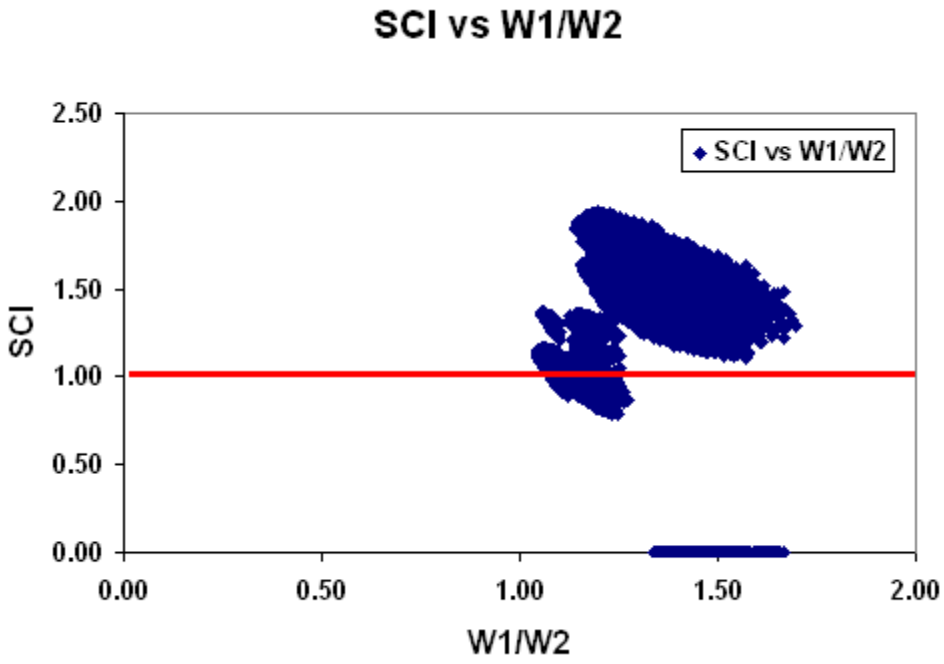
SCI vs W1/W2
SCI vs W1/W2
2.50
2.00
1.50
1.00
0.50
0.00
SCI
0.00
0.50
1.00
1.50
2.00
W1/W2

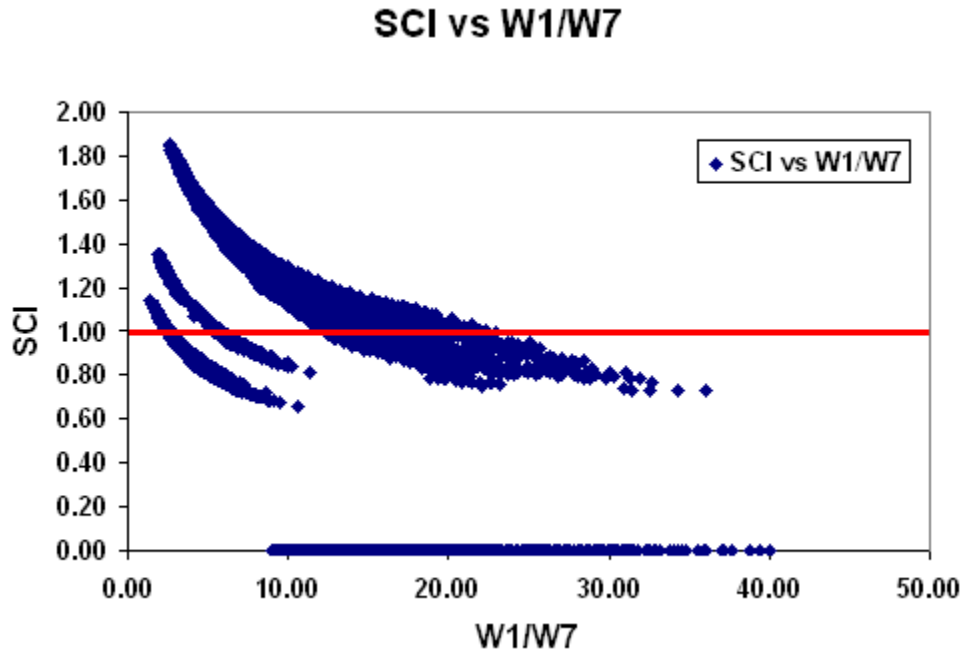
SCI vs W1/W7
SCI vs W1/W7
2.00
1.80
1.60
1.40
1.20
1.00
0.80
0.60
0.40
0.20
0.00
SCI
0.00
10.00
20.00
30.00
40.00
50.00
W1/W7

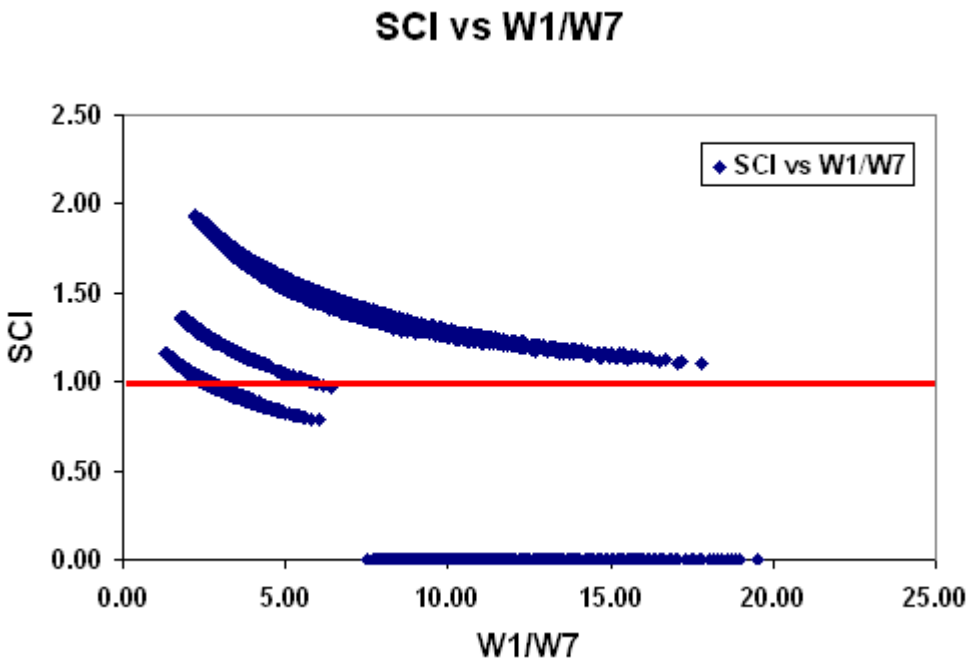
SCI vs W1/W7
SCI vs W1/W7
2.50
2.00
1.50
1.00
0.50
0.00
SCI
0.00
5.00
10.00
15.00
20.00
25.00
W1/W7

APPENDIX J CUT-OFF METHOD EVALUATION RESULTS

J.1 Method I and Pavement Types 1, 2, and 3

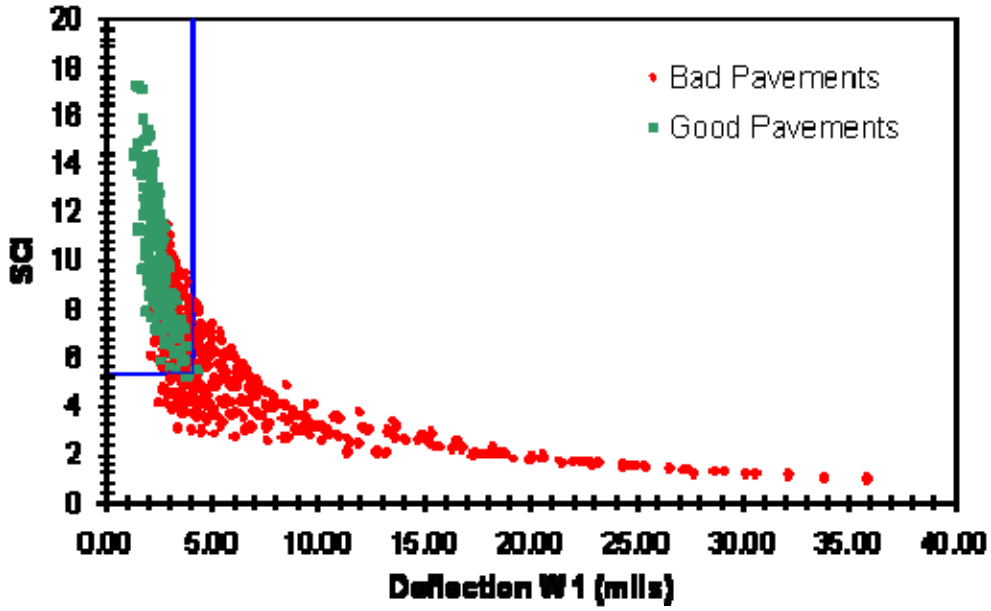

J.2 Method I and Pavement Type 4

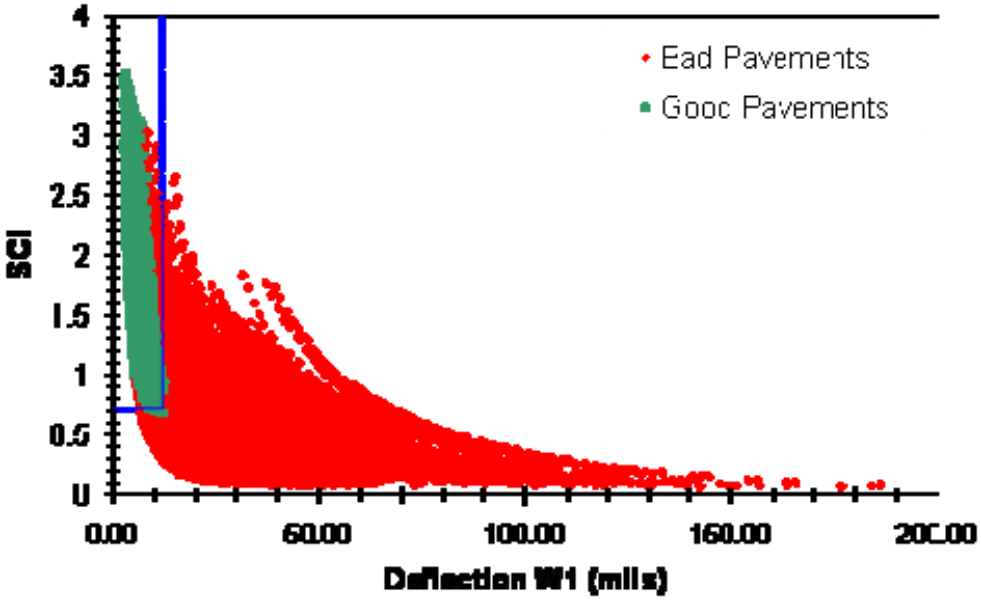

J.3 Method I and Pavement Type 6

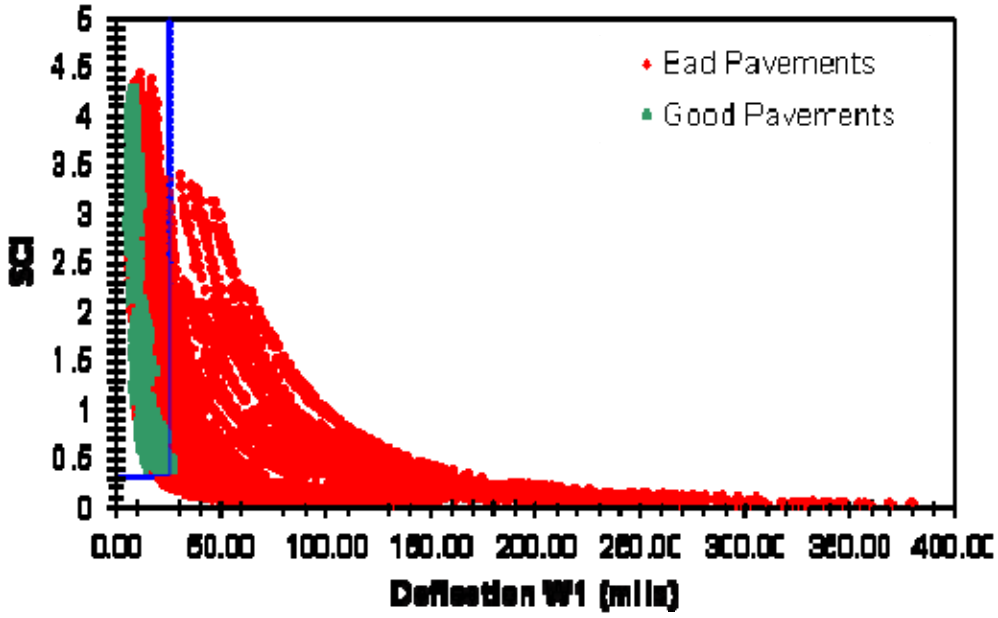

J.4 Method I and Pavement Type 10

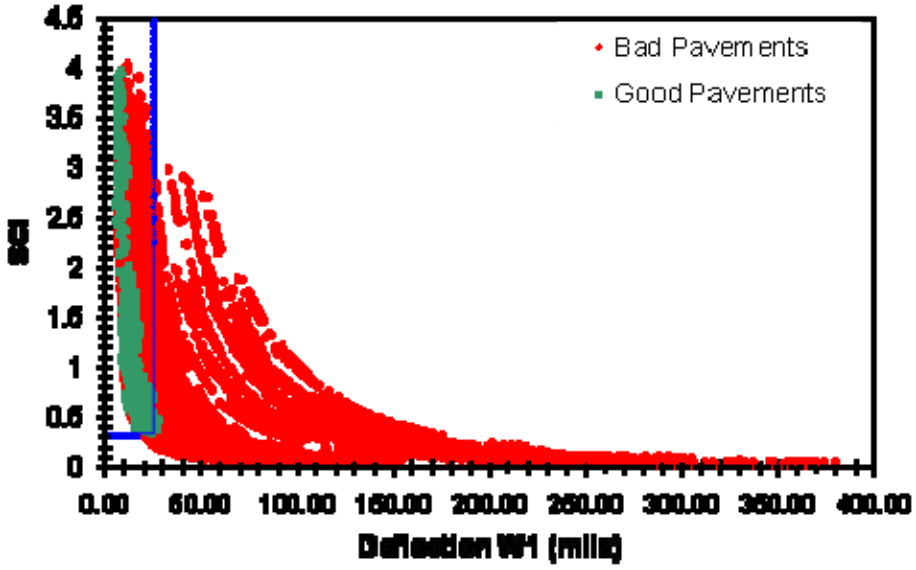

J.5 Method II and Pavement Types 1, 2, and 3

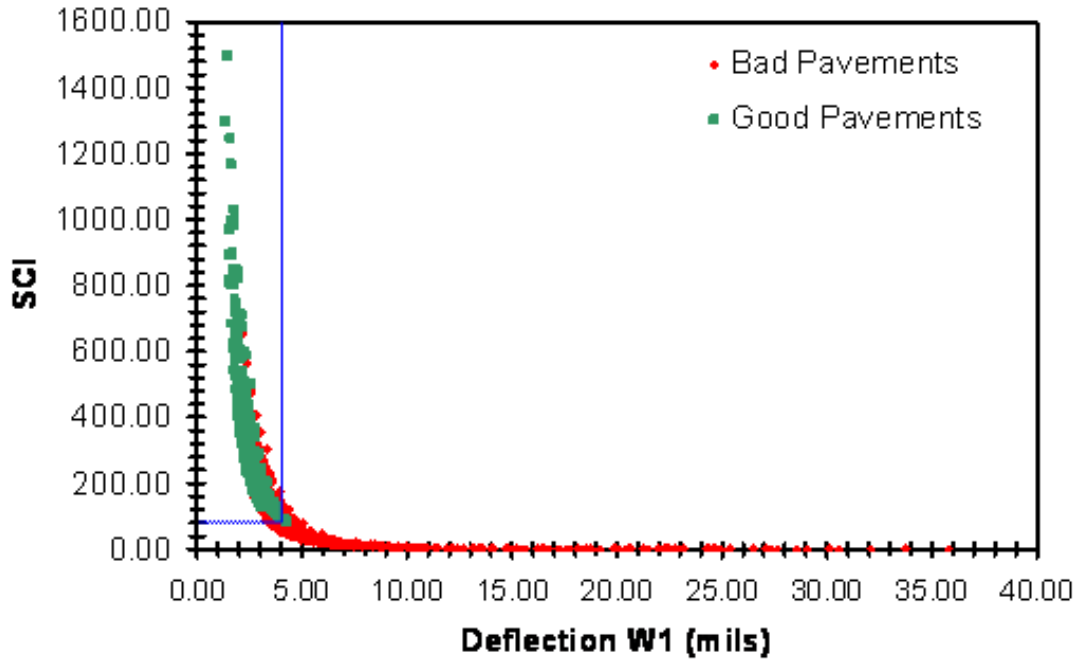

J.6 Method II and Pavement Type 4

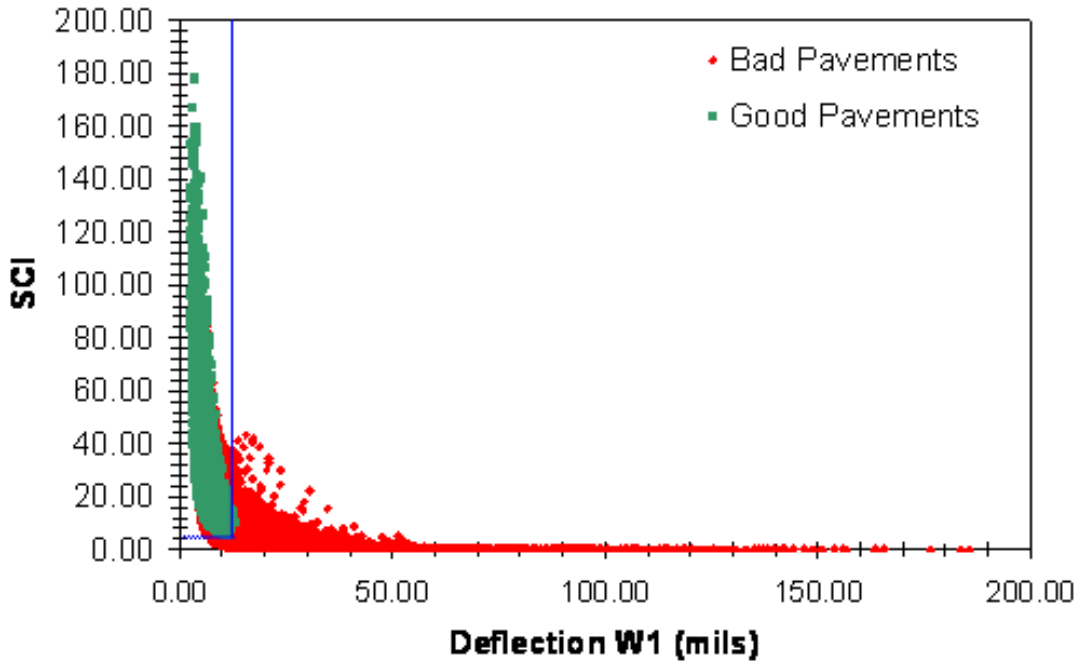

J.7 Method II and Pavement Type 6

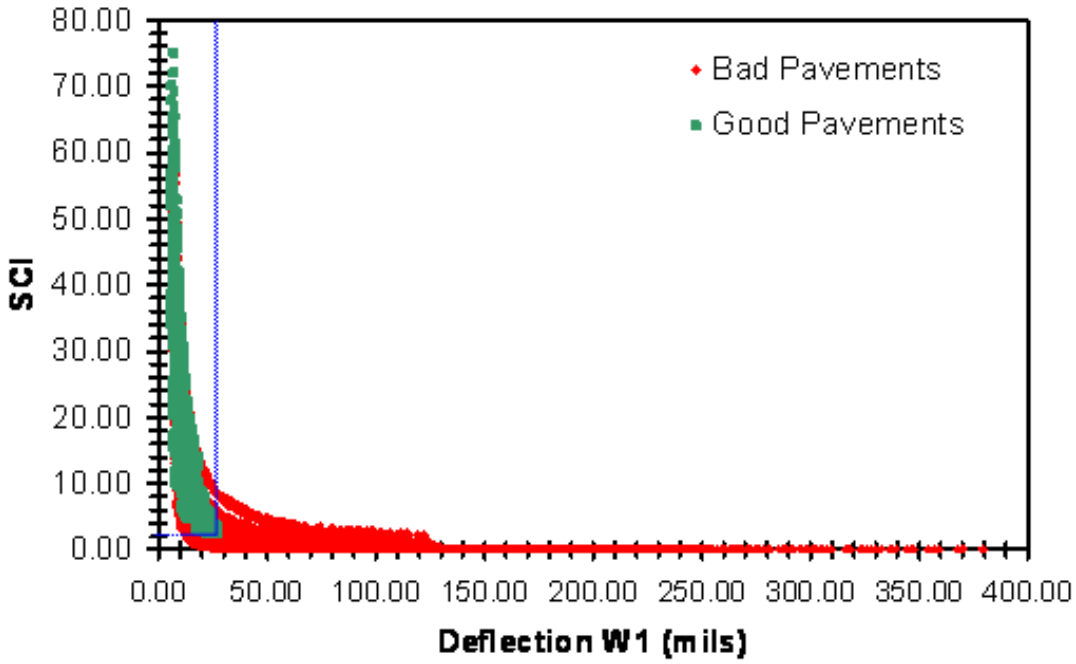

J.8 Method II and Pavement Type 10

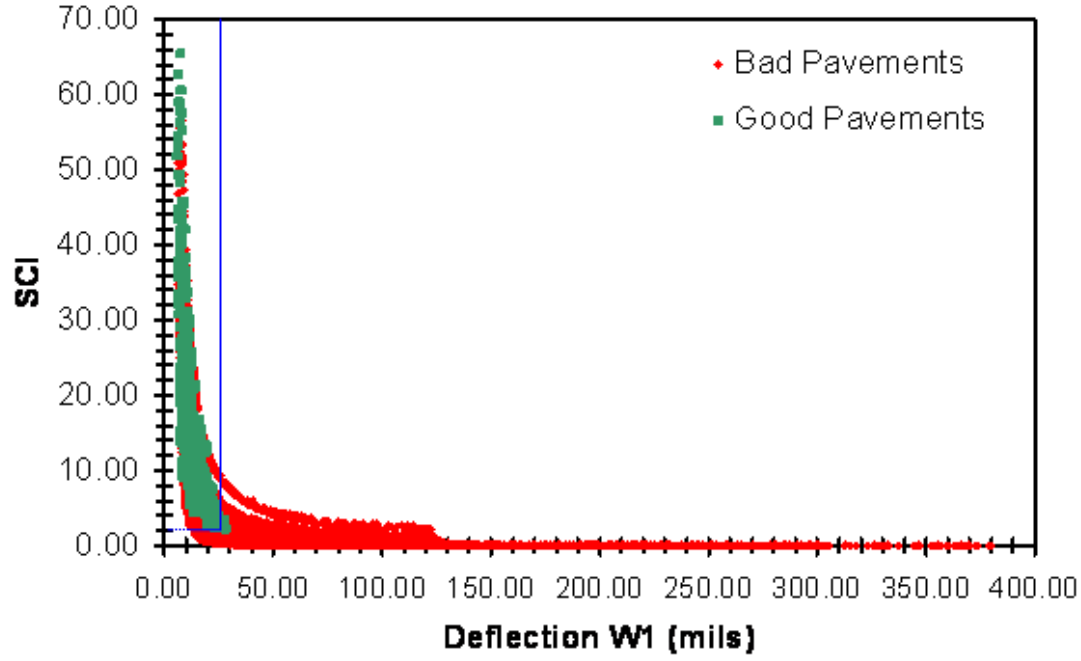

J.9 Method III and Pavement Types 1, 2, and 3

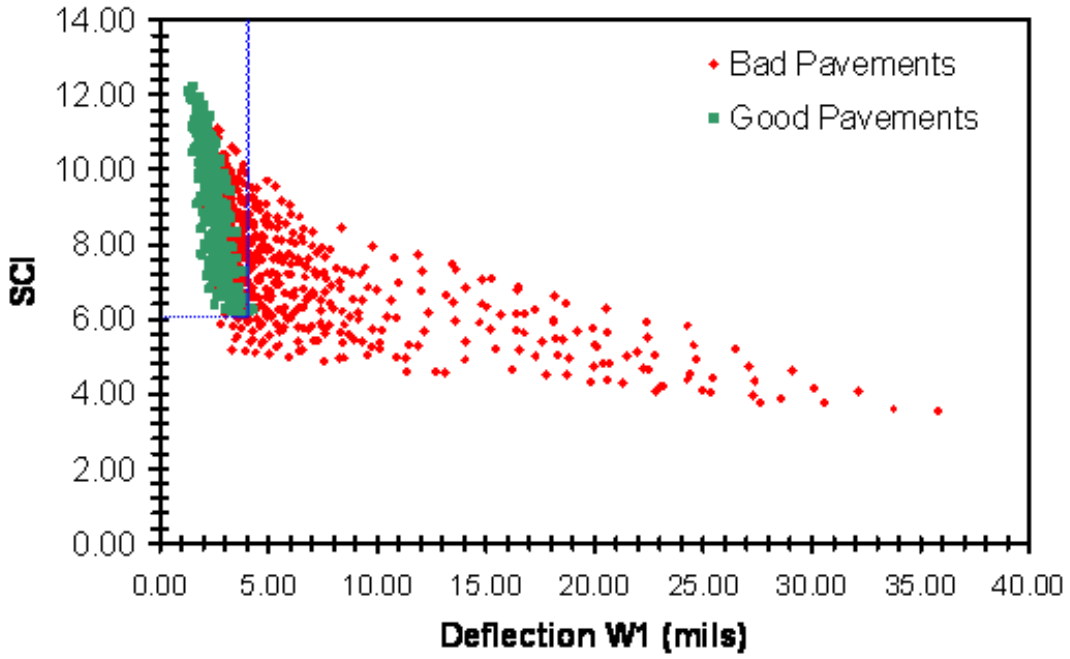

J.10 Method III and Pavement Type 4

J.11

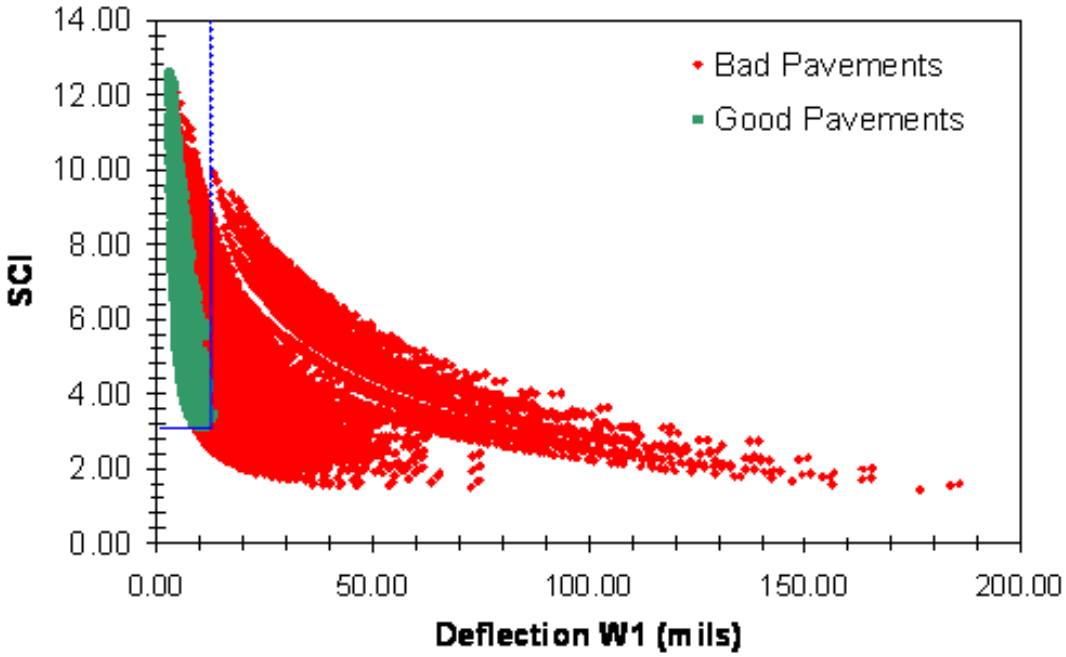

Method III and Pavement Type 6

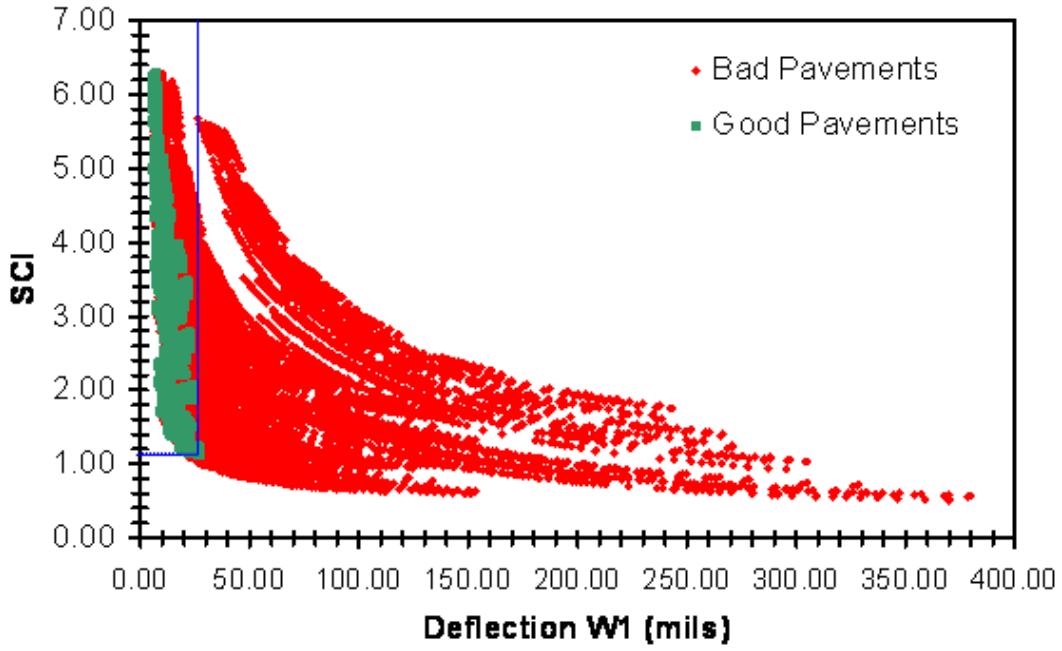

J.12 Method III and Pavement Type 10

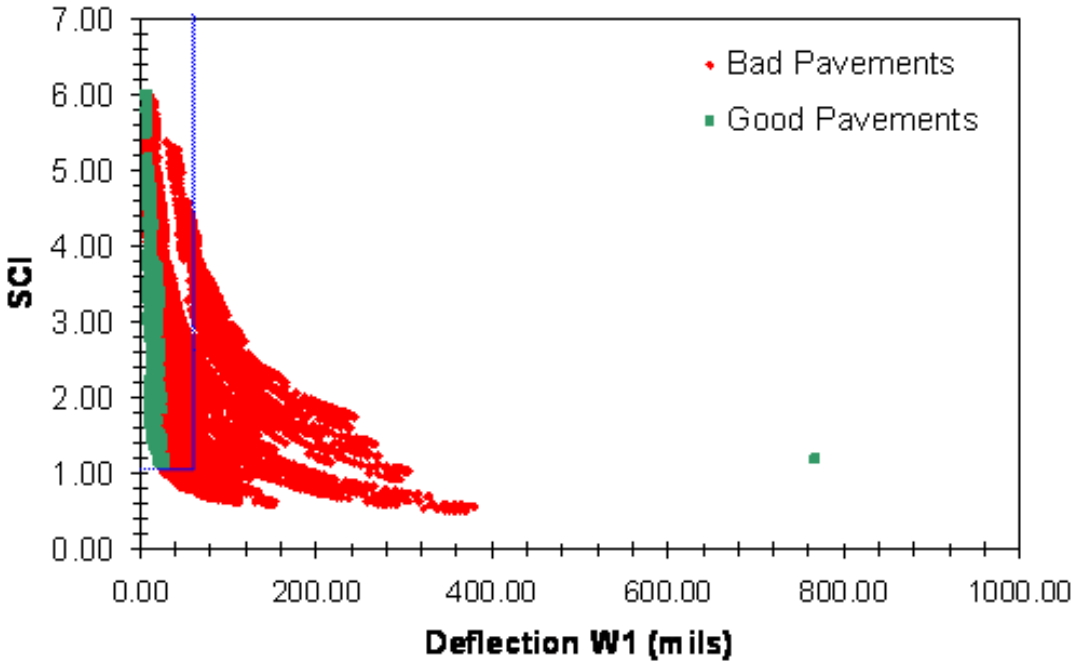

J.13 Method IV and Pavement Types 1,2, and 3

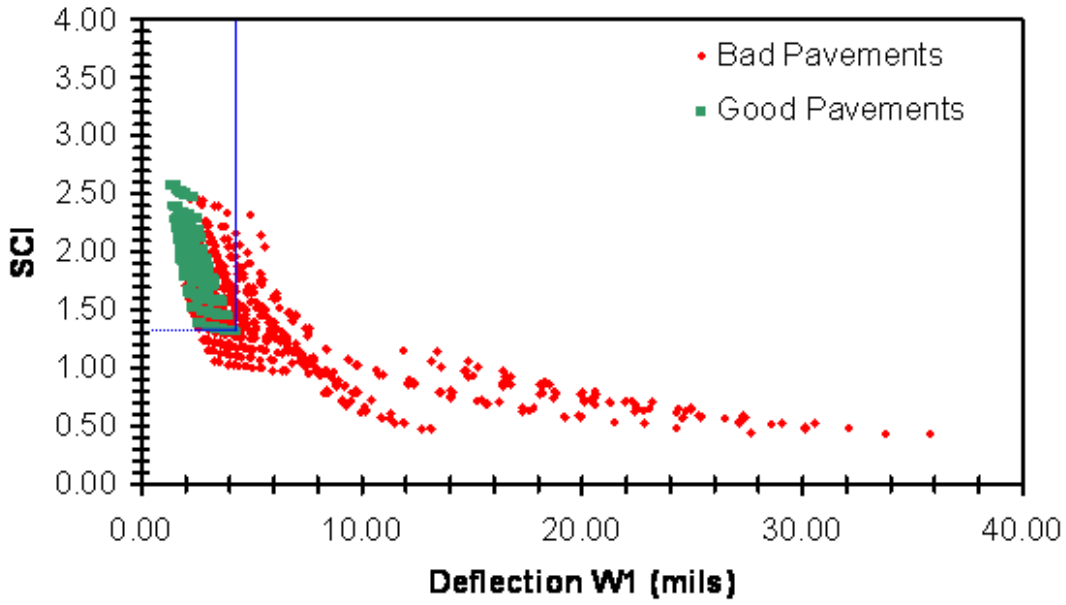

J.14 Method IV and Pavement Type 4

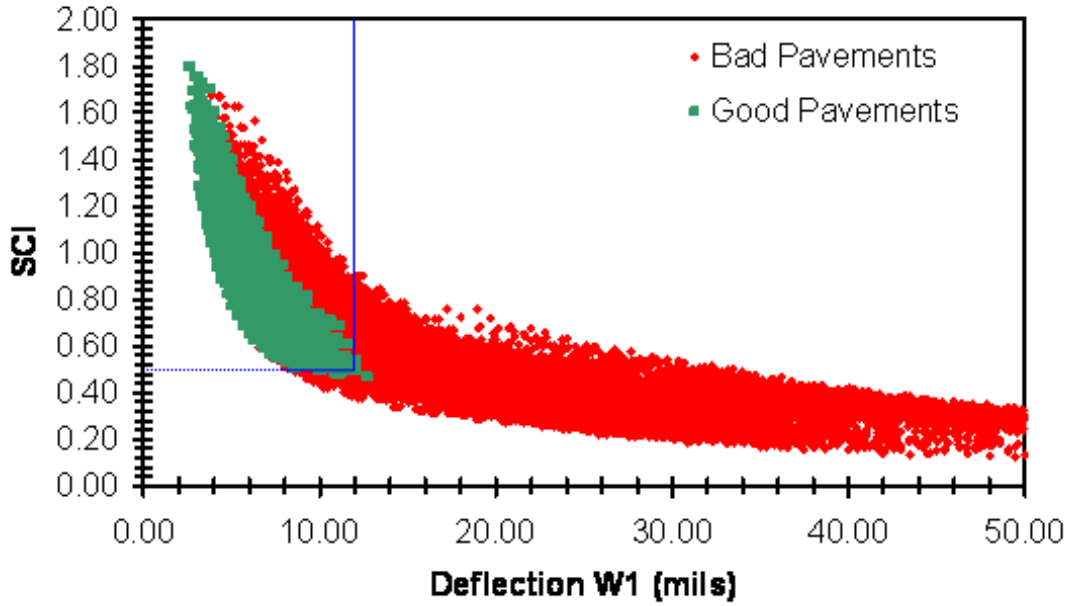

J.15 Method IV and Pavement Type 6

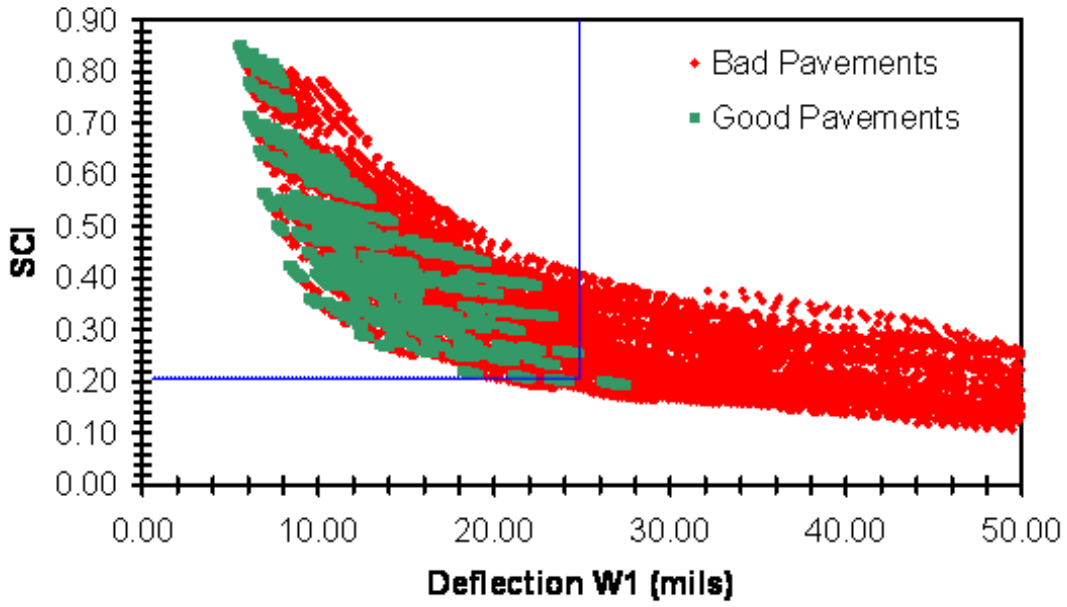

J.16 Method IV and Pavement Type 10

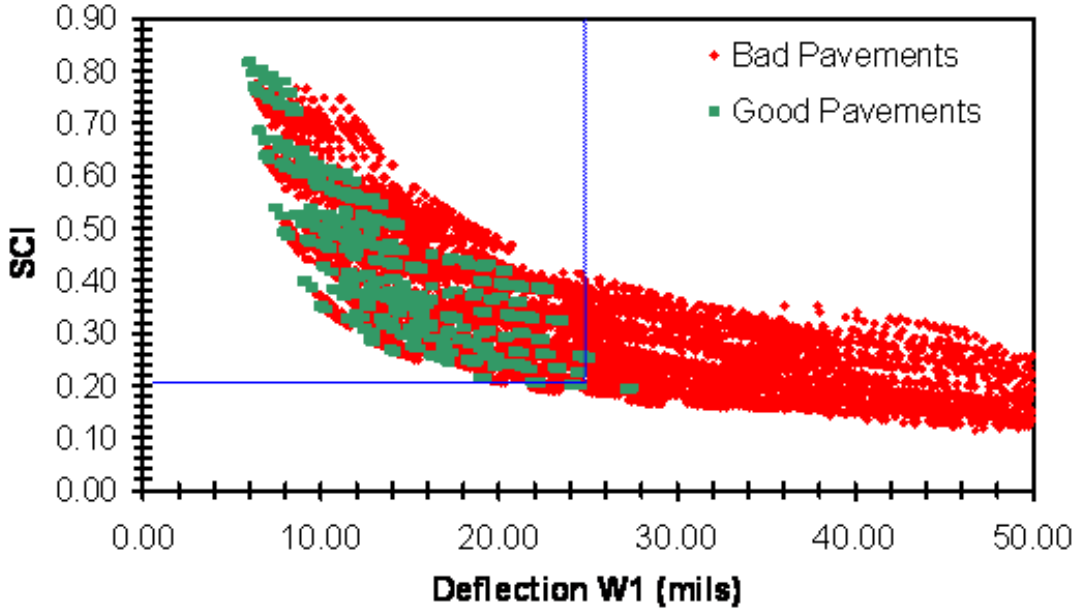

APPENDIX K FALSE POSITIVE AND FALSE NEGATIVE TABLES

K.1 Method IV and Pavement Types 1, 2, and 3

W1 Factors		W1 Cutoffs								
		3.2	**3.4**	**3.6**	**3.8**	**4**	**4.2**	**4.4**	**4.6**	**4.8**
0.8	False Positives	115	135	151	169	185	199	214	224	236
	Percentage	16.0%	18.8%	21.0%	23.5%	25.7%	27.6%	29.7%	31.1%	32.8%
	False Negatives	17	8	5	2	1	0	0	0	0
	Percentage	2.4%	1.1%	0.7%	0.3%	0.1%	0.0%	0.0%	0.0%	0.0%
0.85	False Positives	97	115	133	150	165	181	197	208	219
	Percentage	13.5%	16.0%	18.5%	20.8%	22.9%	25.1%	27.4%	28.9%	30.4%
	False Negatives	28	17	11	7	2	2	0	0	0
	Percentage	3.9%	2.4%	1.5%	1.0%	0.3%	0.3%	0.0%	0.0%	0.0%
0.9	False Positives	81	98	115	132	148	164	176	193	201
	Percentage	11.3%	13.6%	16.0%	18.3%	20.6%	22.8%	24.4%	26.8%	27.9%
	False Negatives	40	28	17	12	7	3	2	0	0
	Percentage	5.6%	3.9%	2.4%	1.7%	1.0%	0.4%	0.3%	0.0%	0.0%
0.95	False Positives	65	81	98	115	131	148	163	174	189
	Percentage	9.0%	11.3%	13.6%	16.0%	18.2%	20.6%	22.6%	24.2%	26.3%
	False Negatives	53	38	27	17	12	7	3	2	1
	Percentage	7.4%	5.3%	3.8%	2.4%	1.7%	1.0%	0.4%	0.3%	0.1%
1	False Positives	51	68	84	98	115	130	147	160	173
	Percentage	7.1%	9.4%	11.7%	13.6%	16.0%	18.1%	20.4%	22.2%	24.0%
	False Negatives	71	51	38	25	17	12	7	4	2
	Percentage	9.9%	7.1%	5.3%	3.5%	2.4%	1.7%	1.0%	0.6%	0.3%
1.05	False Positives	43	53	70	85	99	115	129	146	155
	Percentage	6.0%	7.4%	9.7%	11.8%	13.8%	16.0%	17.9%	20.3%	21.5%
	False Negatives	84	68	49	36	24	17	12	7	4
	Percentage	11.7%	9.4%	6.8%	5.0%	3.3%	2.4%	1.7%	1.0%	0.6%
1.1	False Positives	32	46	55	72	85	100	115	129	144
	Percentage	4.4%	6.4%	7.6%	10.0%	11.8%	13.9%	16.0%	17.9%	20.0%
	False Negatives	105	81	65	46	35	24	17	12	8
	Percentage	14.6%	11.3%	9.0%	6.4%	4.9%	3.3%	2.4%	1.7%	1.1%
1.15	False Positives	24	33	50	58	73	88	102	115	128
	Percentage	3.3%	4.6%	6.9%	8.1%	10.1%	12.2%	14.2%	16.0%	17.8%
	False Negatives	120	101	77	61	44	34	24	17	12
	Percentage	16.7%	14.0%	10.7%	8.5%	6.1%	4.7%	3.3%	2.4%	1.7%
1.2	False Positives	19	30	36	50	60	76	90	102	115
	Percentage	2.6%	4.2%	5.0%	6.9%	8.3%	10.6%	12.5%	14.2%	16.0%
	False Negatives	142	113	91	75	55	43	32	23	17
	Percentage	19.7%	15.7%	12.6%	10.4%	7.6%	6.0%	4.4%	3.2%	2.4%

K.2 Method IV and Pavement Type 5

W1 Factors			W1 Cutoffs								
			16	**17**	**18**	**19**	**20**	**21**	**22**	**23**	**24**
	0.8	False Positives	4458	5129	5798	6427	7033	7622	8192	8712	9173
		Percentage	19.3%	22.3%	25.2%	27.9%	30.5%	33.1%	35.6%	37.8%	39.8%
		False Negatives	344	233	159	108	65	38	23	14	9
		Percentage	1.5%	1.0%	0.7%	0.5%	0.3%	0.2%	0.1%	0.1%	0.0%
	0.85	False Positives	4458	5129	5798	6427	7033	7622	8192	8712	9173
		Percentage	19.3%	22.3%	25.2%	27.9%	30.5%	33.1%	35.6%	37.8%	39.8%
		False Negatives	344	233	159	108	65	38	23	14	9
		Percentage	1.5%	1.0%	0.7%	0.5%	0.3%	0.2%	0.1%	0.1%	0.0%
	0.9	False Positives	4458	5129	5798	6427	7033	7622	8192	8712	9173
		Percentage	19.3%	22.3%	25.2%	27.9%	30.5%	33.1%	35.6%	37.8%	39.8%
		False Negatives	344	233	159	108	65	38	23	14	9
		Percentage	1.5%	1.0%	0.7%	0.5%	0.3%	0.2%	0.1%	0.1%	0.0%
	0.95	False Positives	4458	5129	5798	6427	7033	7622	8192	8712	9173
		Percentage	19.3%	22.3%	25.2%	27.9%	30.5%	33.1%	35.6%	37.8%	39.8%
		False Negatives	344	233	159	108	65	38	23	14	9
		Percentage	1.5%	1.0%	0.7%	0.5%	0.3%	0.2%	0.1%	0.1%	0.0%
	1	False Positives	4458	5129	5798	6427	7033	7622	8192	8712	9173
		Percentage	19.3%	22.3%	25.2%	27.9%	30.5%	33.1%	35.6%	37.8%	39.8%
		False Negatives	344	233	159	108	65	38	23	14	9
		Percentage	1.5%	1.0%	0.7%	0.5%	0.3%	0.2%	0.1%	0.1%	0.0%
	1.05	False Positives	4458	5129	5798	6427	7033	7622	8192	8712	9173
		Percentage	19.3%	22.3%	25.2%	27.9%	30.5%	33.1%	35.6%	37.8%	39.8%
		False Negatives	344	233	159	108	65	38	23	14	9
		Percentage	1.5%	1.0%	0.7%	0.5%	0.3%	0.2%	0.1%	0.1%	0.0%
	1.1	False Positives	4458	5129	5798	6427	7033	7622	8192	8712	9173
		Percentage	19.3%	22.3%	25.2%	27.9%	30.5%	33.1%	35.6%	37.8%	39.8%
		False Negatives	344	233	159	108	65	38	23	14	9
		Percentage	1.5%	1.0%	0.7%	0.5%	0.3%	0.2%	0.1%	0.1%	0.0%
	1.15	False Positives	4458	5129	5798	6427	7033	7622	8192	8712	9173
		Percentage	19.3%	22.3%	25.2%	27.9%	30.5%	33.1%	35.6%	37.8%	39.8%
		False Negatives	344	233	159	108	65	38	23	14	9
		Percentage	1.5%	1.0%	0.7%	0.5%	0.3%	0.2%	0.1%	0.1%	0.0%
	1.2	False Positives	4458	5129	5798	6427	7033	7622	8192	8712	9173
		Percentage	19.3%	22.3%	25.2%	27.9%	30.5%	33.1%	35.6%	37.8%	39.8%
		False Negatives	344	233	159	108	65	38	23	14	9
		Percentage	1.5%	1.0%	0.7%	0.5%	0.3%	0.2%	0.1%	0.1%	0.0%

K.3 Method IV and Pavement Type 6

W1 Factors		W1 Cutoffs								
		20	**21.25**	**22.5**	**23.75**	**25**	**26.25**	**27.5**	**28.75**	**30**
0.8	False Positives	3378	3834	4223	4589	4908	5227	5579	5889	6169
	Percentage	22.0%	25.0%	27.5%	29.9%	32.0%	34.0%	36.3%	38.3%	40.2%
	False Negatives	85	57	22	18	15	0	0	0	0
	Percentage	0.6%	0.4%	0.1%	0.1%	0.1%	0.0%	0.0%	0.0%	0.0%
0.85	False Positives	2974	3378	3810	4189	4518	4830	5134	5455	5763
	Percentage	19.4%	22.0%	24.8%	27.3%	29.4%	31.4%	33.4%	35.5%	37.5%
	False Negatives	168	85	62	25	18	17	4	0	0
	Percentage	1.1%	0.6%	0.4%	0.2%	0.1%	0.1%	0.0%	0.0%	0.0%
0.9	False Positives	2607	2992	3378	3784	4146	4461	4761	5052	5349
	Percentage	17.0%	19.5%	22.0%	24.6%	27.0%	29.0%	31.0%	32.9%	34.8%
	False Negatives	243	162	85	62	26	18	18	8	0
	Percentage	1.6%	1.1%	0.6%	0.4%	0.2%	0.1%	0.1%	0.1%	0.0%
0.95	False Positives	2315	2653	3010	3378	3764	4104	4426	4706	4965
	Percentage	15.1%	17.3%	19.6%	22.0%	24.5%	26.7%	28.8%	30.6%	32.3%
	False Negatives	346	234	160	85	64	33	18	18	11
	Percentage	2.3%	1.5%	1.0%	0.6%	0.4%	0.2%	0.1%	0.1%	0.1%
1	False Positives	2067	2354	2694	3025	3378	3748	4069	4376	4645
	Percentage	13.5%	15.3%	17.5%	19.7%	22.0%	24.4%	26.5%	28.5%	30.2%
	False Negatives	466	329	225	157	85	64	35	18	18
	Percentage	3.0%	2.1%	1.5%	1.0%	0.6%	0.4%	0.2%	0.1%	0.1%
1.05	False Positives	1857	2118	2398	2722	3039	3378	3720	4038	4330
	Percentage	12.1%	13.8%	15.6%	17.7%	19.8%	22.0%	24.2%	26.3%	28.2%
	False Negatives	563	443	314	213	155	85	64	38	18
	Percentage	3.7%	2.9%	2.0%	1.4%	1.0%	0.6%	0.4%	0.2%	0.1%
1.1	False Positives	1687	1916	2186	2450	2751	3061	3378	3705	4024
	Percentage	11.0%	12.5%	14.2%	16.0%	17.9%	19.9%	22.0%	24.1%	26.2%
	False Negatives	704	526	412	298	209	150	85	64	42
	Percentage	4.6%	3.4%	2.7%	1.9%	1.4%	1.0%	0.6%	0.4%	0.3%
1.15	False Positives	1533	1732	1969	2226	2493	2772	3078	3378	3690
	Percentage	10.0%	11.3%	12.8%	14.5%	16.2%	18.0%	20.0%	22.0%	24.0%
	False Negatives	797	656	504	395	290	202	149	85	64
	Percentage	5.2%	4.3%	3.3%	2.6%	1.9%	1.3%	1.0%	0.6%	0.4%
1.2	False Positives	1396	1597	1780	2029	2263	2518	2800	3091	3378
	Percentage	9.1%	10.4%	11.6%	13.2%	14.7%	16.4%	18.2%	20.1%	22.0%
	False Negatives	896	761	619	486	373	275	200	147	85
	Percentage	5.8%	5.0%	4.0%	3.2%	2.4%	1.8%	1.3%	1.0%	0.6%

K.4 Method IV and Pavement Type 10

W1 Factors		W1 Cutoffs								
		20	**21.25**	**22.5**	**23.75**	**25**	**26.25**	**27.5**	**28.75**	**30**
0.8	False Positives	2672	3051	3372	3679	3901	4174	4430	4701	4934
	Percentage	21.7%	24.8%	27.4%	29.9%	31.7%	34.0%	36.1%	38.3%	40.2%
	False Negatives	97	54	33	17	12	7	0	0	0
	Percentage	0.8%	0.4%	0.3%	0.1%	0.1%	0.1%	0.0%	0.0%	0.0%
0.85	False Positives	2369	2672	3027	3340	3621	3846	4105	4329	4598
	Percentage	19.3%	21.7%	24.6%	27.2%	29.5%	31.3%	33.4%	35.2%	37.4%
	False Negatives	161	97	55	36	18	12	10	0	0
	Percentage	1.3%	0.8%	0.4%	0.3%	0.1%	0.1%	0.1%	0.0%	0.0%
0.9	False Positives	2109	2387	2672	3010	3310	3572	3801	4040	4252
	Percentage	17.2%	19.4%	21.7%	24.5%	26.9%	29.1%	30.9%	32.9%	34.6%
	False Negatives	239	159	97	58	39	18	14	11	3
	Percentage	1.9%	1.3%	0.8%	0.5%	0.3%	0.1%	0.1%	0.1%	0.0%
0.95	False Positives	1900	2145	2400	2672	2992	3275	3542	3765	3955
	Percentage	15.5%	17.5%	19.5%	21.7%	24.3%	26.7%	28.8%	30.6%	32.2%
	False Negatives	324	226	154	97	59	41	22	14	12
	Percentage	2.6%	1.8%	1.3%	0.8%	0.5%	0.3%	0.2%	0.1%	0.1%
1	False Positives	1730	1932	2174	2411	2672	2982	3243	3514	3715
	Percentage	14.1%	15.7%	17.7%	19.6%	21.7%	24.3%	26.4%	28.6%	30.2%
	False Negatives	406	306	219	154	97	60	43	24	16
	Percentage	3.3%	2.5%	1.8%	1.3%	0.8%	0.5%	0.3%	0.2%	0.1%
1.05	False Positives	1569	1766	1963	2191	2423	2672	2962	3219	3460
	Percentage	12.8%	14.4%	16.0%	17.8%	19.7%	21.7%	24.1%	26.2%	28.2%
	False Negatives	509	392	292	209	152	97	62	46	24
	Percentage	4.1%	3.2%	2.4%	1.7%	1.2%	0.8%	0.5%	0.4%	0.2%
1.1	False Positives	1433	1606	1811	1995	2211	2439	2672	2943	3206
	Percentage	11.7%	13.1%	14.7%	16.2%	18.0%	19.8%	21.7%	24.0%	26.1%
	False Negatives	581	471	373	278	202	146	97	63	46
	Percentage	4.7%	3.8%	3.0%	2.3%	1.6%	1.2%	0.8%	0.5%	0.4%
1.15	False Positives	1329	1476	1650	1832	2020	2227	2456	2672	2931
	Percentage	10.8%	12.0%	13.4%	14.9%	16.4%	18.1%	20.0%	21.7%	23.9%
	False Negatives	650	551	432	353	268	197	144	97	66
	Percentage	5.3%	4.5%	3.5%	2.9%	2.2%	1.6%	1.2%	0.8%	0.5%
1.2	False Positives	1226	1371	1516	1700	1860	2043	2241	2464	2672
	Percentage	10.0%	11.2%	12.3%	13.8%	15.1%	16.6%	18.2%	20.1%	21.7%
	False Negatives	710	622	539	423	337	259	193	142	97
	Percentage	5.8%	5.1%	4.4%	3.4%	2.7%	2.1%	1.6%	1.2%	0.8%

APPENDIX L SPEFICATIONS FOR CONTINUOUS DEFLECTION MEASUREMENT DEVICE

L.1 General

A continuous measurement device shall be provided that is capable of scanning road network bearing capacity and to point out locations with bearing capacity deviations and thus minimize use of traditional stationary or slow moving equipments. The device shall be able to perform well at traffic speeds of 50 m/h or higher and shall be able to apply loads in excess of 9 kips. The sensor for deflection shall be a Doppler laser that can measure deflection velocity of the pavement surface. The device shall employ a reference sensor to remove unwanted contributions in the measurement. The equipment shall be modular in the sense that it may be synchronized in a digital network with other software packages like "Profilograph", "Pavement LineScan Video", "Right-of-Way Video", "GPS" or TMV.

L.2 Sensor Specifications

The device shall consist of seven Doppler sensors. The sensors shall be placed 12 in. (100 mm) apart in front of the moving load. The remaining sensor shall be placed outside the deflection bowl as a reference. The sensors shall meet the following specifications:

Doppler Specifications:

Sensor head

- Laser type: helium neon
- Wavelength: 633 nm or better
- Laser safety class: II
- Operating temperature: 32/F…104/F (0/C…40/C)
- Storage temperature: 5/F…149/F (-15/C…+65/C)

Signal processing

- Calibration error: < 0.1% of measurement value for |v| > 1.25 in./s
- Measurement units: yd./s, ft./min
- Data rate: max. 2000 measurements/s (internal, without averaging)
- Permissible acceleration: > 790 in./sec^2
- Signal delay: < 5 ms (measured at the analog output)
- Power consumption: max. 100 VA
- Operating temperature: 41/F…104/F (+5/C…+40/C)
- Storage temperature: 5/F…149/F (-15/C…+65/C)

Overall System specification (for 7-sensor configuration)

- Accuracy: 0.2 mils or better

- Precision: 0.08 mils or better
- Resolution: 0.04 mils or better
- Driving Speed: 60 mph

L.3 Other Sensor Specifications

The sensors other than velocity sensors shall meet the following criterion:

Odometer
The device shall include an Odometer which has an accuracy of 0.01% or better. The Odometer shall perform under the following operational/environmental conditions:

- Shock 100 g, 11 ms
- Vibration 10 g (10 to 2000 Hz)
- Temperature -4/F…185/F (-20EC to +85EC)
- Accuracy Resolution: 20.000 pulses per rotation
    - rotational error: <0.2 pulse
- Speed: max. 3000 rpm (typically more than 188 mph)

Gyroscope
The device shall be provided with Gyroscope which provides digital output and meets the following operational/environmental conditions:

- Shock: 30 g, 11 ms
- Vibration: 0.1 g^2/Hz, 1 h/axis
- Temperature: -40/F…150/F (-40EC to +65EC)
- Accuracy:
    - Measuring range ±100 E/s
    - Random walk < 0.5 E/ *h*
    - Output data rate 125 Hz
    - Scale factor < 0.3 % (1 σ)

Accelerometer (vertical)
The device shall consist of an accelerometer to measure vertical movements and shall be a Closed-loop force balance type with pivot-and-jewel bearing. The accelerometer shall meet the following operational/environmental requirements:

- Shock survival: 100 g - 11 ms shock survival
- Operating temp: 67/F…203/F (-55EC to +95EC)
- Storage temp: -85/F…203/F (-65EC to +95EC)
- Accuracy:
    - Resolution: 5 µg
    - Bandwidth: 150 Hz
    - Damping ratio: 0.6
    - Linearity error: < 0.5 mg
    - bias drift: < 20 µg per EF

Data Acquisition System
The system shall be equipped with the data-acquisition system capable to capture and handle output from all sensors and instruments. In addition, the device shall have a rack to properly accommodate power supply electronics, interface electronics for signal conditioning and an industrial computer. The data-acquisition software and software for post-processing of data shall be provided and be compatible with the TxDOT Modular Vehicle (TMV) environment.

L.4 Calibration

A calibration procedure and necessary equipment shall be provided by the manufacturer for calibration of the equipment. In addition, the design requirements for calibration slabs (if needed) shall be provided by the manufacturer before the delivery of the equipment.

L.5 Availability of Spare Parts

The manufacturer shall provide availability of any spare parts for the device for at least 5 (five) years from the date of acceptance of delivery.

L.6 Warranty and Documentation

The system shall be warranted to be free from defects in materials and workmanship for a period of one (1) year from the date of acceptance of delivery. During training five sets of Operator's Guide, Software Manual and Technical Reference containing drawings, detailed diagrams and cabling tables etc. shall be provided.

L.7 Training

The necessary training shall be provided to a minimum of five TxDOT personal. The training shall include demonstration of the equipment, data analysis, calibration of the equipment, and how to trouble shoot in case of problems both in terms of operation and data analysis. The training shall be provided along with the delivery of the equipment.

L.8 Overall Warranty

The system should work according to specifications. Any claims on the warranty shall be dealt with within 30 days after the fault has been reported. The manufacturer should start working on the problem within 48 hours of receipt of the notification. If the device cannot be repaired within the 60 days, the manufacturer shall provide TxDOT with a replacement.